ISSN 1023-9855

# Thoracic Medicine

Volume 38 • Number 2 • June 2023

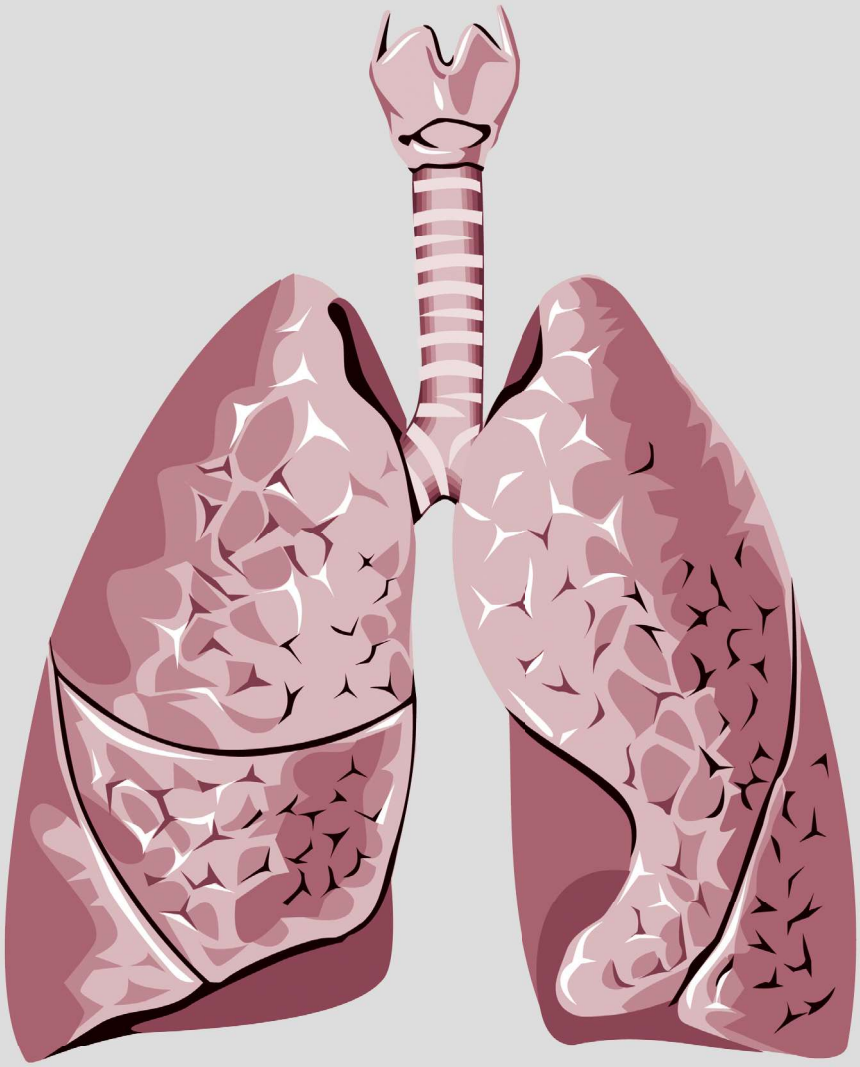

The Official Journal of

Taiwan Society of Pulmonary and Critical Care Medicine

Taiwan Society of Sleep Medicine

Taiwan Society for Respiratory Therapy

Taiwan Society of Tuberculosis and Lung Diseases

# Thoracic Medicine

The Official Journal of
Taiwan Society of Pulmonary and Critical Care Medicine
Taiwan Society for Respiratory Therapy
Taiwan Society of Sleep Medicine
Taiwan Society of Tuberculosis and Lung Diseases

# Thoracic Medicine

The Official Journal of
Taiwan Society of Pulmonary and Critical Care Medicine
Taiwan Society for Respiratory Therapy
Taiwan Society of Sleep Medicine
Taiwan Society of Tuberculosis and Lung Diseases

Volume 38
Number 2
June 2023

## CONTENTS

# The role of Treatment or Incidental Pulmonary Tuberculosis Findings Post-Surgery in a Tuberculosis-Endemic Country

Chien-Te Pan[1], Yu-Ting Tseng[1], Chung-Yu Chen[2], Pei-Ming Huang[1]

**Introduction:** The indications for surgery are limited to the management of complicated forms of tuberculosis (TB), and mostly to cases in which medical treatment is failing. There is, however, limited good quality data on the effectiveness of using surgery alongside drug treatment for TB. This study investigated the prognosis of patients with an incidental pulmonary TB finding after surgical resection.

**Methods:** The study enrolled patients who received video-assisted thoracic surgery (VATS) wedge resection or lobectomy for lung lesions from 2013 to 2017. The Pulmonary TB diagnosis was based on pathological examination with acid-fast stain or the mycobacterial culture result of surgical specimens. Medical records were reviewed and clinical data, including age, gender, surgical type, pathological reports, microbiological cultures, treatment and follow-up duration were analyzed.

**Results:** A total of 443 patients from National Taiwan University Hospital Yunlin Branch, Yunlin County, Taiwan, were included. Of those, 200 patients (45.1%) had primary lung cancer, 31 (7.0%) had metastatic cancer, 20 (4.5%) were diagnosed as having mycobacterial infection, and 11 patients (2.5%) had cryptococcosis. Thirteen of the 20 patients (65.0%) with mycobacterial infection received anti-TB treatment, and the remaining 7 patients (35.0%) were followed at the clinic without a therapeutic medication prescription. All of these patients were stable after lung lesions resection without evidence of pulmonary TB recurrence.

**Conclusion:** Anti-TB treatment may not be essential after surgical resection with an incidental finding of pulmonary TB. There is a need for well-designed trials to provide more information about the effectiveness of surgery. ***(Thorac Med 2023; 38: 96-101)***

Key words: surgery, lung tumor, pulmonary tuberculosis

[1]Department of Surgery, National Taiwan University Hospital Yunlin Branch, [2]Department of Internal Medicine, National Taiwan University Hospital Yunlin Branch
Address reprint requests to: Dr. Yu-Ting Tseng, No.579, Sec.2, Yunlin Rd., Douliou City, Yunlin County, Taiwan

## Introduction

The diagnosis of tuberculosis (TB) is mainly based on medical history, microbiological evidence, radiographic features, clinical manifestation, and laboratory findings. Of all the infectious diseases that occur in Taiwan, TB has the highest incidence and the highest mortality rate, with 9,759 TB cases (41.4 per 100,000 individuals) recorded in 2017. [1]

The histological features suggestive of TB include granulomatous inflammation, caseous necrosis, and positive acid-fast stain (AFS). But these are not pathognomonic for active TB. Granulomatous inflammation and caseous necrosis sometimes are caused by pathogens other than Mycobacterium tuberculosis, such as nontuberculous mycobacteria (NTM) and fungi. [2] Granulomatous inflammation may also be seen in noninfectious diseases, such as Sarcoidosis or hypersensitivity pneumonitis. [3-4]

More and more small nodules are being resected due to the increasing demand for lung tumor screening. Even if histological examination of resected specimens reveals findings suggestive of TB, it is still difficult to differentiate an active disease from old tuberculoma without serial radiographic studies. Therefore, whether patients with such a histological finding should receive standard anti-TB treatment immediately is still debated.

In this study, we identified patients with resected lung nodules who had histological findings suggestive of TB, but no clinical evidence. We also compared clinical characteristics and other factors during the subsequent 2 years between patients receiving and not receiving anti-TB treatment after surgical resection.

## Methods

This study enrolled patients who had undergone video-assisted thoracic surgery (VATS) wedge resection or lobectomy for lung lesions from 2013 to 2018 in a regional teaching hospital. We excluded malignant diseases and other infectious diseases (Figure -1). The pulmonary TB diagnosis was based on a pathological examination that received granulomatous change and characteristic caseous necrosis, with or without an AFS or mycobacterial culture result of surgical specimens. Medical records were reviewed and clinical data, including age, gender, surgical type, pathological reports, microbiological cultures, treatment and follow-up duration were analyzed.

## Results

A total of 443 patients from National Taiwan University Hospital Yunlin Branch, Yunlin County, Taiwan, were included (Figure 1). Of these patients, 200 (45.1%) had primary lung cancer, 31 (7.0%) had metastatic cancer, 20 (4.5%) were diagnosed as having mycobacterial infection, and 11 (2.5%) had cryptococcosis (Table 1).

Thirteen of the 20 patients (65.0%) with mycobacterial infection received anti-TB treatment and the other 7 patients (35.0%) were followed at the clinic without a therapeutic medication prescription. The median of the tracking duration was 57 days (range: 9 to 1610 days) (Table 2). All of these patients were stable after lung lesions resection without evidence of pulmonary TB recurrence.

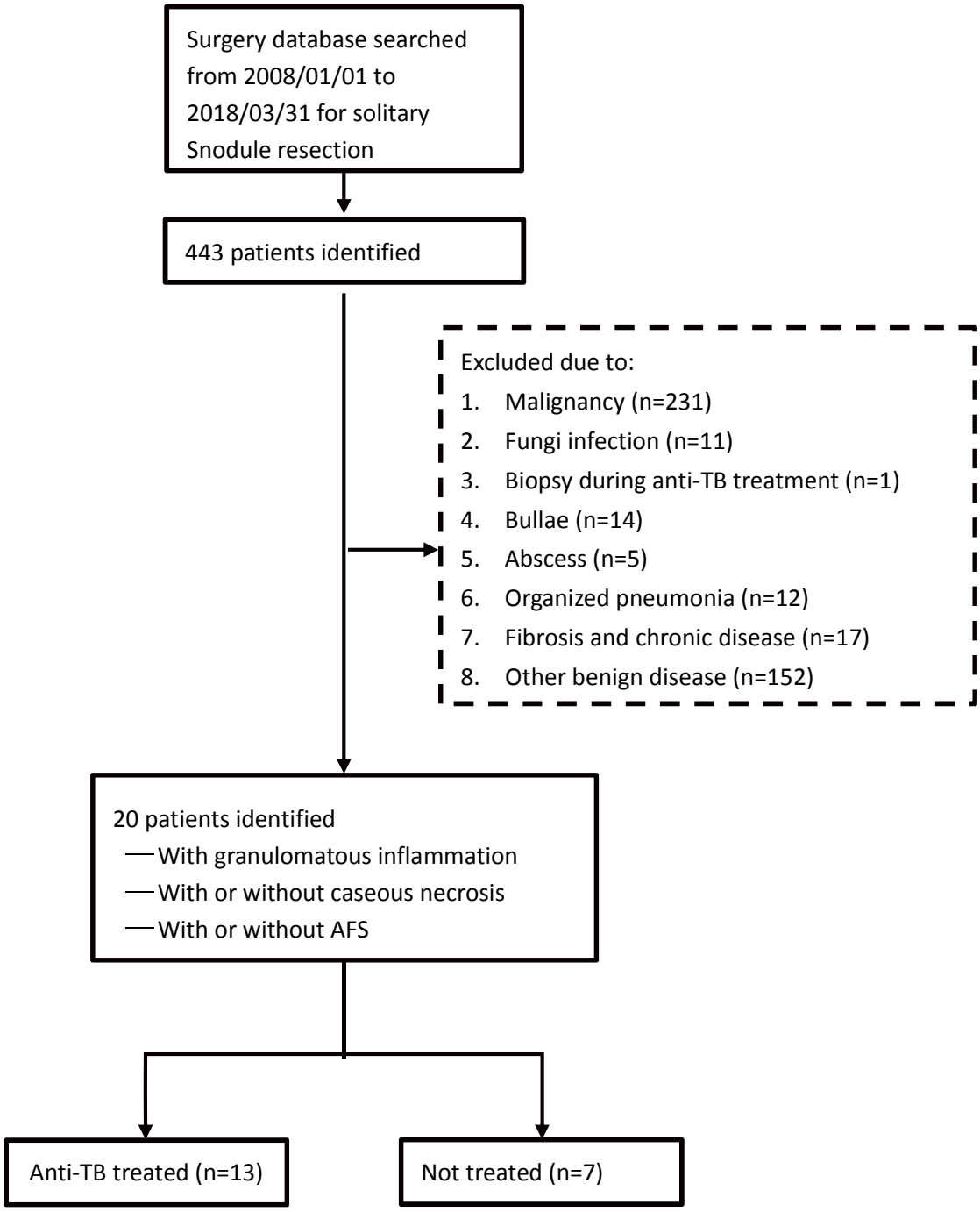


**Fig. 1.** Flowchart of study design and case selection

**Table 1.** Post-Operation Diagnosis

| Post-operation diagnosis | Number | Percentage |
|---|---|---|
| Lung cancer | 200 | 45% |
| Metastatic cancer | 31 | 7% |
| Mycobacterial infection | 20 | 5% |
| Cryptococcosis | 11 | 2% |
| Others | 181 | 41% |
| Total | 443 | |

**Table 2.** Clinical Characteristics and Pathology Data of Treated and Untreated Groups

| | No anti-TB treatment | Anti-TB treatment | *p* value |
|---|---|---|---|
| Number | 7 | 13 | |
| Age | 58.28571 | 55.46154 | 0.300 |
| Gender | 71% | 69% | 0.096 |
| Granulomatous inflammation | 86% | 77% | 0.087 |
| Caseating necrosis | 14% | 38% | 0.054 |
| Necrosis | 43% | 8% | 0.002 |
| Mycobacterial infection | 0% | 31% | 0.035 |
| TB culture positive | 0% | 92% | <0.001 |

TB: tuberculosis

## Discussion

We have 2 major findings in this study. First, the physician tended to give anti-TB medication if there was a histological finding of mycobacterial infection and a positive culture result. Second, the physician would not give anti-TB treatment if the pathology report were necrosis. Therefore, granulomatous inflammation alone should not be a reason to immediately begin anti-TB treatment after surgical resection. A similar conclusion was also reached in a study from a single medical center. [5]

Determining the treatment strategy depends on an understanding of the natural course of pulmonary tuberculoma. About 30-50% of pulmonary tuberculoma may have a stable course. [6-8]. However, since there is still a possibility of progression, anti-TB treatment is still recommended after tuberculoma is noted postoperatively. [8-10]

This study showed that the physician favored anti-TB treatment with a positive AFS in the pathology finding after resection. However,

there are still 2 factors that could influence the result. One is the staining method itself, in that the bacilli are frequently missed or underestimated with AFS microscopically on formalin-fixed, paraffin-embedded tissue. [1] The other is that NTM infection varies within the population, which will reduce the positive predictive value of AFS for pulmonary TB [12-13]. Therefore, no histological finding has been identified to be pathognomonic for active TB. For this reason, whether immediate anti-TB treatment should be administered to patients with histological findings without clinical evidence suggestive of TB remains debatable. [14-15]

Surgery is considered as a diagnostic procedure, an adjuvant for multidrug-resistant TB, and a therapeutic strategy for refractory lesions only because of the high surgical complication rate, despite adequate anti-TB treatment [16-19]. If pulmonary lesions are removed completely, the remaining tissues are macroscopically and microscopically normal. In this study, a patient could be considered to be cured. [20] The decision on whether to begin regular follow-up or immediately initiate anti-TB treatment should be carefully made based on a risk benefit assessment. A prospective study is required to confirm this finding.

## Conclusion

In patients having resected single lung nodules with histological findings, but no clinical evidence suggestive of TB, the incidence rate of active TB is low. Regular follow-up sputum and imaging studies, rather than immediate anti-TB treatment administration, may be considered. More study is necessary to confirm our findings.

## References

1. Centers for Disease Control, Ministry of Health and Welfare, Taiwan: Taiwan tuberculosis control report 2020.
2. Zumla A, James DG. Granulomatous infections: etiology and classification. Clin Infect Dis. 1996; 23(7): 146-58.
3. Ma Y, Gal A, Koss MN. The pathology of pulmonary sarcoidosis: update. Semin Diagn Pathol. 2007; 24(3): 150-61.
4. Selman M, Pardo A, King TE, Jr. Hypersensitivity pneumonitis: insights in diagnosis and pathobiology. Am J Respir Crit Care Med 2012; 186(4): 314-24.
5. Chung CL, Chen YF, Lin YT, et al. Outcome of untreated lung nodules with histological but no microbiological evidence of tuberculosis. BMC Infect Dis.2018; 18:530.
6. Lee HS, Oh JY, Lee JH, *et al*. Response of pulmonary tuberculomas to anti-tuberculous treatment. Eur Respir J. 2004; 23(3): 452-5.
7. Grenville-Mathers R. The Natural history of so-called tuberculoma. J Thorac Surg 1952; 23(3): 251-2.
8. Subotic D, Yablonskiy P, Sulis G, *et al*. Surgery and pleuro-pulmonary tuberculosis: a scientific literature review. J Thorac Dis. 2016; 8(7): E474-85.
9. Pryta S, Hansen JL. Surgical treatment of "tuberculoma". Scand J Thorac Cardiovasc Surg. 1976; 10(2): 179-82.
10. Evman S, Baysungur V, Alpay L, *et al*. Management and surgical outcomes of concurrent tuberculosis and lung cancer. Thorac Cardiovasc Surg. 2016; http://dol.org/10.1055/s-0036-1583167.
11. Fukunaga H, Murakami T, Gondo T, *et al*. Sensitivity of acid-fast staining for mycobacterium tuberculosis in formalin-fixed tissue. Am J Respir Crit Care Med. 2002; 166(7): 994-7.
12. Kendall BA, Varley CD, Choi D, *et al*. Distinguishing tuberculosis from nontuberculous mycobacteria lung disease, Oregon, USA. Emerg Infect Dis. 2011; 17(3): 506-9.
13. Grubek-Jaworska H, Walkiewicz R, Safianowska A, et al. Nontuberculous mycobacterial infections among patients suspected of pulmonary tuberculosis. Eur J Clin Microbiol Infect Dis. 2009; 28(7): 739-44.
14. Aubry MC. Necrotizing granulomatous inflammation: what does it mean if your special stains are negative?

Mod Pathol. 2012; 25(Suppl 1): S31-8.
15. Ulbright TM, Katzenstein AL. Solitary necrotizing granulomas of the lung: differentiating features and etiology. Am J Surg Pathol. 1980; 4(1): 13-28.
16. Freixinet J. Surgical indications for treatment of pulmonary tuberculosis. World J. Surg 1997; 21: 475-479.
17. Sihoe ADL, Shiraishi Y, Yew WW. The current role of thoracic surgery in tuberculosis management. Respiratory. 2009; 14: 954-968.
18. Yen YT, Wu MH, Lai WW, *et al*. The role of video-assisted thoracoscopic surgery in therapeutic lung resection for pulmonary tuberculosis. Ann Thorac. Surg 2013; 95:257-63.
19. Tseng YL, Chang JM, Liu YS, *et al*. The role of video-assisted thoracoscopic therapeutic resection for medically failed pulmonary tuberculosis. Medicine (Baltimore) 2016 May; 95(18): e3511.
20. Getahun H, Matteelli A, Chaisson RE, *et al*. Latent Mycobacterium tuberculosis infection. N Engl. J Med. 2015; 372(22): 2127-35.

# Late-Onset Chylopericardium and Chylothorax after Thoracic Surgery

Huei-Yang Hung[1], Yen-Lung Lee[2], Chih-Jen Yang[1,3]

Chylopericardium is defined as the accumulation of chylous fluid in the pericardial cavity that may progress to cardiac tamponade or constrictive pericarditis. Chylopericardium is very rare, but may occur after thoracic surgery. It can be caused by either direct injury to the branches of the thoracic duct, or indirect injury by occult obstruction of lymphatic drainage. Late-onset chylous fluid leakage can occur when thoracic surgery is combined with lymph node dissection. We reported the case of a patient with a late onset of co-incident chylopericardium and chylothorax 1 month after undergoing video-assisted thoracic surgery for segmentectomy with mediastinal lymph node dissection to treat a pulmonary nodule. Both the chylopericardium and the chylothorax were completely resolved after the immediate surgical creation of a pericardial window and chest tube drainage, and the patient was recommended to follow a low-fat diet. This case reminds us of the rare but crucial complications associated with thoracic surgery. ***(Thorac Med 2023; 38: 109-115)***

Key words: chylopericardium, chylothorax, thoracic surgery

## Introduction

Lung cancer remains the leading cause of cancer-related deaths worldwide, accounting for 1.8 million deaths each year [1]. More than 50% of patients with lung cancer are diagnosed at an advanced stage, and the 5-year survival rate for metastatic non–small cell lung cancer (NSCLC) is below 10% [2]. In a large randomized controlled trial (National Lung Screening Trial), low-dose chest computed tomography (CT) was found to reduce lung cancer mortality by up to 20%, through an increase in the early detection rate of lung cancer in high-risk populations of patients that smoked at least 30 pack-years [3]. Therefore, an increasing number of people are receiving low-dose CT to improve the early detection of lung cancer. Surgical interventions for patients with lung cancer are becoming increasingly popular due to advances in thoracic surgery, and thoracic surgery is often the final step for determining a definite diagnosis when lung nodules are identified on a CT scan.

[1]Division of Pulmonary and Critical Care Medicine, Department of Internal Medicine, Kaohsiung Medical University Hospital, Kaohsiung Medical University, Kaohsiung, Taiwan, [2]Department of Surgery, Kaohsiung Municipal Ta-Tung Hospital, Kaohsiung Medical University, Kaohsiung, Taiwan, [3]School of Post-Baccalaureate Medicine, College of Medicine, Kaohsiung Medical University, Kaohsiung, Taiwan
Address reprint requests to: Dr. Chih-Jen Yang, Department of Internal Medicine, Kaohsiung Medical University Hospital, Kaohsiung Medical University,No. 100, Tzyou First Road, Kaohsiung City, Taiwan

However, thoracic surgery is associated with very rare but critical complications, such as chylopericardium and chylothorax. The thoracic duct, which passes through the mediastinum, transports lymph chyle, which contains triglycerides, proteins, T lymphocytes, and immunoglobulins, to the venous system. Due to the anatomical location of the thoracic duct, it can be injured either directly or indirectly during thoracic surgery, leading to the development of chylopericardium or chylothorax.

Chylous leakage is typically diagnosed when fluid is detected with a milky, yellowish appearance and a high triglyceride level. Delayed management of chylous leakage can result in the progression to respiratory failure, cardiac tamponade, or cardiac arrest [4]. Late-onset chylopericardium can be easily overlooked due to the initial nonspecific symptoms, leading to fatal outcomes. A systematic review revealed that cardiac tamponade developed in 29.4% of patients who experienced cardiac surgery-related chylopericardium [5]. Chylothorax is another uncommon but potentially serious complication of pulmonary surgery combined with mediastinal lymph node dissection [6]. Chylothorax after pulmonary resection and mediastinal lymph node dissection has been reported to occur in 1.4% to 2.4% of cases [6, 7]. A review of 17 cases of late-onset chylothorax after various surgeries or traumas revealed that it could occur at any time, ranging from less than 1 week to 20 years after the initiating event [8].

Conservative treatment or surgical intervention, such as thoracic duct ligation or the creation of a pericardial window, may be necessary in cases of chylopericardium or chylothorax. We report a very rare case of late-onset chylopericardium and chylothorax 1 month after thoracic surgery in a healthy 59-year-old woman.

## Case presentation

This healthy 59-year-old woman underwent a right lower lung segmentectomy and mediastinal lymph node dissection via video-assisted thoracic surgery (VATS) to remove a 0.6-cm nodule that was incidentally found on low-dose CT. A benign nodule was identified, and the patient was discharged uneventfully. A chest radiograph taken 4 days after VATS showed a normal heart size and no pleural effusion (Figure 1A). Another chest radiograph obtained approximately 2 weeks later revealed mild cardiomegaly (Figure 1B), but the patient reported no discomfort. One month later, the patient began to experience dyspnea on exertion and presented to the emergency department with massive right pleural effusion and pericardial effusion (Figure 1C). Echocardiography revealed a large amount of circumferential pericardial effusion, measuring 3.15 cm at its greatest width [9]. Thoracentesis was rapidly performed, and a study of the pleural effusion revealed transudative chylothorax (pleural fluid/serum lactate dehydrogenase: 93/211 IU/L; pleural fluid/serum protein: 2.4/5.9 g/dL) containing 203 mg/dL triglycerides with predominant mononuclear cells (polymorphonuclear cells/mononuclear cells: 7%/93%).

To avoid the rapid accumulation of pericardial effusion, which may result in cardiac tamponade, a pericardial window was surgically created, and a total of 775 mL of milk-like effusion was drained (Figure 2). This fluid contained a high level of triglycerides, up to 376 mg/dL, indicating chylopericardium. No leakage or obstructed site over the pericardium was detected by CT with enhancement. The Gram stain, acid-fast stain, adenosine deaminase test,

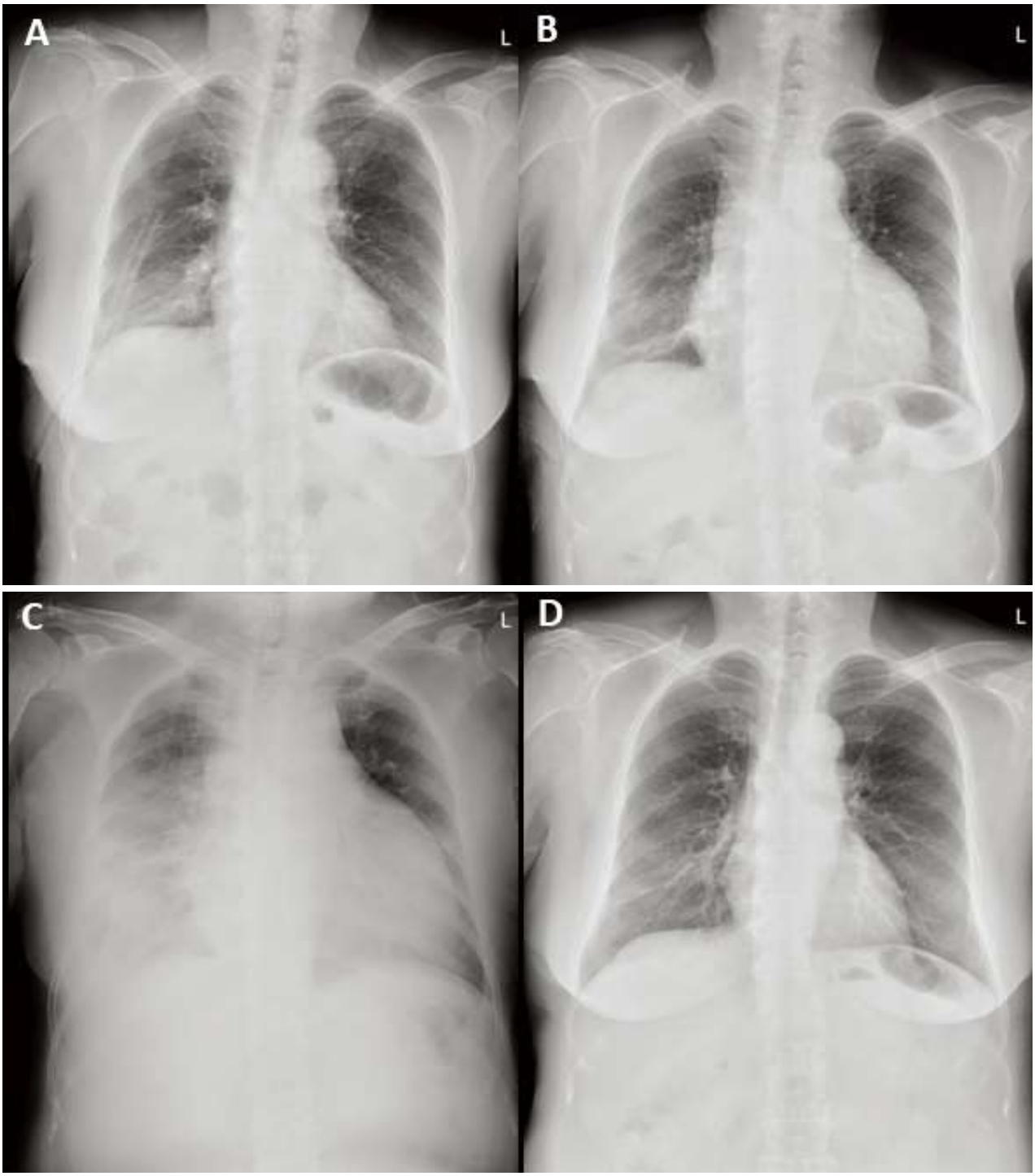


**Fig. 1.** (A). Post-right lower lobe video-assisted thoracic surgery (VATS) segmentectomy. (B). Cardiomegaly was noted approximately 2 weeks after the operation. (C). Massive right-side pleural effusion and cardiomegaly progression were noted approximately 1 month after the operation. (D). Follow-up 5 months after the operation revealed no evidence of recurrent chylothorax or chylopericardium.

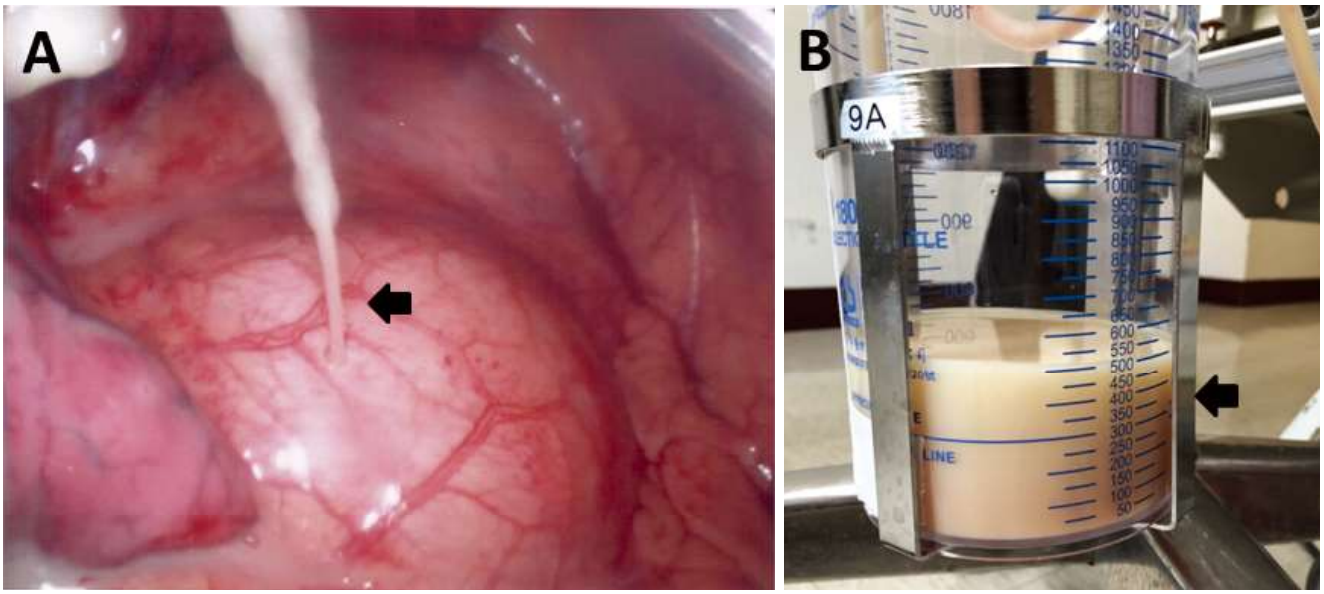


**Fig. 1.** (A). Milk-like pericardial effusion was released when the pericardium was dissected. (B). Pericardial effusion contained with Chyle and high level of triglyceride was drained and collected in a chest bottle.

and pleural fluid cultures were all negative. A low-fat diet was encouraged, and the drainage of chylous effusion from the chest tube decreased gradually. The chest tube was removed 2 weeks later, and no recurrent pericardial or pleural effusion was detected during 5 months of follow-up (Figure 1D).

## Discussion

We report a very rare case of late-onset chylopericardium and simultaneous chylothorax in a healthy, 59-year-old woman after VATS to remove a lung nodule. These rare complications were successfully resolved by immediate surgical intervention and a low-fat diet. No recurrence was observed during 5 months of follow-up.

Chylopericardium is a rare condition defined as the accumulation of chylous fluid in the pericardial cavity. A definite diagnosis of chylopericardium can be challenging to determine, and a scoring system was proposed by Dib et al. to facilitate the diagnosis. [10] The score is calculated by assessing the presence of the following 4 features of the pericardial fluid: a milky yellowish appearance, a triglyceride level greater than 500 mg/dL, a cholesterol/triglyceride ratio less than 1, and negative cultures with lymphocyte predominance on cytologic examination. Each feature that is present is awarded 1 point, and a score of 2 is required for a diagnosis of chylopericardium (with a specificity and sensitivity of 100%) [10].

The most common etiology for chylopericardium is secondary injury to the thoracic duct, typically as a complication following cardiothoracic surgery and thoracic trauma. In addition, congenital lymphangiomatosis, radiotherapy, subclavian vein thrombosis, infection, mediastinal neoplasm, cystic hygroma, acute pancreatitis, and Gorham's disease have also been reported as possible chylopericardium etiologies.

The thoracic duct ascends from the cisterna chyli at the level of the first or second lumbar vertebra. It is a single channel that ascends along the posterior mediastinum to the right of the vertebral column, coursing obliquely behind the esophagus at the seventh thoracic vertebra, crossing from right to left at the level of the fifth to sixth thoracic vertebrae, ascending into the neck posterior to the aortic arch, and emptying into the left jugulosubclavian junction [11, 12]. The thoracic duct is proximal to the trachea and to highly variable collateral channels that may be injured during pulmonary resection, particularly mediastinal lymph node dissection, leading to the disruption of lymphatic flow [13].

Although chylopericardium is a rare entity, it has been reported to occur after lung resection with mediastinal lymph node dissection, lobectomy for lung cancer, and radical esophagectomy [14-16]. In addition to direct injury to the thoracic duct or its branches during cardiac surgery, extensive mediastinal lymph node dissection might hinder lymphatic drainage from the pericardium into the mediastinal lymph node chain, resulting in indirect injury to the thoracic duct, and leading to chylopericardium [14, 17]. According to cadaver studies, lymphatic drainage from the pericardium is predominantly directed to the mediastinal and peritracheobronchial nodes, which may contribute to the development of chylopericardium [18, 19]. Lymphatic flow from the pericardium might be interrupted or damaged during thoracic surgery combined with mediastinal lymph node dissection [16].

Lymphoscintigraphy is a useful tool for confirming the leakage site in the thoracic duct. In a primary chylopericardium case series, 3 cases were found to have direct communication between the thoracic duct and the pericardial space, 3 had no direct communication but presented with the pericardial accumulation of technetium-99 m sulfur colloid, and 3 showed negative results by lymphoscintigraphy [20].

Pericardial effusion is generally graded as minimal (<5 mm of pericardial separation during diastole, corresponding to a fluid volume of 50 to 100 mL), small (5 to 10 mm of separation, corresponding to a fluid volume of 100 to 250 mL), moderate (10 to 20 mm of separation, corresponding to a fluid volume of 250 to 500 mL), or large (>20 mm separation, corresponding to a fluid volume greater than 500 mL) [9]. Generally speaking, the speed of chylous fluid accumulation in the pericardium depends on the degree of thoracic duct injury (either direct or indirect) [5]. Direct injury to the thoracic duct during surgery results in the rapid accumulation of chyle in the pericardium, followed soon by the development of symptoms including dyspnea, because the pericardial cavity is not as large as the pleural cavity. By contrast, late-onset chylopericardium, such as in our presented case, might indicate the development of chylopericardium due to the occult obstruction of lymphatic drainage, also known as indirect thoracic duct injury.

An average chylopericardium onset time of 22.1 ± 54.0 days following cardiac surgery was reported in a systematic review [5]. Some cases were misdiagnosed at the beginning, and the time interval between the onset of chylopericardium and the establishment of the definite diagnosis was 8.5 ±11.0 days [5]. Late-onset chylopericardium after lung resection accompanied by a mediastinal lymph node dissection may occur, but be overlooked by both surgeons and patients. Therefore, when a patient develops unexpected dyspnea on exertion, or progressive cardiomegaly is noted on the chest radiograph

after cardiothoracic surgery, further examination, such as echocardiography, chest CT, or lymphangiography, is necessary to determine the presence of chylopericardium.

In addition to chylopericardium, chylothorax is an important complication of thoracic surgery. Chylothorax is typically exudative; transudative chylothorax is less common. The mechanism through which transudative chyle in the lymphatic system transforms into exudative chylous pleural effusion remains unclear. One hypothesis is that the physiological conditions of transcapillary hydrostatic gradients and water reabsorption lead to a relative increase in protein concentrations [21]. Transudative chylothorax has been reported in patients with liver cirrhosis, nephrotic syndrome, and heart failure. Cerfolio *et al*. reported a 1.4% chylothorax incidence rate in 2838 patients who underwent pulmonary resection with complete thoracic mediastinal lymph node dissection, with a particularly high incidence among those with pathologic stage N2 disease and those who underwent robotic resection [5]. Shimizu et al. also reported a 2.4% chylothorax rate in 1110 patients who underwent pulmonary resection (at least lobectomy) and systematic mediastinal lymph node dissection for lung cancer [7].

Chylothorax is typically diagnosed within 3 days after pulmonary resection because oral intake generally starts on postoperative day 1 [7, 22]. Chylothorax most commonly occurs on the right side, because most of the thoracic duct branches are located in the right hemithorax, and leakage typically occurs from a branch of the main duct due to lymph node dissection [13]. Late-onset chylothorax is very rare. Sakaizawa et al. reported a case of late-onset chylothorax occurring 15 days after surgery in a 79-year-old woman who underwent right upper lobectomy and mediastinal dissection for lung cancer [23]. Zhang et al. reviewed the literature and identified 17 cases of late-onset chylothorax after various surgeries or traumas, with onset times ranging from less than 1 week to 20 years [8].

In conclusion, we presented a very rare case of late-onset chylopericardium simultaneous with chylothorax after VATS-based segmentectomy and mediastinal lymph node dissection. Chylopericardium and chylothorax are crucial complications of thoracic or cardiac surgery, particularly those involving mediastinal lymph node dissection. We should be aware of the possibility of the late-onset complication of chylous fluid leakage secondary to thoracic surgery.

## Acknowledgment

The authors thank Kaohsiung Municipal Ta-Tung Hospital for its assistance.

## References

1. Sung H, Ferlay J, Siegel RL, *et al*. Global cancer statistics 2020: GLOBOCAN estimates of incidence and mortality worldwide for 36 cancers in 185 countries. CA Cancer J Clin 2021; 71(3): 209-49.
2. Lemjabbar-Alaoui H, Hassan OU, Yang YW, *et al*. Lung cancer: Biology and treatment options. Biochim Biophys Acta 2015; 1856(2): 189-210.
3. National Lung Screening Trial Research Team, Aberle DR, Adams AM, *et al*. Reduced lung-cancer mortality with low-dose computed tomographic screening. N Engl J Med 2011; 365(5): 395-409.
4. Uchikawa T, Ohtani K, Muramatsu K, *et al*. Constrictive pericarditis and worsening mitral annular disjunction after long-term chylopericardium. Circ Heart Fail 2018; 11(8): e004698.
5. Yuan SM. Post-cardiac surgery chylopericardium. J Coll Physicians Surg Pak 2020; 30(6): 627-32.
6. Bryant AS, Minnich DJ, Wei B, *et al*. The incidence and management of postoperative chylothorax after

pulmonary resection and thoracic mediastinal lymph node dissection. Ann Thorac Surg 2014; 98(1): 232-5; discussion 5-7.
7. Shimizu K, Yoshida J, Nishimura M, *et al*. Treatment strategy for chylothorax after pulmonary resection and lymph node dissection for lung cancer. J Thorac Cardiovasc Surg 2002; 124(3): 499-502.
8. Zhang C, Zhang RM, Pan Y, *et al*. Late-onset chylothorax during chemotherapy after lobectomy for lung cancer: A case report and review of the literature. Medicine (Baltimore) 2019; 98(22): e15909.
9. Jung HO. Pericardial effusion and pericardiocentesis: role of echocardiography. Korean Circ J 2012; 42(11): 725-34.
10. Dib C, Tajik AJ, Park S, *et al*. Chylopericardium in adults: a literature review over the past decade (1996-2006). J Thorac Cardiovasc Surg 2008; 136(3): 650-6.
11. Johnson OW, Chick JF, Chauhan NR, *et al*. The thoracic duct: clinical importance, anatomic variation, imaging, and embolization. Eur Radiol 2016; 26(8): 2482-93.
12. Chen L, Yu S, Chen S, *et al*. Application of imaging technique in thoracic duct anatomy. Ann Palliat Med 2020; 9(3): 1249-56.
13. Tabu M, Imai K, Ogawa J, *et al*. Late-onset chylothorax after pulmonary resection for lung cancer. Gen Thorac Cardiovasc Surg 2011; 59(3): 205-8.
14. Mizushima Y, Yoshida Y, Inoue A, *et al*. Chylopericardium following right thoracotomy for lung cancer. Tumori 1996; 82(3): 264-5.
15. Yang W, Luo C, Liu Z, *et al*. Chylous pericardial effusion after pulmonary lobectomy. Interact Cardiovasc Thorac Surg 2017; 25 (1): 145-6.
16. Nakamura S, Ohwada S, Morishita Y. Isolated chylopericardium following radical esophagectomy: report of a case. Surg Today 1996; 26(8): 629-31.
17. Tomimaru Y, Kodama K, Okami J, *et al*. Pericardial effusion following pulmonary resection. Jpn J Thorac Cardiovasc Surg 2006; 54(5): 193-8.
18. Riquet M, Le Pimpec-Barthes F, Hidden G. Lymphatic drainage of the pericardium to the mediastinal lymph nodes. Surg Radiol Anat 2001; 23(5): 317-9.
19. Eliskova M, Eliska O, Miller AJ. The lymphatic drainage of the parietal pericardium in man. Lymphology 1995; 28(4): 208-17.
20. Han Z, Li S, Jing H, *et al*. Primary idiopathic chylopericardium: a retrospective case series. BMC Surg 2015; 15: 61.
21. Maldonado F, Hawkins FJ, Daniels CE, *et al*. Pleural fluid characteristics of chylothorax. Mayo Clin Proc 2009; 84(2): 129-33.
22. Shimizu K, Otani Y, Ibe T, *et al*. Late-onset chylothorax after pulmonary resection and systematic mediastinal lymph node dissection for lung cancer. Jpn J Thorac Cardiovasc Surg 2005; 53(1): 39-41.
23. Sakaizawa T, Toishi M, Ozawa K, *et al*. [Late-onset chylothorax after right upper lobectomy; report of a case]. Kyobu Geka 2018; 71(12): 1052-5.

# Pleura-contact Sign of Lung Nodules and Association with Benign Etiology in Asymptomatic Patients Without Cancer History

Chun-Fu Chung[1],Yu-Cheng Tung[2], Sheng-Wei Tu[1], Kuo-Tung Huang[1], Hung-Chen Chen[1], Chien-Hao Lai[1], Meng Chih Lin[1,3], Yu-Ping Chang[1]

**Introduction:** Pulmonary nodules are commonly observed in clinical practice. We aimed to analyze various features of pulmonary nodules and their association with the risk of malignancy.

**Methods:** We retrospectively reviewed patients with lung nodules equal to or less than 3cm in size, detected on chest computed tomography, and those who had received pulmonary nodules resection from January 2001 to December 2015. Ultimately, 302 resected pulmonary nodules from 258 patients were included in the study. Their characteristics and correlations with malignancy were analyzed.

**Results:** Pulmonary nodules with larger diameters were associated with higher risks of malignancy, were more irregular in shape, and had a higher percentage of solid nodules and pleural tag signs. Lung nodules measuring 1-2 cm had the highest percentage of pleura-contact signs (PCSs). Patients with larger pulmonary nodules had more symptoms and higher white blood cell counts. Among asymptomatic patients without known cancer histories, malignant pulmonary nodules tended to be large in diameter, irregular in shape, have a high percentage of pleura tag signs, have a low percentage of PCSs, and appear frequently in elderly patients. Multivariant analysis of factors associated with the malignancy risk of a pulmonary nodule in asymptomatic patients without a cancer history revealed that the patient's age and nodule diameter were significant positive predictors of cancer risk, while PCS was a negative predictor of malignancy.

**Conclusion:** For asymptomatic patients without a cancer history, PCSs may predict a benign nature in pulmonary nodules ≤ 3 cm in diameter. ***(Thorac Med 2023; 38: 102-108)***

Key words: Pulmonary nodule, pleural-contact sign, malignancy risk, lung cancer

[1]Division of Pulmonary and Critical Care Medicine, Department of Internal Medicine, Kaohsiung Chang Gung Memorial Hospital and Chang Gung University College of Medicine, Kaohsiung, Taiwan, [2]Department of Diagnostic Radiology, Kaohsiung Chang Gung Memorial Hospital, Chang Gung University College of Medicine, Kaohsiung 83301, Taiwan, [3]Department of Respiratory Therapy, Kaohsiung Chang Gung Memorial Hospital and Chang Gung University College of Medicine, Kaohsiung, Taiwan

Address reprint requests to: Dr. Yu-Ping Chang, Division of Pulmonary and Critical Care Medicine, Department of Internal Medicine, Kaohsiung Chang Gung Memorial Hospital, Chang Gung University College of Medicine, Kaohsiung, Taiwan

## Introduction

Pulmonary nodules are defined as round or irregular opacities (measuring ≤ 3 cm in diameter)located in the lungs, and are common findings in computed tomography (CT) scans [1]. Pulmonary nodules are frequently encountered in clinical practice; therefore, the assessment of malignancy risk may be critical to clinical decisions. The malignancy risk of pulmonary nodules is principally correlated with their size and growth rate [2].Features suggestive of a nodule with a high probability of malignancy include large size, spiculation, pleural indentation, size increment, upper lobe location, irregular border, pure ground-glass opacities, or a subsolid appearance [1,3]. In addition to nodular characteristics, clinical factors, such as the patient's age, and a history of cigarette smoking, chronic obstructive pulmonary disease, and asbestos exposure, should also be considered [3-4]. Low-dose CT screening in high-risk patients can reduce the lung cancer mortality risk by up to 20% [5].

This study aimed to analyze the characteristics of pulmonary nodules and the risk of malignancy, especially among asymptomatic patients without a known cancer history.

## Material and methods

### *Participants*

Patients with lung nodules ≤ 3 cm in maximum diameter detected on chest CT and who underwent pulmonary nodule resection from1 January2001 to31 December 2015 at Kaohsiung Chang Gung Memorial Hospital were retrospectively screened. A total of 409 resected nodules were identified. Twenty-five nodules were excluded owing to incomplete data, and 82 nodules were excluded because more than 3 lung nodules were synchronously detected on chest CT. Finally, 302 nodules resected from 258 patients were included in the analysis. This study was approved by the Institutional Review Board of Chang Gung Memorial Hospital, and the requirement for patient consent was waived (IRB:201901664B0).

### *CT protocols*

A CT scan was performed to evaluate the entire lung and estimate the extent of nodules with a CT section thickness of 2–5 mm (lower dose CT: 2–3 mm; contrast-enhanced CT:5 mm; high-resolution CT:5 mm). The CT scanner used the following parameters:120 kVp and auto exposure control; beam pitch, 0.875–1.675. The images were reconstructed with a field of view of 15–20 cm. The lung was displayed with a window level of -500 HU and a window width of 1500 HU as the lung window setting, and with a window level of 50 HU and a window width of 350 HU as the mediastinal window setting for tumor assessment.

### *Definition of pleural-contact sign*

A pulmonary nodule was defined as positive for pleural-contact sign (PCS) if it was directly in contact with the pleura and the distance from the pleura was 0 mm on the CT images, as shown in Supplemental Figure 1.

**Fig. 1.** A chest CT image illustrating PCS of a lung nodule. An arrow was used to mark a lung nodule that directly contacted the pleura and the distance from the pleura was 0 mm. (CT: computed tomography; PCS: pleura-contact sign)

### *Statistics analysis*

We used the non-parametric Mann–Whitney U-test or Kruskal–Wallis test to compare continuous variables and presented them as medians with interquartile ranges. We used the chi-square test to compare categorical variables, which were presented as frequencies with percentages. Multivariate analysis was performed using binary logistic regression analysis to adjust for confounding factors, and all covariates with a p-value< 0.05 were considered in the analysis. Statistical analyses were performed using SPSS version 21.0 (IBM Corp., Armonk, New York, USA). Statistical significance was set at a p-value of< 0.05.

## Results

This analysis comprised 302 lung nodules with a maximum diameter of ≤ 3 cm that were resected from 258 patients. Lung nodules were categorized into 3 groups according to the maximum diameter detected on chest CT in the lung window: ≤ 1,>1 to ≤ 2, and > 2 to ≤3 cm.

**Table 1.** Clinical Parameters and Nodule Characteristics Classified by Nodule Size

| Lung nodule size | ≤ 1 cm | >1 to ≤ 2 cm | >2 to ≤ 3 cm | *p*-value |
|---|---|---|---|---|
| n | 120 | 132 | 50 | |
| Age (years) | 58.0 (52.0–63.0) | 59.0 (54.0–65.0) | 58.5 (51.8–65.8) | 0.219 |
| BMI (kg/m2) | 24.6 (21.7–26.8) | 24.2 (22.2–26.4) | 24.4 (22.2–25.8) | 0.922 |
| Sex | | | | |
| Male (total 166) | 59 (35.5%) | 75 (45.2%) | 32 (19.3%) | 0.177 |
| Female (total 136) | 61 (44.9%) | 57 (41.9%) | 18 (13.2%) | |
| Symptoms | 22 (18.3%) | 36 (27.3%) | 20 (40.0%) | 0.012 |
| Never-smoker | 96 (80.0%) | 95 (72.0%) | 38 (76.0%) | 0.331 |
| White blood cell count (/uL) | 5.0 (3.5–6.1) | 6.0 (4.6-7.3) | 6.6 (4.9-7.7) | <0.001 |
| Lymphocyte (%) | 29.8 (22.8–34.9) | 30.3 (22.9–36.7) | 27.8 (22.7–34.9) | 0.776 |
| Monocyte (%) | 5.7 (4.6–7.2) | 5.6 (4.5–6.9) | 5.0 (4.4–6.2) | 0.143 |
| Cancer history | 67 (55.8%) | 58 (43.9%) | 14 (28.0%) | 0.004 |
| Pathology malignancy | 39 (32.5%) | 64 (48.5%) | 27 (54.0%) | 0.009 |
| GGO | 28 (23.3%) | 5 (3.8%) | 1 (2.0%) | |
| Subsolid nodule | 16 (13.3%) | 31 (23.5%) | 9 (18.0%) | <0.001 |
| Solid nodule | 76 (63.3%) | 96 (72.7%) | 40 (80.0%) | |
| Irregular nodule shape | 11 (9.2%) | 73 (55.3%) | 41 (92%) | <0.001 |
| Pleura-contact sign | 31 (25.8%) | 51 (38.6%) | 11 (22%) | 0.030 |
| Pleura tag sign | 4 (3.3%) | 24 (18.2%) | 23 (46%) | <0.001 |

BMI: body mass index; GGO: ground-glass opacity.

All clinical characteristics and pertinent laboratory data were compared and are listed in Table 1. There were no differences in age, body mass index, sex, smoking habits, or percentage of blood lymphocytes and monocytes among the groups. Patients with larger nodules may present more symptoms, and have higher risks of malignancy, more irregular shapes, more solid nodules, more pleural tag signs, and higher white blood cell counts. Lung nodules measuring >1 to ≤ 2 cm had the highest percentage of PCSs.

We then selected pulmonary nodules from asymptomatic patients with no cancer history and categorized them as malignant or benign by etiology. A comparison of their clinical features and laboratory data are displayed in Table 2. In asymptomatic patients without a cancer history, malignant pulmonary nodules tended to be large in diameter, have an irregular shape, have pleura tag signs, have a low percentage of PCSs, and appear frequently in elderly patients.

Multivariate analysis of factors associated with malignancy risk of pulmonary nodules, as shown in Table 3, revealed that the patient's age and nodule diameter were significant positive predictors of cancer risk, whereas PCS was a negative predictor of malignancy.

**Table 2.** Lung Nodules in Patients Without Cancer History and Symptoms

| | Benign | Malignant | *p*-value |
|---|---|---|---|
| n | 67 | 28 | |
| Age (years) | 56.0 (49.0-62.0) | 63.0 (58.3-70.0) | <0.001 |
| BMI (kg/m$^2$) | 24.8 (22.9-26.0) | 23.4 (21.6-25.6) | 0.123 |
| Sex | | | 0.821 |
| Male (total 55) | 38 (69.1%) | 17 (30.9%) | |
| Female (total 40) | 29 (72.5%) | 11 (27.5%) | |
| Never-smoker | 53 (79.1%) | 22 (78.6%) | 1.000 |
| White blood cell count (/uL) | 5.8 (3.9–7.3) | 5.9 (5.1–7.5) | 0.267 |
| Lymphocyte (%) | 27.1 (21.9–37.6) | 31.0 (24.5–36.0) | 0.304 |
| Monocyte (%) | 5.6 (4.5–7.2) | 5.8 (4.7–6.4) | 0.928 |
| Maximum diameter (cm) | 1.1 (0.7–1.6) | 1.9 (1.2–2.3) | <0.001 |
| GGO | 11 (16.4%) | 2 (7.1%) | 0.272 |
| Subsolid nodule | 17 (25.4%) | 5 (17.9%) | |
| Solid nodule | 39 (58.2%) | 21 (75.0%) | |
| Irregular nodule shape | 23 (34.3%) | 21 (75.0%) | 0.001 |
| Pleura-contact sign | 22 (32.8%) | 2 (7.1%) | 0.009 |
| Pleura tag signs | 9 (13.4%) | 15 (53.6%) | <0.001 |

BMI: body mass index; GGO: ground-glass opacity.

**Table 3.** Multivariate analysis of Factors associated With risk of Lung Nodule Malignancy

| | Odds ratio | 95% confidence interval | *p*-value |
|---|---|---|---|
| Age | 1.10 | 1.03–1.17 | 0.004 |
| Lung nodule maximum diameter (cm) | 4.65 | 2.01–10.75 | <0.001 |
| Pleura-contact sign | 0.18 | 0.03–0.98 | 0.047 |

## Discussion

### *1. PCSs and risk of malignancy*

The PCSs of pulmonary nodules defined nodules that were directly in contact with the pleura on CT images [6].Kim et al. reported that malignant subsolid pulmonary nodules, pleural attachment, and indentation may be independently associated with visceral pleural invasion, especially in patients with large solid portions [7]. Hsu et al. concluded that linear pleural tags with a soft tissue component at the pleural end of the mediastinal window can predict visceral pleural invasion in non-small cell lung cancer [8]. However, a retrospective review analyzed 569 participants with 943 solid pulmonary non-calcified nodules attached to the pleura and found that nodules < 1 cm, with smooth margins and lentiform, oval, semicircular, or triangular shapes were benign[9].The PCSs in the cancer population suggested visceral pleural invasion[7].In the NELSON study, smooth or attached solid indeterminate nodules (0.5 cm) were all benign after a 1-year follow-up, and none of the identified cancers were attached to the pleura, vessels, or fissures [10].

### *2. Nodule diameter and risk of malignancy*

The NELSON 1-year follow-up study concluded that nodule growth assessed by volume doubling time at the 1-year follow-up was the only potential predictor of malignancy [10]. The PanCan dataset study, which included 1,871 persons with 7,008 nodules, confirmed that nodule diameter is associated with lung cancer probability, with a significant non-linear relationship in patients undergoing low-dose CT screening [11].The American College of Chest Physicians (ACCP) evidence-based clinical practice guidelines reviewed 7 studies assessing nodule size and found a proportional increase in the risk of malignancy with an increase in the diameter of the nodule [4]. The risk of malignancy was exceedingly low in nodules < 5 mm in size (range 0-1%), while the risks were high in nodules 5-10 mm in size (range 6-28%) and nodules >2 cm in size (range 64-82%) [4].

### *3. Age and risk of malignancy*

Cancer can be considered an age-associated condition because the incidence of most cancers increases with age [12]. According to statistics from Cancer Research UK during the period 2016-2018, people aged 85-89 years had the highest incidence of lung cancer, and more than 44% of all new lung cancer cases in the UK are diagnosed in people aged 75 years and over each year [13].Using the Taiwan National Health Insurance Research Database to retrospectively review 33,919 lung cancer patients between 2002 and 2008, it was found that age > 65years at the time of diagnosis could be identi-

fied as an independent prognostic factor of lung cancer [14]. Venuta *et al*. reported less than 0.5% of lung cancer-related deaths occurred at< 40 years of age, and there was only a 0.03% likelihood of lung cancer development up to age 39, without significant sex differences [15]. A longitudinal study in Hungary enrolled lung cancer patients aged > 20 years during 2011-2016 and found that lung cancer incidence and mortality increased with age, peaking in the 70-79 and 60-69 years age groups among men and women, respectively [16].

In our study, we found that PCSs may predict the benign nature of pulmonary nodules ≤ 3 cm in asymptomatic patients without a cancer history, and this is commonly observed during health examinations. Our study was also in accordance with previous studies showing that nodular size and age were significant positive predictors of malignancy risk.

***Limitations***

This study had several limitations. First, the sample size was relatively small and restricted. The study focused on asymptomatic patients without a cancer history, which may not apply to the general population. Second, we could not measure the volume of pulmonary nodules, and there was a lack of uniformity in the CT protocols.

## Conclusion

For asymptomatic patients without a cancer history, PCSs may predict the benign nature of pulmonary nodules ≤3 cm in diameter.

## Acknowledgements

We thank Prof. Sheng-Nan Lu, Prof. Hsueh-Wen Chang, Shin-Yi Chien, Chih-Yun Lin, and the Biostatistics Center, Kaohsiung Chang Gung Memorial Hospital, for the statistical analysis.

## Funding

The authors received no financial support for the research, authorship, or publication of this article.

## Declaration of conflicting interests

The authors declare that there are no conflicts of interest.

## References

1. Sánchez M, Benegas M, Vollmer I. Management of incidental lung nodules <8 mm in diameter. J Thorac Dis 2018; 10(Suppl 22): 2611-2627.
2. Bankier AA, MacMahon H, Goo JM, *et al*. Recommendations for measuring pulmonary nodules at CT: a statement from the Fleischner Society. Radiology 2017 Nov; 285(2): 584-600.
3. Ost DE, Gould MK. Decision making in patients with pulmonary nodules. Am J Resp Crit Care Med 2012 Feb; 185(4): 363-372.
4. Gould MK, Donington J, Lynch WR, *et al*. Evaluation of individuals with pulmonary nodules: when is it lung cancer? Diagnosis and management of lung cancer, 3rd ed: American College of Chest Physicians evidence-based clinical practice guidelines. Chest 2013 May; 143(5 Suppl): 93-120.
5. The National Lung Screening Trial Research Team. Reduced lung-cancer mortality with low-dose computed tomographic screening. N Engl J Med 2011; 365: 395-409.
6. Eriguchi T, Takeda A, Tsurugai Y, *et al*. Pleural contact decreases survival in clinical T1N0M0 lung cancer patients undergoing SBRT. Radiother Oncol 2019; 134: 191-198.
7. Kim HJ, Cho JY, Lee YJ, *et al*. Clinical significance of

pleural attachment and indentation of subsolid nodule lung cancer. Cancer Res Treat 2019; 51(4): 1540-1548.

8. Hsu JS, Han IT, Tsai TH, *et al*. Pleural tags on CT scans to predict visceral pleural invasion of non-small cell lung cancer that does not abut the pleura. Radiology 2016 May; 279(2): 590-596.
9. Zhu Y, Yip R, You N, *et al*. Management of nodules attached to the costal pleura at low-dose CT screening for lung cancer. Radiology 2020; 297: 710-718.
10. Xu DM, van der Zaag-Loonen HJ, Oudkerk M, *et al*. Smooth or attached solid indeterminate nodules detected at baseline CT screening in the NELSON study: cancer risk during 1 year of follow-up. Radiology 2009 Jan; 250(1): 264-272.
11. McWilliams A, Tammemagi MC, Mayo JR, *et al*. Probability of cancer in pulmonary nodules detected on first screening CT. N Engl J Med 2013; 369: 910-919.
12. White MC, Holman DM, Boehm JE, *et al*. Age and cancer risk: A potentially modifiable relationship. Am J Prev Med 2014 Mar; 46(3 Suppl 1):S7-15.
13. Cancer Research UK; https://www.cancerresearchuk.org/health-professional/cancer-statistics/statistics-by-cancer-type/lung-cancer.
14. Wang BY, Huang JY, Cheng CY, *et al*. Lung cancer and prognosis in Taiwan: a population-based cancer registry. J Thorac Oncol 2013 Sep; 8(9): 1128-1135.
15. Venuta F, Diso D, Onorati I, et al. Lung cancer in elderly patients. J Thorac Dis2016; 8(Suppl 11): S908-S914.
16. Tamási L, Horváth K, Kiss Z, *et al*. Age and gender specific lung cancer incidence and mortality in Hungary: trends from 2011 through 2016. Pathol Oncol Res 2021 Apr 30; 27: 598862.

# Central Diabetes Insipidus as the First Manifestation of Pulmonary Langerhans Cell Histiocytosis – Report of 2 Cases

Chung-Fu Lin[1], Sy-Harn Lian[1], Ye-Fong Du[1], Han-Yu Chang[1], Cheng-Lin Wu[2]
Tang-Hsiu Huang[1]

Langerhans cell histiocytosis (LCH) is a rare disease that is characterized by the recruitment and accumulation of abnormal histiocytes, and can involve multiple organs. LCH is more common in children than in adults, and adult-onset LCH is strongly associated with cigarette smoking. Pituitary involvement can cause central diabetes insipidus (CDI). In this report, we describe 2 patients with LCH who had a positive smoking history and presented initially with CDI-related polyuria and nocturia; their pulmonary disease was revealed only later by the typical radiographic features during the subsequent systematic workup. A concise and updated review of the relevant literature is also included. Through the report of these 2 cases, we aim to highlight the potentially systemic and progressively destructive nature of LCH, and the importance of monitoring for possible extra-pulmonary involvement, even in patients with prominent pulmonary LCH. ***(Thorac Med 2023; 38: 116-121)***

Key words: central diabetes insipidus, pulmonary Langerhans cell histiocytosis

## Introduction

Langerhans cell histiocytosis (LCH) is a rare disease that can involve single or multiple organs. The prognosis of systemic LCH is generally worse than that of isolated LCH. The etiology is related to the aberrant accumuation and function of histiocytes ("Langerhans cells") originating from the myeloid lineage [1, 2]. These Langerhans cells form granulomatous nodules with associated infiltration of inflammatory cells. Tissue destruction may follow in the later stage. The incidence rate of LCH in children under age 15 is around 4.6 cases per million, and it is even rarer in adults -- about 1 to 2 cases per million [1, 3, 4].

The exact incidence and prevalence of pulmonary LCH (PLCH) is unknown. PLCH occurs mostly in cigarette smokers of both sexes, with the age of onset between 20 and 40 years

[1]Department of Internal Medicine, [2]Department of Pathology, National Cheng Kung University Hospital, College of Medicine, National Cheng Kung University, Tainan, Taiwan
Address reprint requests to: Dr. Tang-Hsiu Huang, Division of Chest Medicine, Department of Internal Medicine, National Cheng Kung University Hospital, College of Medicine, National Cheng Kung University, No 138, Sheng-Li Road, Tainan 704, Taiwan

old [5]. Patients with PLCH may present with dyspnea, cough, constitutional symptoms (fever, body weight loss, and sweating), or spontaneous pneumothorax, while some patients may be asymptomatic [5, 6]. Typical chest computed tomography (CT) findings include reticulomicronodular lesions that are intermixed with many bizarre-shaped cysts; they exhibit an upper-to-middle-lobe predominance and spare the basal costophrenic regions [7]. The number of cysts may increase as the disease progresses. PLCH can be either isolated or part of a systemic manifestation. The co-presentation of PLCH and central diabetes incipidus (CDI) is quite uncommon. CDI also results from histiocytic infiltration of the pituitary and hypothalamus, leading to the destruction of vasopressin-producing magnocellular neurons in the paraventricular and supraoptic nuclei [8, 9, 10]. In this case report, we describe the clinical presentatons of 2 patients with PLCH whose major initial manifestation was CDI-related polyuria. Despite the initial inconspicuousness of the respiratory symptoms, pulmonary parenchymal destruction by the disease process was radiographically evident in both patients.

## Case Report

**Case 1:** A 47-year-old man presented initially to our general medicine outpatient clinic with polyuria and nocturia. He used to smoke 2 packs of cigarette per day, but quit 7 years ago. Water deprivation test confirmed the diagnosis of CDI, and magnetic resonance imaging (MRI) of the brain showed features suggesting hypothalamus-pituitary infiltrative disease (Figure 1). The CDI-related symptoms improved following intra-nasal desmopressin. He also suffered from chronic dry cough. Chest radiograph and CT scan revealed extensive mixed nodular and cystic lesions, predominantly in the bilateral upper lung fields (Figure 2). The nodules had ill-defined margins and a centrilobular distribution, whereas the cysts were variable in size and shape, with a confluence between adjacent cysts being frequently observed. Pulmonary

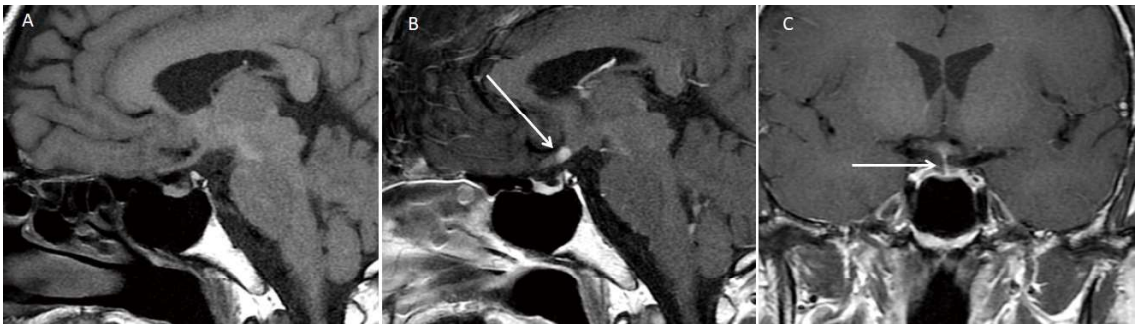


**Fig. 1.** (A) Sagittal T1-weighted image shows absence of a normal posterior pituitary bright spot. (B) Post-contrast sagittal T1-weighted image and (C) coronal image show nodular enhancement at the hypothalamus (arrow in B) and the infundibulum (arrow in C).

**Fig. 2.** CT scan reveals an extensive mixed nodular and cystic change that was most prominent in the bilateral upper lung fields.

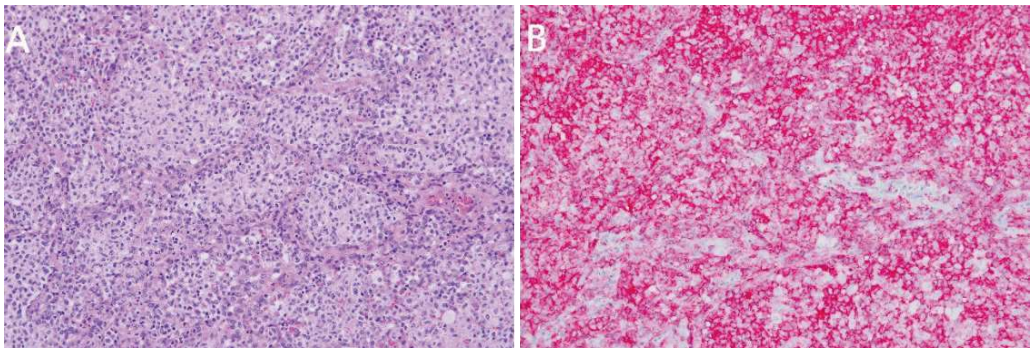


**Fig. 3.** Histology of the wedge-biopsied right upper lobe of the lung shows (A) numerous proliferative Langerhans cells that (B) stained immunohistochemically positive for CD1a.

screening spirometry was within normal ranges. Video-assisted thoracoscopic wedge biopsy of the lung was done, and histological examination of the specimen revealed numerous Langerhans cells infiltrating the alveolar interstitium, which stained immunohistochemically positive for CD1a and S-100 (Figure 3). Chemotherapy with vinblastine and methylprednisolone was administered, but the patient later died from hospital-acquired pneumonia with acute respiratory distress syndrome (ARDS).

**Case 2:** A 35-year-old man with a smoking habit (2 packs per day for 20 years) had developed polyuria, nocturia, and erectile dysfunction for several months. CDI was confirmed by water deprivation test, while further endocrine surveys revealed pan-hypopituitarism. MRI of the brain showed an absence of posterior pituitary hyperintensity on T1-weighted images and thickening of the pituitary stalk (Figure 4). His polyuria and nocturia improved after intranasal desmopressin. Chest CT showed multiple pulmonary nodules intermixed with cystic lesions, mainly in the upper lung regions, sparing the basal and peri-diaphragmatic zones (Figure 5A). The diagnosis of LCH was made based

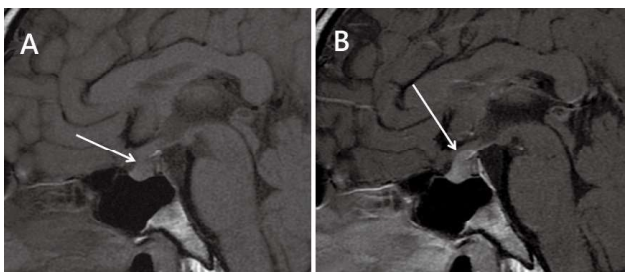


**Fig. 4.** (A) Sagittal T1-weighted MRI shows a thickened pituitary infundibulum (arrow) and absence of a posterior bright spot. (B) Post-contrast sagittal T1-weighted MRI shows enhancement of the pituitary infundibulum and hypothalamus (arrow), consistent with pituitary axis LCH.

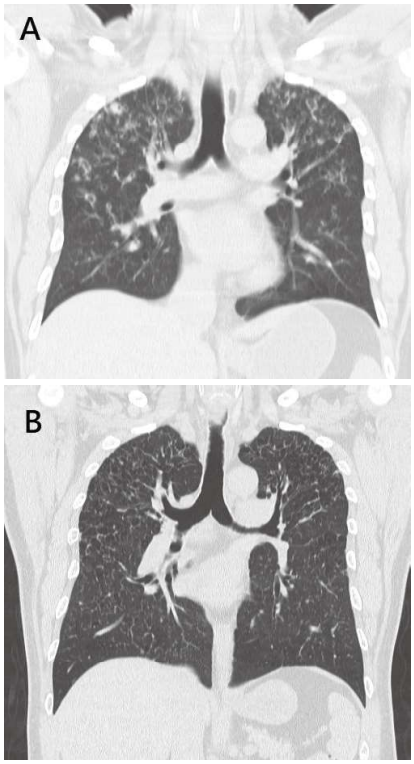


**Fig. 5.** (A) Baseline CT shows multiple nodular, mixed with cystic, lesions mainly in the upper lung regions. (B) Follow-up CT 6 years later shows decreased nodular lesions, but increased cystic changes.

on the radiographic findings and after a multidisciplinary discussion. Meanwhile, the patient has had minimal airway symptoms, and he has therefore declined any diagnostic or therapeutic intervention for his pulmonary condition. A follow-up CT scan 6 years later showed diminishment of the nodular lesions, but an increased extent of cystic changes (Figure 5B). Specifically, many nodular densities had been replaced by thin-walled and bizarre-shaped cysts of variable sizes, all still with an upper-lobe predominance. Serial pulmonary function tests reported mild impairment in the diffusion capacity of carbon monoxide and a trend toward an obstructive ventilatory deficit. The patient still receives regular follow-up at our hospital.

## Discussion

LCH results from dysregulated differentiation and recruitment of histiocytes that form granulomatous nodules in single or multiple organs. The histiocytes are characterized immunohistochemically by the expression of langerin (CD207), S100, and CD1a [11]. There have been controversies regarding whether LCH is a reactive and inflammatory process or a type of neoplasm. Although this issue is still not resolved, findings from recent genetic studies appear to support a clonal neoplastic nature. In many patients (both children and adults) with LCH, mutation of the genes participating in the mitogen-activated protein kinase (MAPK) pathway (which is associated with cellular differentiation, migration, and apoptosis) could be identified in the pathological histiocytes, particularly mutations of the BRAF gene [1, 5, 12, 13]. We did not check the lesion-site genetic profile of our 2 patients. Nevertheless, considering the very high frequency (>80%) of MAPK-associated mutations in systemic and pulmonary LCH, as was recently reported by Jouenne et al [13], it appears reasonable to suspect that such mutations might have also existed in the abnormal histiocytes of our patients. Besides, it has been reported that CDI occurs with increased frequency in patients with a BRAFV600E mutation [12].

In PLCH, numerous abnormal histiocytes accumulate in the small airways (particularly the respiratory bronchioles), as well as the interstitium. They may form granulomatous nodules accompanied by the infiltration of mixed chronic inflammatory cells. Destruction and remodeling of the surrounding tissue may follow as the disease progresses [5, 14, 15]. The pulmonary lesions are mainly bilateral and symmetrical, and predominate in the upper and middle lung fields, but spare the basal costophrenic regions. The corresponding radiographic findings on chest CT scan include a small nodular opacity, cavitation, or cysts, or a combination of such. Patients may be asymptomatic or may have mild respiratory symptoms. Both patients that we described in this report initially sought medical attention for CDI-related symptoms, and not due to respiratory complaints. While 1 patient exhibited only nonspecific chronic cough, the other had no respiratory symptom at all (despite the progressive parenchymal cystic and destructive changes as observed in his serial CT images). The variable and nonspecific manifestation of PLCH potentially makes the diagnosis challenging. The prognosis of PLCH can be quite variable and has not been well defined. Older age at diagnosis, pulmonary function impairment, ongoing cigarette smoking, and the presence of symptomatic pulmonary hypertension are potentially negative prognostic factors [3, 5, 6, 16, 17, 18].

CDI is a common neuro-endocrinological manifestation of LCH, occurring in up to 43% of patients with systemic LCH and in 7% of patients with PLCH, and can be irreversible [3, 9, 10, 16]. Patients typically present with polyuria and subsequent polydipsia, and a lack of response to water restriction during the water deprivation test. Typical brain MRI findings include loss of a bright spot in the posterior pituitary gland on T1-weighted images, infundibular enlargement, and hypothalamic involvement [19]. Desmopressin is the standard treatment for CDI. Both of our patients exhibited CDI-related symptoms, and they responded well to intra-nasal desmopressin. One patient (case 2) also needed other hormonal supplements on a regular basis to correct the panhypopituitarism. To the best of our knowledge, CDI or even panhypopituitarism as the initial and main presentation of PLCH has been very rarely described in the literature [9, 10, 20], and has not been reported from Taiwan.

Smoking cessation is of utmost importance in the management of PLCH [5,17]. Corticosteroid is frequently used as the first-line therapy, though there has been no consensus on either the dosing or the duration of treatment [5, 6]. For patients with obstructive ventilatory impairment, inhaled corticosteroid and long-acting β2-agonist may be considered [6, 17]. Systemic chemotherapy involving vinblastine and high-dose corticosteroid has been previously administered to treat LCH, particularly systemic LCH. However, recent evidence suggests that systemic chemotherapy might be ineffective in halting pulmonary function decline [21]. Our case 1 patient also received systemic chemotherapy, but he succumbed to infectious complications shortly thereafter. Myeloid-cytotoxic cladribine [5, 22, 23] and novel small-molecule agents specifically targeting mutations of the MAPK pathway [1, 5, 24, 25, 26, 27, 28, 29] are potentially promising future therapies, but further clinical evidence is needed to validate their safety and efficacy for PLCH. Moreover, LCH-related CDI is often refractory to treatment for LCH alone [20]. Long-term desmopressin administration is usually necessary.

In conclusion, the aberrant histiocytes in LCH may infiltrate multiple organs simultaneously, including the lungs and pituitary gland. In this case report, we highlight the variable and potentially multi-systemic nature of PLCH. Patients with PLCH need to be followed and checked for extra-pulmonary involvement, such as pituitary dysfunction, while patients with unexplained CDI must receive workups to exclude LCH and concurrent lung involvement. Considering the progressively destructive sequelae of PLCH, even in asymptomatic patients, careful monitoring is important for the timely detection of radiographic and functional deterioration.

## References

1. Allen CE, Merad M, McClain KL. Langerhans-cell histiocytosis. N Engl J Med 2018; 379(9): 856-868.
2. Brabencova E, Tazi A, Lorenzato M, *et al*. Langerhans cells in Langerhans cell granulomatosis are not actively proliferating cells. Am J Pathol 1998; 152: 1143-149.
3. Arico M, Girschikofsky M, Genereau T, *et al*. Langerhans cell histiocytosis in adults: report from the International Registry of the Histiocyte Society. Eur J Cancer 2003; 39: 2341-2348.
4. Guyot-Goubin A, Donadieu J, Barkaoui M, et al. Descriptive epidemiology of childhood Langerhans cell histiocytosis in France, 2000-2004. Pediatr Blood Cancer 2008;51:71-75
5. Vassallo R, Harari S, Tazi A. Current understanding and management of pulmonary Langerhans cell histiocytosis. Thorax 2017; 72(10): 937-945.
6. Lorillon G, Tazi A. How I manage pulmonary Langerhans

cell histiocytosis. Eur Respir Rev 20176; 26(145): 170070.

7. Bonelli FS, Hartman TE, Swensen SJ, *et al*. Accuracy of high-resolution CT in diagnosing lung diseases. Am J Roentgenol 1998; 170(6): 1507-12.
8. Maghnie M. Diabetes insipidus. Horm Res 2003; 59 Suppl 1: 42-54.
9. Brys ADH, Vermeersch S, Forsyth R, *et al*. Central diabetes insipidus: beware of Langerhans cell histiocytosis! Neth J Med 2018; 76(10): 445-449.
10. Lourenço J, Ferreira C, Marado D. Adult pulmonary Langerhans cell histiocytosis revealed by central diabetes insipidus: a case report and literature review. Mol Clin Oncol 2020; 13(4): 30.
11. Sholl LM, Hornick JL, Pinkus JL, *et al*. Immunohistochemical analysis of langerin in Langerhans cell histiocytosis and pulmonary inflammatory and infectious diseases. Am J Surg Pathol 2007; 31(6): 947-952.
12. Héritier S, Emile JF, Barkaoui MA, *et al*. BRAF mutation correlates with high-risk Langerhans cell histiocytosis and increased resistance to first-line therapy. J Clin Oncol 2016; 34(25): 3023-3030.
13. Jouenne F, Chevret S, Bugnet E, *et al*. Genetic landscape of adult Langerhans cell histiocytosis with lung involvement. Eur Respir J 2020; 55(2): 1901190.
14. Colby TV, Lombard C. Histiocytosis X in the lung. Hum Pathol 1983; 14:847-56.
15. Vassallo R, Ryu JH, Colby TV, *et al*. Pulmonary Langerhans'-cell histiocytosis. N Engl J Med 2000; 342(26): 1969-1978.
16. Vassallo R, Ryu JH, Schroeder DR, *et al*. Clinical outcomes of pulmonary Langerhans'-cell histiocytosis in adults. N Engl J Med 2002; 346: 484-90
17. Tazi A, de Margerie C, Naccache JM, *et al*. The natural history of adult pulmonary Langerhans cell histiocytosis: a prospective multicentre study. Orphanet J Rare Dis 2015; 10: 30.
18. Le Pavec J, Lorillon G, Jaïs X, *et al*. Pulmonary Langerhans cell histiocytosis-associated pulmonary hypertension: clinical characteristics and impact of pulmonary arterial hypertension therapies. Chest 2012; 142: 1150-7.
19. Grois N, Prayer D, Prosch H, *et al*. Course and clinical impact of magnetic resonance imaging findings in diabetes insipidus associated with Langerhans cell histiocytosis. Pediatr Blood Cancer 2004; 43: 59-65.
20. Mendoza ES, Lopez AA, Valdez VA, *et al*. Adult-onset Langerhans cell histiocytosis presenting with adipsic diabetes insipidus, diabetes mellitus and hypopituitarism: a case report and review of literature. J Clin Transl Endocrinol Case Rep 2015; 1: 1-5.
21. Tazi A, Lorillon G, Haroche J, *et al*. Vinblastine chemotherapy in adult patients with Langerhans cell histiocytosis: a multicenter retrospective study. Orphanet J Rare Dis 2017; 12: 95.
22. Lorillon G, Bergeron A, Detourmignies L, *et al*. Cladribine is effective against cystic pulmonary Langerhans cell histiocytosis. Am J Respir Crit Care Med 2012; 186(9): 930-932.
23. Grobost V, Khouatra C, Lazor R, *et al*. Effectiveness of cladribine therapy in patients with pulmonary Langerhans cell histiocytosis. Orphanet J Rare Dis 2014; 9: 191.
24. Hyman DM, Puzanov I, Subbiah V, *et al*. Vemurafenib in multiple nonmelanoma cancers with BRAF V600 mutations. N Engl J Med 2015; 373(8): 726-736.
25. Diamond EL, Subbiah V, Lockhart AC, *et al*. Vemurafenib for BRAF V600-mutant Erdheim-Chester disease and Langerhans cell histiocytosis: analysis of data from the histology-independent, phase 2, open-label VE-BASKET study. JAMA Oncol 2018; 4(3): 384-388.
26. Hazim AZ, Ruan GJ, Ravindran A, *et al*. Efficacy of BRAF-inhibitor therapy in BRAFV600E-mutated adult Langerhans cell histiocytosis. Oncologist 2020; 25(12): 1001-1004.
27. Papapanagiotou M, Griewank KG, Hillen U, *et al*. Trametinib-induced remission of an MEK1-mutated Langerhans cell histiocytosis. JCO Precis Oncol 2017; 1: 1-5.
28. Lorillon G, Jouenne F, Baroudjian B, *et al*. Response to trametinib of a pulmonary Langerhans cell histiocytosis harboring a MAP2K1 deletion. Am J Respir Crit Care Med 2018; 198(5): 675-678.
29. Messinger YH, Bostrom BC, Olson DR, *et al*. Langerhans cell histiocytosis with BRAF p.N486_P490del or MAP2K1 p.K57_G61del treated by the MEK inhibitor trametinib. Pediatr Blood Cancer 2020; 67(12): e28712.

# Rare Cause of Pleural Effusion, Intestinal-type Mucinous Borderline Ovarian Tumor with Pseudo-Meigs' Syndrome: A Case Report

Chuan-Chuan Wang[1], Jia-Hao Zhang[1]

Meigs' syndrome is characterized by pleural effusion and ascites associated with benign ovarian solid tumors such as fibroma, Brenner tumor, or granulosa cell tumor. However, pseudo-Meigs' syndrome is composed of ascites, pleural effusion, and ovarian tumors other than that described by Meigs. The incidence of pseudo-Meigs' syndrome is lower than that of Meigs' syndrome. We reported a 54-year-old woman who had progressive dyspnea and abdominal distension for 6 months. Image study revealed ascites, massive right side pleural effusion, and a huge multicystic ovarian mass (26 x 25 x 14cm in size). The patient had elevated carbohydrate antigen (CA)-125 (189.6 U/mL). The final pathologic report revealed an intestinal-type mucinous borderline ovarian tumor. Removal of the ovarian mass led to resolution of the pleural effusion and ascites. Mucinous borderline ovarian tumor rarely lead to pleural effusion, and pseudo-Meigs' syndrome is a rare differential diagnosis in an exudative pleural effusion. ***(Thorac Med 2023; 38: 122-125)***

Key words: pseudo-Meigs' syndrome, intestinal-type mucinous borderline ovarian tumor

## Introduction

Pleural effusion is a common cause of shortness of breath in patients. The etiologies of pleural effusion can be divided into 2 categories: exudative and transudative. The most common cause of transudative pleural effusion is congestive heart failure; exudative pleural effusion is usually caused by pneumonia, malignancy, or pulmonary embolism. A rare etiology of pleural effusion is Meigs' syndrome and pseudo-Meigs' syndrome. Meigs' syndrome was defined by Meigs and Cass in 1937 as the hydrothorax and ascites that resolved after removal of a coexisting benign ovarian fibroma [1]. Pseudo-Meigs' syndrome is similar to Meigs' syndrome except the tumor is not a benign ovarian fibroma, but may be a malignant tumor or emanate from the ovary, uterus, or colon [2-3]. We report a rare case of intestinal-

[1]Division of Pulmonary Medicine, Department of Internal Medicine, Far Eastern Memorial Hospital
Address reprint requests to: Dr. Chuan-Chuan Wang, Division of Pulmonary Medicine, Department of Internal Medicine, Far Eastern Memorial Hospital, No.21, Sec. 2, Nanya S. Rd., Banciao Dist., New Taipei City 220, Taiwan (R.O.C.)

type mucinous borderline ovarian tumor with pseudo-Meigs' syndrome.

## Case Report

A 54-year-old woman had a history of type II diabetes mellitus and uterine myoma status post abdominal total hysterectomy 7 years before this admission. She experienced a progressively enlarged lower abdomen for half a year, but did not pay attention to it. Owing to progressive dyspnea, she visited our emergency department. Chest X-ray showed massive right pleural effusion (Fig. 1). A pigtail was inserted and the effusion was found to be characteristically exudative (total protein 7.4 g/dL; lactate dehydrogenase (LDH) 135 IU/L; glucose 109 mg/dL, compared with blood total protein 7.5 g/dL; LDH 191 IU/L). Cytology showed the pleural effusion was negative for malignant cells. Abdominal sonography revealed multiple anechoic cystic lesions occupying the whole abdomen and pelvis (Fig. 2). The abdominal computed tomography scan showed a large ovarian tumor (27.3 x 25.6 x 14.5 cm) with a multicystic mass and ascites (Fig. 3). Elevated serum CA-125 (189.6 U/mL) was also detected. Exploratory laparotomy was performed and a huge cystic tumor with mucinous content was seen. Bilateral salpingo-oophorectomy and tumor resection were performed. The final patho-

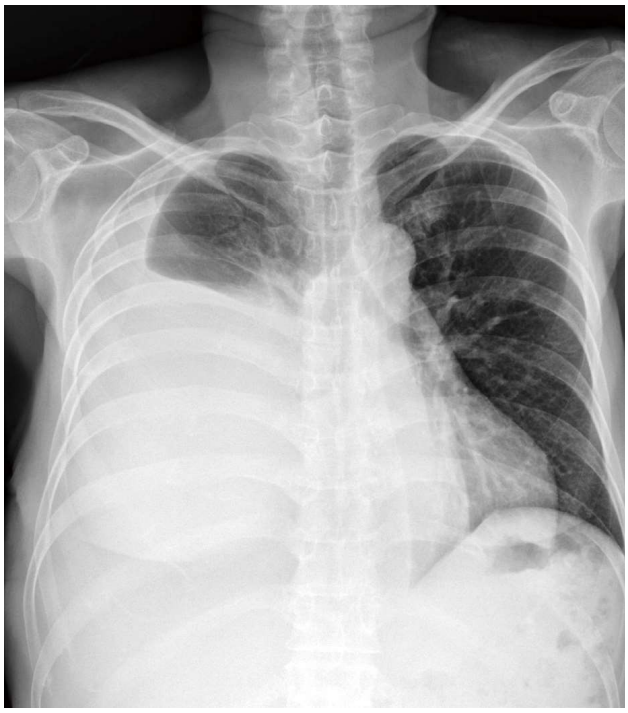

**Fig. 1.** Chest AP view revealed right massive pleural effusion.

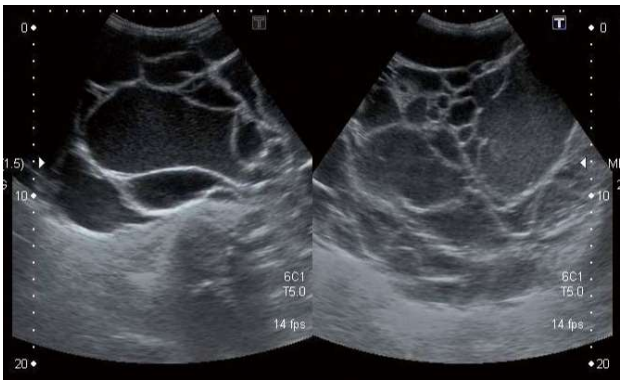

**Fig. 2.** Abdominal sonography showed multiple anechoic cystic lesions.

**Fig. 3.** Computed tomography scan revealed a large ovarian tumor (27.3 x25.6 x14.5 cm) with a multicystic mass and ascites.

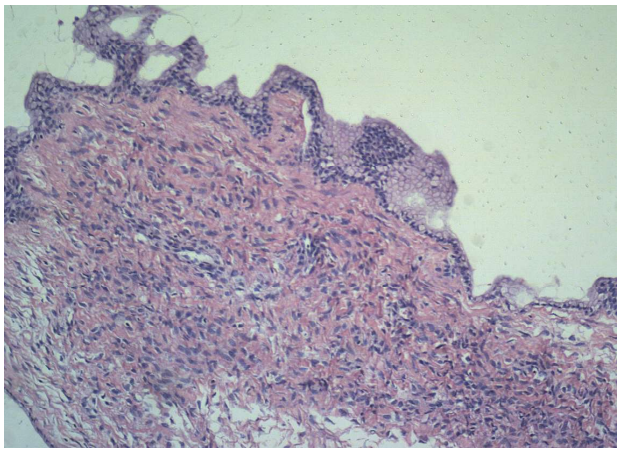

**Fig. 4.** Pathologic examination revealed epithelial cells with nuclear stratification and with forming papillae and mucinous deprivation; no inflammatory cells were detected in the stroma. (H&E stain, 100X)

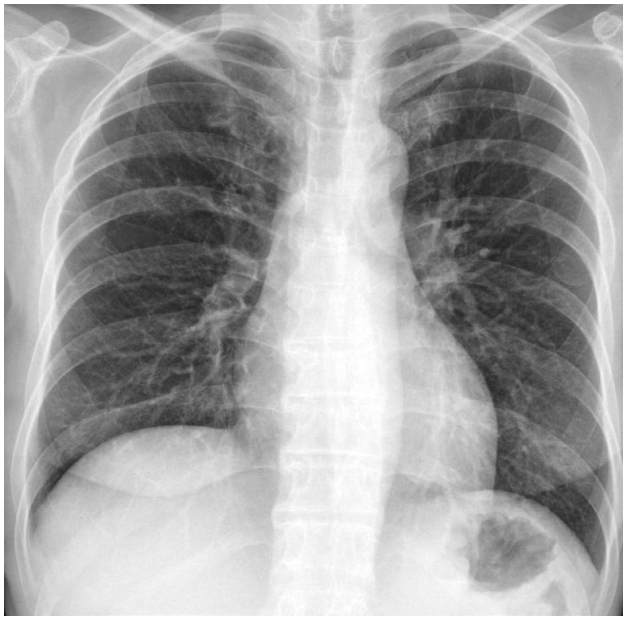

**Fig. 5.** Six months after surgical intervention, there was no recurrence of right pleural effusion.

logic report confirmed that this mass lesion was an intestinal-type mucinous borderline ovarian tumor (Fig. 4). After the operation, the patient's pleural effusion and ascites were resolved. Chest X-ray revealed no pleural effusion half year later (Fig. 5).

## Discussion

Meigs' syndrome is defined as the hydrothorax and ascites that resolves after removal of a coexisting benign ovarian fibroma. Pseudo-Meigs' syndrome occurs when the coexisting ovarian fibroma is not benign. The pleural effusion is a minority part of both syndromes. According to current knowledge, the pleural effusion is right-side predominant, but bilateral and left side effusion has also been reported [4,5]. The definite mechanism of the pleural effusion and ascites in Meigs' and pseudo-Meigs' syndrome is still unknown, and this may be due to most studies stopping at the negative result for malignant cells in the pleural fluid cell block exam.

Conventional concepts including lymphatic obstruction resulting in increased permeability of pelvic lymphatics and transdiaphragmatic shifting of ascites have been hypothesized [1,5]. However ovarian hyperstimulation by the hypersecretion of vascular endothelial growth factor (VEGF) due to abnormal VEGF that was normalized after resection of an intraabdominal tumor was observed recently, and the specimen showed positive immunostaining for VEGF [6]. There are many kinds of ovarian tumors associated with pseudo-Meigs' syndrome. However, the more relevant factor in the formation of ascites and pleural effusion may be tumor size, especially a diameter of more than 6 cm, rather than histologic type [7], but only 2 case reports of pseudo-Meigs' syndrome were associated with intestinal-type mucinous borderline ovarian tumors [8,9]. In these 2 cases, the tumor size was more than 10 cm; the ascites and pleural effusion were both improved after surgical removal of the ovarian tumor.

The mucinous borderline ovarian tumor

has low malignant potential, and long-term survival rates were 98% at 5 years and 96% at 10 years [10]. In a recent study of pure borderline tumors, all were stage I and none metastasized [11]. Surgical intervention is a very important part of the complete remission of this kind of disease, the ascites, and the pleural effusion.

In conclusion, pseudo-Meigs' syndrome is a rare differential diagnosis for the coexistence of pleural effusion and ascites. The internist should keep in mind that a patient presenting with pleural effusion, ascites, and an intra-abdominal tumor may be successfully treated by removal of the intra-abdominal tumor.

## References


1. Meigs JV. Fibroma of the ovary with ascites and hydrothorax; Meigs' syndrome. Am J Obstet Gynecol 1954; 67: 962-985.
2. Loizzi V, Cormio G, Resta L, *et al*. Pseudo-Meigs syndrome and elevated CA125 associated with struma ovarii. Gynecol Oncol 2005; 97(1): 282-284.
3. Cetin B, Aslan S, Akinci M *et al*. A long surviving case of pseudo-Meigs' syndrome caused by Krukenberg tumor of the stomach. Jap J Clin Oncol 2005; 35(4): 221-223.
4. Terada S, Suzuki N, Uchide K *et al*. Uterine leiomyoma associated with ascites and hydrothorax. Gynecol Obstet Invest 1992; 33(1): 54-58.
5. Nagakura S, Shirai Y, Hatakeyama K. Pseudo-Meigs' syndrome caused by secondary ovarian tumors from gastrointestinal cancer. A case report and review of the literature. Dig Surg 2000; 17(4): 418-419.
6. Okuchi Y, Nagayama S, Mori Y, *et al*. VEGF hypersecretion as a plausible mechanism for pseudo-Meigs' syndrome in advanced colorectal cancer. Jpn J Clin Oncol. 2010;40(5): 476-481.
7. Papanikolaou C, Fortounis K, Ainalis S, *et al*. Pseudo-Meigs'syndrome: a case report. Internet J Patho. 2004; v. 4, No. 2.
8. Wiatrowska B, Krajci P, Berner A. Pseudo-Meigs' syndrome. Tidsskr Nor Laegeforen 2000; 120: 364-366.
9. Chen YY, Hsiao SM, Hsu YP, *et al*. Borderline mucinous ovarian tumor presenting as pseudo-Meigs' syndrome. J Obstet Gynaecol Res 2013 ;39(1): 434-6.
10. Hart WR, Norris HJ. Borderline and malignant mucinous tumors of the ovary. Histologic criteria and clinical behavior. Cancer 1973; 31: 1031-1045.
11. Rodriguez IM, Prat J. Mucinous tumors of the ovary: a clinicopathologic analysis of 75 borderline tumors (of intestinal type) and carcinomas. Am J Surg Pathol 2002;26: 139-152.

# An Excavated Pulmonary Lesion in an Immunocompetent Young Man

Chun-Yen Chen[1], Kuang-Tai Kuo[1,2], Wei-Hwa Lee[3], Wei-Ciao Wu[1]

We reported the case of a 32-year-old male non-smoking white-collar worker who visited our hospital due to an abnormal chest radiograph found during a health check-up. He had no known disease and also denied a recent history of travel. Chest radiograph revealed an excavated lesion in the right upper lung field. Chest high-resolution computed tomography without contrast further confirmed the excavated lesion located at the superior segment of the right lower lobe, and also disclosed some small nodules, which were all less than 1 cm and scattered around the excavated lesion. Wedge resection of right lower lobe was done, and the pathological picture revealed cryptococcosis. Furthermore, tissue culture for fungus documented the presence of *Cryptococcus neoformans*. The patient was treated successfully with oral fluconazole. ***(Thorac Med 2023; 38: 132-135)***

Key words: Cryptococcus neoformans, Immunocompetent, Excavate

## Introduction

Cryptococcosis is a fungal infection that usually occurs in immunocompromised patients, and sometimes in immunocompetent individuals. Cavitation in cryptococcocal lesions is more commonly seen in immunocompromised patients, and usually represents an aggressive course. The radiologic presentation of our patient was unique, because only a ring-like lesion was seen on the initial chest radiograph. Further diagnostic tools, including bronchoscopic brushing or CT/sono-guided biopsy, are usually needed; our patient agreed to undergo video-assisted thoracic surgery for tissue diagnosis. Although there are no established criteria for the treatment of immunocompetent patients diagnosed with cryptococcosis, our patient was treated successfully with oral fluconazole.

## Case Report

A 32-year-old male non-smoking white-collar worker visited our hospital due to an

[1]Division of Thoracic Surgery, Department of Surgery, Shuang Ho Hospital, Taipei Medical University, Taipei, Taiwan, [2]Division of Thoracic Surgery, Department of Surgery, School of Medicine, College of Medicine, Taipei Medical University, Taipei, Taiwan, [3]Department of Pathology, Shuang Ho Hospital, Taipei Medical University, Taipei, Taiwan.
Address reprint requests to: Dr. Wei-Ciao Wu, Division of Thoracic Surgery, Department of Surgery, Shuang Ho Hospital, Taipei Medical University, No.291, Zhongzheng Rd., Zhonghe District, New Taipei City 23561, Taiwan

abnormal chest radiograph found during health check-up. He had no known disease prior to this visit, and denied any respiratory symptoms in the past 6 months. He also denied a recent history of travel. Chest radiograph revealed an excavated lesion in the right upper lung field (Figure 1A). Chest high-resolution computed tomography (HRCT) without contrast further confirmed the excavated lesion located at the superior segment of the right lower lobe (RLL), and also disclosed some nodules, all less than 1 cm in size, scattered around the excavated lesion as well as other parts of the RLL (Figure 1B). Acid-fast stain of the sputum yielded negative results, and blood examination, including a serologic test for cryptococcal antigen, were all unremarkable. The patient declined bronchoscopy for personal reasons, but agreed to video-assisted thoracic surgery (VATS) exploration for tissue diagnosis.

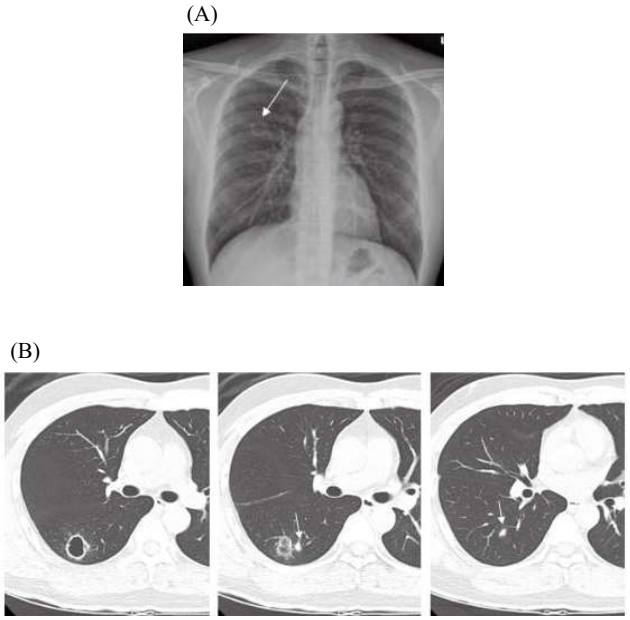


**Fig. 1.** (A) Chest radiograph showed a ring-like lesion at the right upper lung field (arrow). (B) Computed tomography scans showed the location of the ring-like lesion (left panel), the surrounding nodule (arrow, middle panel), and 1 of the other small nodules at the right lower lobe (arrow, right panel).

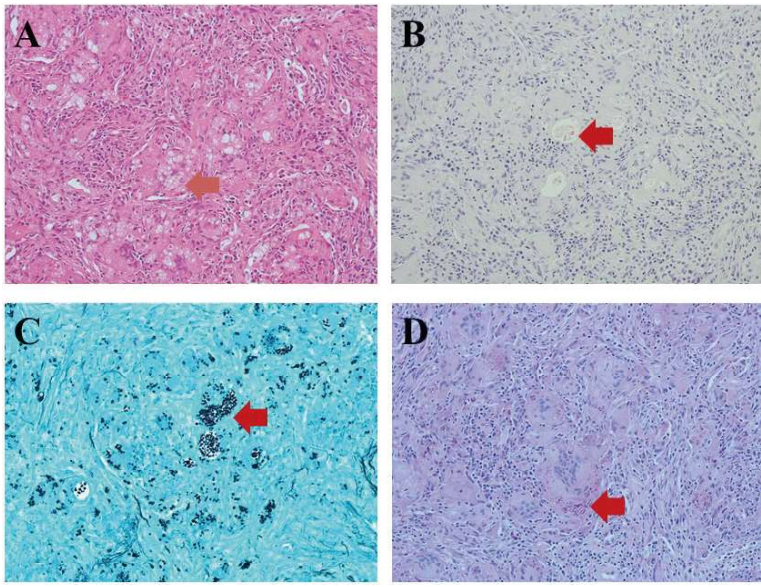


**Fig. 2.** Pathology photos of the resected specimen. Red arrows indicate fungal spores. Hematoxylin and eosin stain (A), periodic-acid Schiff (PAS) stain (B), Grocott's methenamine silver (GMS) stain (C), and mucicarmine stain (D) are shown. Original magnification, × 200

Wedge resection of the RLL was performed, and a thin-walled cavitating nodule, 2.1 cm in diameter, plus a surrounding nodule, 0.8 cm in diameter, were identified in the resected specimen. Necrotizing granulomatous inflammation was revealed microscopically in the lung lesion. Many yeasts with capsules highlighted by periodic-acid Schiff (PAS) stain, Grocott's methenamine silver (GMS) stain and mucicarmine stain were found in the histiocytes, the multinucleated giant cells and the necrotic tissues (Figure 2). The whole pathological picture was that of cryptococcosis. Furthermore, tissue culture for fungus documented *Cryptococcus neoformans*. The postoperative course was uneventful and the patient was discharged on the third postoperative day. After the diagnosis, oral fluconazole 400 mg per day was administered for 3 months. Four months after the diagnosis of cryptococcosis, follow-up chest CT showed resolution of all small nodules in the residual RLL (Figure 3).

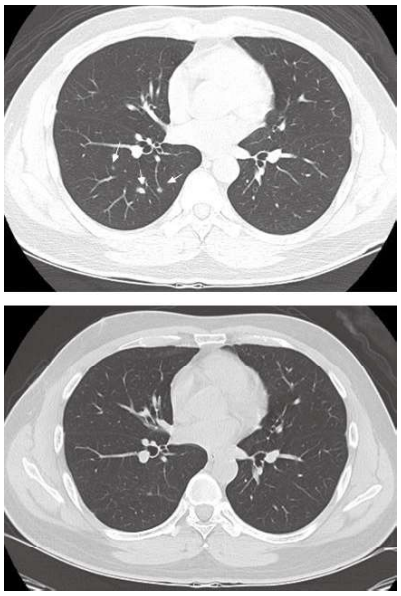

**Fig. 3.** After treatment with oral fluconazole for 3 months, the follow-up computed tomography scan revealed a disappearance of the small nodules (lower panel), as compared with the scan before treatment (upper panel, arrows).

## Discussion

Cryptococcosis is a fungal infection that usually occurs in immunocompromised patients, but can also be seen in immunocompetent individuals at times. Cavitation in cryptococcocal lesions is more commonly seen in immunocompromised patients, as it usually represents an aggressive course [1]. However, the rate of occurrence of cavitation in immunocompetent hosts has been reported to be up to 40% [2]. The radiologic presentation of our patient was unique, because only a ring-like lesion was seen on the initial chest radiograph. Although it has been suggested that thin-walled cavitating nodules usually indicate benign lesions [3], it is difficult to make an accurate diagnosis based on this single finding. Further diagnostic tools, including bronchoscopic brushing or CT/sono-guided biopsy, are usually needed, with the latter method once reported to have had a higher diagnostic yield [4].

We considered that CT/sono-guided biopsy was not suitable for this patient because of the limited solid components of the lesions. Since the patient declined bronchoscopy for personal reasons, surgical diagnosis became a feasible option. Meanwhile, we also learned that a serologic test was not absolutely determinative, and this was not uncommon in clinical practice. For this patient, we used the latex agglutination (LA) method for the serologic test. LA has been reported to have an overall sensitivity and specificity of 93-100% and 93-98%, respectively [5]. Newer tools, such as a lateral flow assay (LFA), have been reported to have higher sensitivity and specificity than LA [6]; however, this assay is not yet widely available.

As for the necessity of treatment for immunocompetent patients diagnosed with cryptococcosis, there are no established criteria. However, oral fluconazole has been recommended for infected patients, because even in immunocompetent patients, dissemination still occurs occasionally [7]. With regard to the optimal treatment duration, there is still no consensus -- reported treatment periods have ranged from 6 weeks to 12 months [7-9]. Our patient was found to have multiple nodules upon presentation, and therefore was considered infected rather than colonized, making active treatment mandatory. Subsequent CT scans showed the disappearance of all nodules, indicating the justification of our management.

In conclusion, even in immunocompetent patients without risk factors, cryptococcosis should still be taken into account, and can present as an excavated pulmonary lesion. Negative results on the serologic test can't totally exclude cryptococcal infection, and surgical diagnosis may be needed if percutaneous biopsy is difficult.

## References


1. Chang WC, Tzao C, Hsu HH, *et al*. Pulmonary cryptococcosis: comparison of clinical and radiographic characteristics in immunocompetent and immunocompromised patients. Chest 2006; 129: 333-40.
2. Fox DL, Müller NL. Pulmonary cryptococcosis in immunocompetent patients: CT findings in 12 patients. AJR 2005; 185: 622-6.
3. Erasmus JJ, Connolly JE, McAdams HP, *et al*. Solitary pulmonary nodules: Part I. Morphologic evaluation for differentiation of benign and malignant lesions. Radiographics 2000; 20: 43-58.
4. Lee LN, Yang PC, Kuo SH, *et al*. Diagnosis of pulmonary cryptococcosis by ultrasound-guided percutaneous aspiration. Thorax 1993; 48: 75-8.
5. Perfect JR, Bicanic T. Cryptococcosis diagnosis and treatment: What do we know now. Fungal Genet Biol 2015; 78: 49-54.
6. Prattes J, Heldt S, Eigl S, *et al*. Point of care testing for the diagnosis of fungal infections: are we there yet? Curr Fungal Infect Rep 2016; 10: 43-50.
7. Limper AH, Knox KS, Sarosi GA, *et al*. An official American Thoracic Society statement: Treatment of fungal infections in adult pulmonary and critical care patients. Am J Respir Crit Care Med 2011; 183: 96-128.
8. Núñez M, Peacock JE Jr, Chin R Jr. Pulmonary cryptococcosis in the immunocompetent host. Therapy with oral fluconazole: a report of four cases and a review of the literature. Chest 2000; 118: 527-34.
9. La Hoz RM, Pappas PG. Cryptococcal infections: changing epidemiology and implications for therapy. Drugs 2013; 73: 495-504.

# Good's Syndrome With Opportunistic Infection – A Case Report and Literature Review

Chung Lee[1], Wen-Lin Su[1,2], Yao-Kuang Wu[1,2], Mei-Chen Yang[1,2], Lun-Yu Jao[1]
Chou-Chin Lan[1,2*], Yi-Chih Huang[1,2*]

Good's syndrome (GS) is a rare condition in which thymoma is associated with hypogammaglobulinemia. It is characterized by autoimmunity and increased susceptibility to bacterial, viral, and fungal infections. Here, we presented the case of a patient with thymoma after thymectomy and hypogammaglobulinemia, diagnosed as GS. A 56-year-old Taiwanese woman had undergone thymectomy approximately 17 years previous to this admission. She also underwent retinal detachment surgery due to retinal cytomegalovirus (CMV) infection 7 years before this admission. In the years after her thymectomy, she developed Pneumocystis jirovecii pneumonia and CMV pneumonitis. The serum immunoglobulin levels were significantly low (IgG, 154 mg/dL; IgA, 24 mg/dL; IgM, < 20 mg/dL), suggesting that these infectious diseases were associated with GS. The patient received regular human immunoglobulin treatment without fatal infection. Increased awareness regarding the clinical and immunological profile of this syndrome may lead to early recognition and prevent mortality. ***(Thorac Med 2023; 38: 126-131)***

Key words: Good's syndrome, thymoma, cytomegalovirus infection

## Introduction

Good's syndrome (GS) is a rare association of thymoma and immunodeficiency that was first described more than 50 years ago. Patients are most commonly between the ages of 40 and 70 years and have a thymoma, low to absent B cells in the peripheral blood, hypogammaglobulinemia, and defects in cell-mediated immunity. Patients often present with recurrent infections due to encapsulated bacteria, fungi, and viruses. Herein, we describe a patient with GS and a presentation of unusual infections, and review the literature.

## Case Report

A 56-year-old Taiwanese woman with a history of thymoma underwent thymectomy approximately 17 years prior to this admission,

[1]Division of Pulmonary Medicine, Taipei Tzu Chi Hospital, Buddhist Tzu Chi Medical Foundation, New Taipei City, Taiwan, [2]School of Medicine, Tzu-Chi University, Hualien, Taiwan, *These authors contributed equally to this work.
Address reprint requests to: Dr. Yi-Chih Huang, Division of Pulmonary Medicine, Taipei Tzu Chi Hospital, Buddhist Tzu Chi Medical Foundation, 289, Jianguo Road, Xindian City, New Taipei City 23142, Taiwan, Republic of China

and retinal detachment surgery due to cytomegalovirus (CMV) infection approximately 7 years before this admission. She was a non-smoker and a non-drinker.

The patient was admitted to our hospital with a 10-day history of productive cough and a 5-day history of dyspnea and fever. She denied experiencing an altered mental status, hemoptysis, gastrointestinal symptoms, skin lesions, or constitutional symptoms, such as night sweats and loss of appetite. Chest X-ray (CXR) (Figure 1A) revealed extensive mixed consolidation and ground-glass opacity (GGO) in the bilateral lower lungs. The patient received empirical parenteral antibiotics with intravenous cefoperazone/sulbactam (4 mg Q8H). However, spiking fever and dyspnea persisted after 3 days of the intravenous antibiotics. Follow-up chest X-ray (Figure 1B) revealed mixed consolidation and GGO during progression. Owing to the progression of her pneumonia, we further investigated other pathogens associated with pneumonia. COVID-19 RT polymerase chain reaction (PCR) results were negative, her serum CMV PCR result was 13000 IU/ml, and she was seronegative for IgM CMV. The sputum Pneumocystis jir-

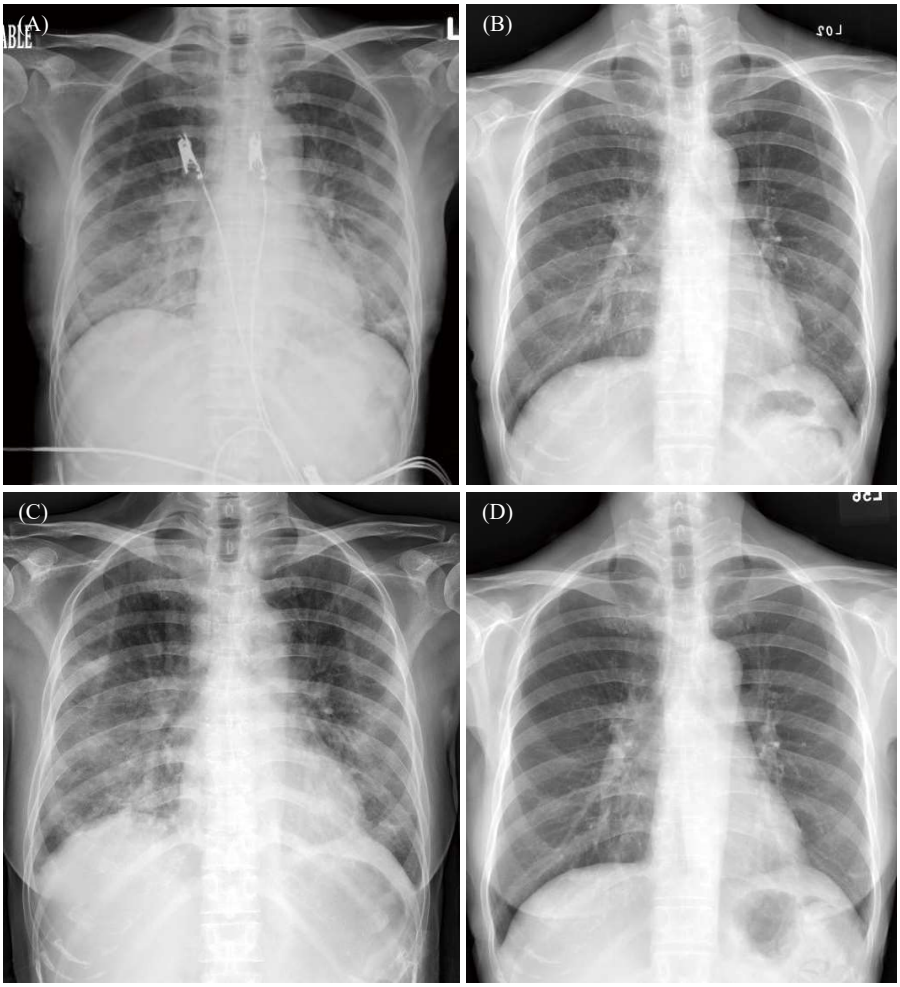


**Fig. 1.** (A). Extensive, mixed consolidation and ground glass opacity in bilateral lungs. (B). Progressive mixed consolidation and ground glass opacity in bilateral lungs. (C). Hazy areas indicate increased ground glass opacity in bilateral lungs, lower lung zones-predominant. (D).Mildly increased lung markings without specific ground glass opacity or pneumonia patch.

ovecii DNA PCR results were positive. She was seronegative for hepatitis B/C and human immunodeficiency virus. Sputum acid-fast smears and bacterial and fungal cultures were negative. Autoimmune screening, including antinuclear antibody, C3, C4, anti-SSA/SSB antibody, anti-Scl-70 antibody, anti-Jo-1 antibody, anti-Smith antibody, antinuclear ribonucleoprotein antibody, anti-double-stranded DNA antibody, and anti-neutrophil cytoplasmic antibodies yielded negative results. Computed tomography (CT) of the thorax revealed the presence of GGO with superimposed interlobular septal thickening and intralobular septal thickening, without evidence of thymoma recurrence (Fig 2).

Due to opportunistic CMV and Pneumocystis jirovecii pneumonia (PJP) infections, an immunodeficiency workup, including flow cytometric lymphocyte subset enumeration and quantitation of immunoglobulin, was performed. She was found to have a complete absence of B cells and evidence of hypogammaglobulinemia (IgG 154 mg/dL, IgA 24 mg/dL, and IgM < 20 mg/dL) (Table 1). Based on her thymoma resection, the hypogammaglobulinemia, and opportunistic infections, she was diagnosed with GS, complicated with CMV and PJP pneumonitis.

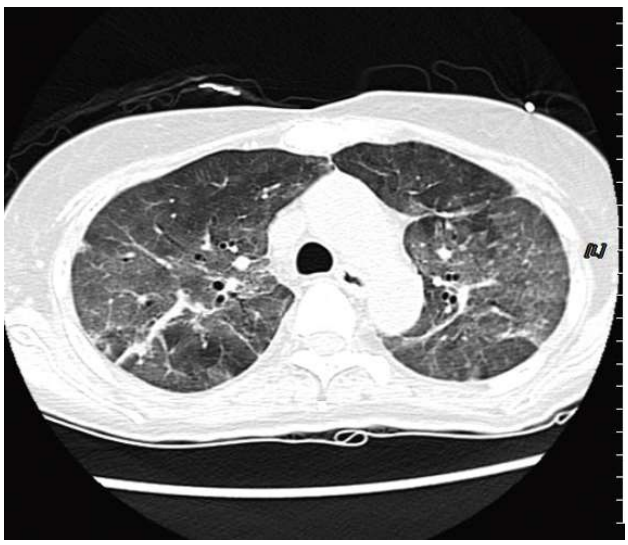

**Fig. 2.** Diffuse interstitial change in both lungs with peripheral lung predominance.

Intravenous immunoglobulin (IVIG) replacement therapy was initiated monthly. A 2-week antiviral treatment with intravenous ganciclovir (200 mg twice daily) and a 3-week antibiotic treatment with oral sulfamethoxazole 400 mg/trimethoprim 80 mg (2tab Q6H) was administered for the CMV and PJP infections. Her IgG levels tripled after the second course of IVIG therapy (154–494 mg/dL). After 2 weeks of treatment, CXR (Fig. 1C) showed a noticeable improvement in bilateral lung infiltrates. Monthly IVIG was subsequently administered, and no further episodes of infection were observed after the second course of IVIG treatment. After 1 month, CXR (Fig. 1D) showed almost complete resolution of the bilateral infiltrates.

## Discussion

GS is a rare immunodeficiency condition that develops in patients with thymoma, and is most common in those aged between 40 and 70 years. The association between thymoma and adult-onset hypogammaglobulinemia was first described by Dr. Good in 1955 [1]. It was initially regarded as a subset of the common variable immunodeficiency disorders (CVIDs) that accompany thymomas. In 1999, it was classified as a distinct primary immunodeficiency disorder, separate from CVIDs, by the expert committee of the World Health Organization/International Union of Immunological Societies [1]. The disease is characterized by low or absent B cells in the peripheral blood, hypogammaglobulinemia, defects in cell-mediated

**Table 1.** Laboratory Profiles of the Patient

| | Patient's data | Normal range |
|---|---|---|
| IgG | 154 mg/dL | 635-1741 mg/dL |
| IgA | 20 mg/dL | 66-433 mg/dL |
| IgM | <20 mg/dL | 45-281 mg/dL |
| WBC | 7.60*1000 | 3.8-9.8*1000 |
| Lymphocytes | 43.8% | 25-40% |
| Lymphocyte count | 3330/uL | |
| CD3+/CD4+ Helper T | 66.6% | 27-51.0% |
| CD3+/CD4+ Helper TC | 2218/uL | 404-1612/uL |
| CD3+/CD8+ Suppre. T | 32.4% | 15-44.0% |
| CD3+/CD8+ Suppre. TC | 1079/uL | 220-1129/uL |
| CD4/CD8 ratio | 2.1 | |
| T cells (CD3) | 97.7% | |
| B cells (CD19) | 0% | |

immunity with CD4+ T lymphopenia, and an inverted CD4:CD8+ T cell ratio. Hypogammaglobulinemia develops in 3–6% of patients with thymoma [2]. A reduced mature B cell count or even the absence of B cells from the peripheral blood was noted in 87% of cases [3].

Thymoma is characterized by an association with humoral and cellular immunodeficiency, and patients with thymoma are thus susceptible to opportunistic infections. Recurrent infections mainly involve the upper or lower respiratory tract, as seen in CVIDs. Haemophilus influenzae and Streptococcus pneumoniae are the most commonly identified pathogens, while Pseudomonas spp, Klebsiella spp, and other Gram-negative organisms have also been isolated from patients with bronchiectasis [4]. CMV and Candida spp are the most common opportunistic pathogens reported [3]. Recent reports have suggested that viral infections may play a role in the etiological mechanisms of thymoma development associated with dysregulated immunity [5]. Approximately 40% of patients with GS have viral infections, with the most common being CMV (24%) [6]. Defects in cell-mediated immunity in GS predispose patients to the opportunistic infections (fungal and viral) observed in acquired immune deficiency syndrome.

In this case, GS was diagnosed 17 years after thymectomy. A systematic review of 152 cases of GS in the literature revealed that the diagnosis of thymoma preceded the diagnosis of hypogammaglobulinemia, infection, or diarrhea in 42.4% of patients, with an interval of 3 months to 18 years [3]. This finding suggests that hypogammaglobulinemia is difficult to recognize during the clinical course of thymoma; GS is thus under-recognized in patients with thymoma [3]. Few studies have been conducted

on patients with thymoma excision, visual loss, and GS. The aqueous humor and vitreous fluid samples from 2 patients with thymoma were positive for CMV DNA by PCR analysis, which is clinically consistent with CMV retinitis [5]. As in our case, CMV retinitis developed 10 years after thymoma excision, and 7 years earlier than GS with CMV pneumonitis. Early detection of the autoimmune status may be necessary in this group of patients.

Data on abnormalities in T cell counts and function are limited, although CD4+ T cell lymphopenia and an abnormal CD4+:CD8+ T cell ratio are seen in a large number of patients. In the present case, the patient's CD4:CD8 ratio was normal (Table 1). Most patients have impaired T cell responses to mitogens such as phytohemagglutinin (PHA) [4]; however, analysis of cellular immunity in GS has revealed that opportunistic infections, such as CMV, can occur in the presence of significantly greater T cell numbers. CMV infection has been documented in the presence of normal CD4+ T cell counts and normal T cell proliferative responses to PHA stimulation. [4]

The use of intravenous immunoglobulins has been reported to improve outcome by improving infection control, reduce hospitalization, and decrease antibiotic use [7]. A previous review reported that approximately 38% of patients with GS had a reduced incidence of infections after treatment with gamma globulin [3]. Accordingly, IVIG is recommended to maintain appropriate immunoglobulin G levels in all patients.

The prognosis of GS is worse than that of other primary immunodeficiencies, with a global mortality rate of 46%, which is mainly dependent on the severity of infection [3]. One study reported that 33% of patients with GS were alive 10 years after diagnosis; in contrast, 95% of patients with common variable types of immunodeficiency were alive 10 years after diagnosis [8]. Astute clinical acumen and increased awareness of the clinical and immunological profile of this syndrome may increase its early recognition and prevent mortality.

Patients with GS and thymoma may also have other associated autoimmune manifestations -- most prominently, pure red cell aplasia and myasthenia gravis [3]. Therefore, physicians should consider such conditions when clinical suspicion arises. We hope this case report encourages physicians to consider immunodeficiency in patients with thymoma by measuring serum immunoglobulin levels. Early screening of patients for immunodeficiency may lead to their identification as candidates for IVIG, which could prevent morbidity and mortality from infection. Moreover, IgG antibodies against CMV should be determined to evaluate whether a patient is at risk of reactivation. Patients with GS who are CMV antibody-negative or whose CMV serology is unknown or cannot be determined should receive CMV-negative blood to avoid the potential risk of iatrogenic disease.

## Conclusions

GS is associated with a high mortality rate. Thymectomy has favorable effects on other parathyroid syndromes, but is ineffective at improving immunological deficiencies in this syndrome. Immunoglobulin replacement has been reported to decrease infections, hospitalizations, and antibiotic use in these patients. Clinical outcomes depend on the severity of infections and associated hematologic and autoimmune diseases rather than thymoma itself. When phy-

sicians encounter patients with multiple opportunistic infections who have a medical history of thymoma, or even those who have undergone thymectomy, monitoring for hypogammaglobulinemia could provide an important clue for the diagnosis of GS.

## Conflict of Interest Disclosure:

The authors declare no financial or other potential conflicts of interest.

## References

1. Chen YD, Wen ZH, Wei B, *et al*. Clinicopathologic features of Good's syndrome: two cases and literature review. Open Med (Wars) 2021; 16: 532-539, https://doi.org/10.1515/med-2021-0256.
2. Tarr PE, Sneller MC, Mechanic LJ, *et al*. Infections in patients with immunodeficiency with thymoma (Good syndrome). Report of 5 cases and review of the literature. Medicine (Baltimore) 2001; Mar; 80(2): 123-33.
3. Kelesidis T, Yang O. Good's syndrome remains a mystery after 55 years: a systematic review of the scientific evidence. Clin Immunol 2010; 135: 347-363.
4. Kelleher P, Misbah SA. What is Good's syndrome? Immunological abnormalities in patients with thymoma. J Clin Pathol 2003; 56: 12-16.
5. Chang R, Duan S, Li S, *et al*. Viral infection in thymoma and thymic tumors with autoimmune diseases. Thorac Cancer 2021; 12: 2971-2980.
6. Bernard C, Frih H, Pasquet F, *et al*. Thymoma associated with autoimmune diseases: 85 cases and literature review. Autoimmun Rev 2016; 15: 82-92.
7. Malphettes M, Gérard L, Galicier L *et al*. Good syndrome: an adult-onset immunodeficiency remarkable for its high incidence of invasive infections and autoimmune complications. Clin Infect Dis 2015; 61: e13-e19.
8. Hermaszewski RA, Webster AD. Primary hypogammaglobulinaemia: a survey of clinical manifestations and complications QJ Med 1993; 86: 31-42.

# Peribronchiolar Metaplasia - Interstitial Lung Disease: Case Report and Review of the Literature

Chen-Chieh Lin[1], Mong-Wei Lin[2], Kuei-Pin Chung[3,4], Yih-Leong Chang[5,6]

Peribronchiolar metaplasia (PBM) is a histological change that features the extension of bronchiolar-type epithelial cells along the alveolar walls adjacent to the bronchioles. The exact mechanisms leading to PBM are not well understood, and may be related to non-specific reactions to tissue injury. Peribronchiolar metaplasia – interstitial lung disease (PBM-ILD) is rarely reported in the literature, and is considered as a subtype of ILD with bronchiolocentric patterns. While focal PBM commonly appears in various chronic ILDs, diffuse PBM in the lungs is the principal pathological hallmark of PBM-ILD. Here, we reported a case of PBM-ILD that may have been caused by long-term incense smoke exposure. Our report indicates that surgical biopsy is crucial for diagnosis of ILD with unusual clinical and radiological presentation. ***(Thorac Med 2023; 38: 136-141)***

Key words: interstitial lung disease, peribronchiolar metaplasia, bronchiolocentric pattern, incense smoke exposure

## Introduction

The classifications of rare idiopathic interstitial pneumonia (IIP), based on the American Thoracic Society / European Respiratory Society statement in 2013, described interstitial lung disease (ILD) that was associated with unusual histopathological features [1]. ILD with bronchiolocentric patterns, which were categorized under this IIP classification, are characterized by bronchiolocentric fibroinflammatory changes, and represent a unique form of small airway disease. Several variants of ILD with bronchiolocentric patterns were reported in the literature, including idiopathic bronchiolocentric interstitial pneumonia, bronchiolitis interstitial pneumonia, airway-centered interstitial fibrosis (ACIF), and peribronchiolar metaplasia (PBM)-related ILD. PBM is a histological feature characterized by the extension

[1]Department of Internal Medicine, National Taiwan University Hospital, Taipei, Taiwan, [2]Department of Surgery, National Taiwan University Hospital, Taipei, Taiwan, [3]Department of Laboratory Medicine, National Taiwan University Hospital, Taipei, Taiwan, [4]Department of Laboratory Medicine, National Taiwan University College of Medicine, Taipei, Taiwan, [5]Department of Pathology, National Taiwan University Hospital and National Taiwan University Cancer Center, Taipei, Taiwan, [6]Department and Graduate Institute of Pathology, College of Medicine, National Taiwan University, Taipei, Taiwan.
Address reprint requests to: Dr. Kuei-Pin Chung, Department of Laboratory Medicine, National Taiwan University Hospital and National Taiwan University College of Medicine, No. 7, Chung Shan S. Rd., Zhongzheng Dist., Taipei 100, Taiwan

of bronchiolar epithelial cells along the alveoli adjacent to the bronchioles, and may represent post-injury non-specific tissue reactions [2]. Focal PBM is commonly associated with various chronic ILDs, such as usual interstitial pneumonitis, non-specific interstitial pneumonitis, desquamative interstitial pneumonitis, respiratory bronchiolitis ILD, and hypersensitivity pneumonitis [3]. Diffuse PBM changes are the main histopathological changes in PBM-ILD, and are rarely reported in the literature. Here, we report a case of PBM-ILD that was proven by surgical biopsy pathology.

## Case Presentation

A 71-year-old woman visited our hospital in September 2019, due to intermittent chest tightness and exertional dyspnea, grade 2, based on the modified Medical Research Council (mMRC) scale, for 3 months. She did not have cough, sputum expectoration, orthopnea, or pedal edema. She was a never-smoker, and had hypertension and diabetes mellitus under regular medical control. She cooked meals at home, but otherwise did not have a remarkable occupational exposure, and did not breed any pets at home. However, she had burned more than 3 incense sticks daily for nearly 30 years. Physical examination did not reveal abnormal breathing sounds, such as rhonchi, wheezes, or rales/crackles. Chest radiograph showed borderline cardiomegaly, with mildly increased infiltration in bilateral lower lung fields (Figure 1A). She reported that her echocardiogram in the cardiovascular clinics did not reveal any abnormalities, including left ventricular systolic dysfunction.

Computed tomography (CT) scan was thus performed for further evaluation, and showed diffuse mosaic attenuation with mildly thickened bronchial walls in bilateral lungs (Figure 1B), without an enlarged pulmonary arterial trunk (Figure 1C). Laboratory screening for autoimmune diseases, including anti-nuclear antibody, anti-extractable nuclear antigen, and erythrocyte sedimentation rate, did not reveal significant findings, and the serum D-dimer level was within normal limits. Although the mosaic attenuation in her lungs may have been

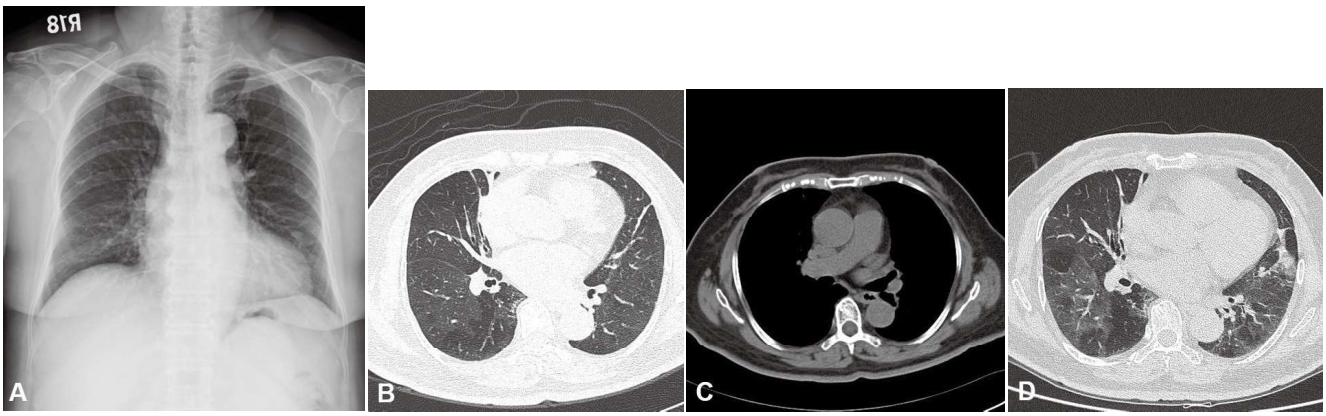


**Fig. 1.** Radiologic figures at presentation and during clinical follow-up. (A) Chest radiograph at presentation showed mildly increased infiltration at bilateral lower lung fields. (B) Chest computed tomography (CT) images in September 2019 showed bilateral diffuse mosaic attenuation with thickened bronchial walls, suggesting small airway diseases with air trapping. (C) Soft tissue window in CT images in September 2019 showed no enlargement of the pulmonary trunk. (D) Chest CT image in April 2021 showed that the mosaic attenuation had progressed slightly within the last 2 years.

due to occlusive pulmonary vascular diseases [4], these diseases were less likely considering the laboratory finding and the lack of evidence of pulmonary hypertension by echocardiogram and chest CT scan. Small airway disease with air trapping was thus highly suspected. Screening spirometry showed that forced expiratory volume in 1 second ($FEV_1$), forced vital capacity (FVC), and the ratio of $FEV_1$ to FVC were all within normal limits. (Table 1). Considering that her dyspneic symptom may be due to small airway disease, a therapeutic trial with a tiotropium bromide monohydrate inhaler (Spiriva® Respimat®) was conducted, and successfully and completely relieved her symptom. Meanwhile, due to the potential causal link between incense smoke exposure and the patient's symptoms, she was asked to stop burning incense to prevent disease progression.

During follow-up, her screening spirometry (Table 1) was re-checked around April 2021, and was compared to the results of her previous exam in September 2019; a modest increase in FVC (around 300 ml) was found. Although her symptoms remained well controlled with tiotropium inhalation (mMRC grade 0), a chest CT scan in April 2021 showed progression of bilateral diffuse mosaic attenuation (Figure 1D). Given that the histopathological nature of the patient's disease was undetermined, and that the prognosis of some small airway diseases, such as bronchiolitis obliterans, is poor, video-assisted thoracoscopic surgery lung biopsy was thus considered. She agreed to undergo lung biopsy, and wedge resections of the left upper and lower lobes of the lungs were performed. Histopathological examination revealed diffusely prominent PBM, given metaplastic extension of the bronchiolar epithelium towards the alveolar ducts and adjacent alveoli, with slight septal fibrosis. (Figure 2). On the basis of the pathological findings, the diagnosis of PBM-ILD was considered. Tiotropium inhalation was maintained to control her symptoms, and her condition has remained stable up to the time of this report.

## Discussion

The clinical characteristics of PBM-ILD are rarely reported in the literature. Fukuoka and associates were the first to propose the term

**Table 1.** Treatment Highlights and Serial Pulmonary Function Tests of the Presented Case

| Date (yyyy/mm) | $FEV_1$/FVC | $FEV_1$ (L) (%predicted) | FVC (L) (%predicted) | DLCO (ml/min/mmHg) (%predicted) | $FEF_{25-75\%}$ (L/S) (%predicted) |
|---|---|---|---|---|---|
| **2019/09** | 84.3% | 1.50 (97.1%) | 1.78 (88.5%) | N/A | 1.60 (84.0%) |
| **2019/10** | Tiopropium (Spiriva Respimat) inhaler added | | | | |
| **2021/04** | 80.5% | 1.69 (112.9%) | 2.10 (106.6%) | 17.9 (111.8%) | 1.40 (76.6%) |
| **2021/08** | 84.6% | 1.65 (112.7%) | 1.95 (100.8%) | N/A | 1.80 (99.5%) |
| **2021/08** | Surgical lung biopsy | | | | |

Acronyms: $FEV_1$, forced expiratory volume in 1 second; FVC, forced vital capacity; DLCO, diffusion capacity of the lung for carbon monoxide; FEF25-75%, forced expiratory flow at 25–75% of forced vital capacity.

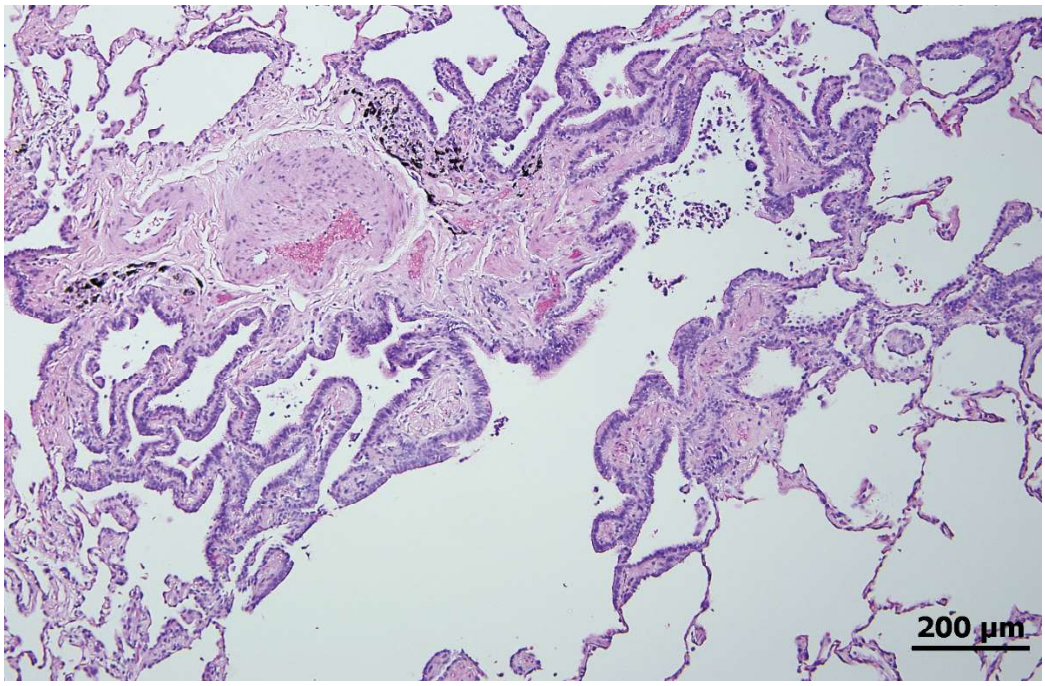


**Fig. 2.** Pathology. Microphotograph of the lung parenchyma showed metaplastic extension of the bronchiolar epithelium towards adjacent alveolar ducts accompanied by slight fibrosis.

"peribronchiolar metaplasia", and reported 15 patients who had PBM as the only major histological finding in surgical lung biopsy samples [3]. In their series, a female predominance was noticed, and the mean age of the population was 57 years. Smoking history (6 of 15) and collagen vascular diseases (3 of 15) were associated with PBM development, and dyspnea was the main presenting symptom. Pulmonary function tests revealed restrictive ventilatory defects in most of the patients. The chest CT scan images featured diffuse ground-glass opacities and mosaic attenuation, together with varying degrees of fibrotic changes. Clinical features of PBM-ILD similar to those reported by Fukuoka and associates were found in 2 other small case series [5, 6]. The outcomes of PBM-ILD were favorable and without progression in most of the patients [3]. The optimal treatment for PBM-ILD currently is unknown, although immunosuppressants, such as corticosteroids, azathioprine, and mycophenolate mofetil, were tried in some patients in one case series [6].

Although our patient had presenting symptoms similar to those reported in the literature, she was older, and had nearly normal spirometry. We did not find evidence of autoimmune disease in our patient, and her disease severity did not worsen with time. We did not prescribe immunosuppressants, but gave her an inhaled long-acting anticholinergic agent as a trial. The response of our patient suggested the potential efficacy of inhaled triotropium in relieving dyspneic symptoms related to PBM-ILD. However, since the mechanisms underlying its therapeutic efficacy are unknown and placebo effects cannot be fully excluded, the therapeutic role of inhaled triotropium needs to be evaluated in other patients with PBM-ILD.

Of all the variants of IIP with bronchiolocentric patterns, ACIF is reported more frequently than PBM-ILD. The clinical features

of ACIF, including demographic predominance and the restrictive ventilatory defect revealed by spirometry, are similar to those of PBM-ILD [7]. In contrast to the benign nature of PBM-ILD, the clinical course of ACIF varies, but may be aggressive, and is associated with 30% 2-year mortality after diagnosis [7, 8]. The chest CT scan image of ACIF is completely different from that of PBM-ILD, and is characterized by diffuse peribronchovascular interstitial thickening and traction bronchiectasis [7-9]. Histological features of ACIF show variable degrees of interstitial fibrosis involving lung parenchyma surrounding membranous and respiratory bronchioles, and the fibrotic reactions in ACIF may account for the poor prognosis [7, 8]. Therefore, it is important to distinguish PBM-ILD from ACIF, due to different clinical outcomes, and surgical lung biopsy is indicated for a definite histological diagnosis.

The etiology of PBM-ILD is not well understood. The peribronchiolar involvement suggests that PBM-ILD may be chronic responses to tissue damage caused by persistent inhalation-related exposure, such as cigarette smoking. Other noxious environmental substances may also lead to PBM development, and Orriols and associates reported that long-term exposure to hydrochloride inhalation may be the cause of PBM-ILD in cleaning personnel [6]. In our patient, long-term incense smoke exposure may have been the cause of PBM-ILD. Inorganic gas, volatile organic compounds, and aldehydes are found in the smoke generated during incense burning, and all of these are respiratory irritants and can induce bronchial constriction and cough [10]. In addition, the particulate matter in incense smoke is more abundant than that in cigarette smoke, which increases the risk of malignancy and the development of various ILD, including idiopathic pulmonary fibrosis and hypersensitivity pneumonitis [11]. Exposure to incense smoke may lead to neutrophil infiltration in alveolar lumens, and cause degenerative and necrotic changes in the alveolar lining. The chronic inflammatory responses and the production of various cytokines, such as interleukin (IL)-4, IL-5, IL-10, and IL-13, may promote airway remodeling, and lead to the development of PBM [10]. Due to religious practice, incense burning is very popular in East Asia, and predisposes those nearby to the development of PBM and PBM-ILD. The exact prevalence of PBN and PBM-ILD in East Asian thus warrants further studies to investigate.

Mosaic attenuation is the major feature in PBM-ILD, and describes the inhomogeneous attenuation in the involved lung parenchyma. In addition to air trapping, micro-circulatory regulation, leading to blood shunting away from the involved lung parenchyma, may also account for the image pattern of mosaic attenuation in small airway diseases [12]. While mosaic attenuation may suggest small airway diseases with air trapping, other diagnoses, particularly occlusive vascular diseases, pulmonary congestion, and an infection process, should be considered and differentiated [12]. Our patients did not have infectious symptoms or signs, and had normal echocardiogram results. Of note, the chest CT image did not reveal features of pulmonary thrombo-embolism or pulmonary hypertension, such as organizing thrombi in the vessels, increased diameters of pulmonary vessels compared to the associated bronchi, and an increased ratio pulmonary trunk-to-aorta ratio. In addition, our patient did not have a relevant family history, and pulmonary function tests did not show an impaired diffusion capacity, a critical feature of pulmonary veno-occlusive disease [4].

Overall, the clinical characteristics of our patient indicate that the most favorable etiology of mosaic attenuation in chest CT images is small airway disease. Importantly, our report further emphasizes the essential role of surgical lung biopsy, though it is an invasive procedure, in clarifying the diagnoses of ILD with unusual clinical and radiological presentations. Detailed clinical and laboratory assessments to identify the causes of unusual ILDs will help clinicians evaluate the diagnostic need for surgical lung biopsy.

## Conclusion

For an ILD with an unusual clinical and radiological presentation, surgical biopsy remains crucial to obtain pathologic proof. We reported a case of biopsy-proven PBM-ILD that may have been caused by long-term incense smoke exposure. Further studies are warranted to advance our understandings of PBM-ILD and other ILD variants with a bronchiolocentric pattern.

**Acknowledgments:** none

## Conflicts of interest:

All authors declared no conflicts.

## References

1. Travis WD, Costabel U, Hansell DM, *et al*. An Official American Thoracic Society/European Respiratory Society Statement: Update of the International Multidisciplinary Classification of the Idiopathic Interstitial Pneumonias. Am J Respir Crit Care Med 2013; 188: 733-48.
2. Wallace AH, Simpson AJ, and Hirani N. Interstitial lung diseases. In: Hasleton P, F.D., Spencer's pathology of the lung. 6th ed. 2014.
3. Fukuoka J, Franks TJ, Colby TV, *et al*. Peribronchiolar metaplasia: A common histologic lesion in diffuse lung disease and a rare cause of interstitial lung disease - Clinicopothologic features of 15 cases. Am J Surg Pathol 2005; 29: 948-54.
4. Montani D., Lau E.M., Dorfmüller P., Girerd B., Jaïs X., Savale L., *et al*. Pulmonary veno-occlusive disease. Eur Respir J 2016;47:1518-34.
5. Cano-Jiménez E, Molina-Molina M, Ramírez J, *et al*. Diffuse Interstitial Lung Disease Related to Peribronchiolar Metaplasia. Arch Bronconeumol 2009; 45: 57-9.
6. Orriols R, Costa R, Montero MA, *et al*. Peribronchiolar metaplasia interstitial pneumonia in cleaning workers. Int J Clin Exp Med 2017; 10: 3778-86.
7. Churg A, Myers J, Suarez T, *et al*. Airway-centered Interstitial Fibrosis: A Distinct Form of Aggressive Diffuse Lung Disease. Am J Surg Pathol 2004; 28: 62-8.
8. Kuranishi LT, Leslie KO, Ferreira RG, *et al*. Airway-centered interstitial fibrosis: etiology, clinical findings and prognosis. Respir Res 2015; 16: 1-8.
9. Silbernagel E, Morresi-Hauf A, Reu S, *et al*. Airway-centered interstitial fibrosis – an under-recognized subtype of diffuse parenchymal lung diseases. Sarcoidosis Vasc Diffuse Lung Dis 2018; 35: 218-29.
10. Lin TC, Krishnaswamy G, and Chi DS. Incense smoke: clinical, structural and molecular effects on airway disease. Clin Mol Allergy 2008; 6: 3.
11. Singh N and Singh S. Interstitial Lung Diseases and Air Pollution: Narrative Review of Literature. Pulm Ther 2021; 7: p. 89-100.
12. Kligerman SJ, Henry T, Lin CT, *et al*. Mosaic Attenuation: Etiology, Methods of Differentiation, and Pitfalls. Radiographics 2015; 35: 1360-1380.

# A Rare Case of Lung Cancer With Initial Presentation of Symptomatic Choroidal Metastasis

Chin-Shui Yeh[1,3], Jian-Sheng Wu[2,3]

Symptomatic choroidal metastasis is a rare presenting manifestation of lung cancer. We reported the case of a 57-year-old woman who was a non-smoker throughout her life, and who had initially presented with blurred vision in her left eye. The ophthalmologist referred her to the chest medicine department for testing for occult primary lung malignancy. Pathologic diagnosis of the computed tomography-guided fine needle aspiration from the left lower lobe lung mass was adenocarcinoma. The final diagnosis was adenocarcinoma of the lung, with metastases to the choroid, liver, left adrenal gland, and multiple bones. Clinical staging was T2bN3M1c, stage IVB. She received radiation therapy to the posterior pole of the left eye. However, her visual acuity decreased to 20/200, and progression of retinal detachment at the macula was noted. A subtenon triamcinolone acetonide injection was administered monthly, and the retinal detachment subsided with visual acuity improving to 20/25 3 months later. Genetic analysis of the tumor cells revealed a mutation in epidermal growth factor receptor exon 19. She received an oral tyrosine kinase inhibitor, dacomtinib, as first-line therapy with a good response, and tumor regression was observed. Choroidal metastasis is relatively uncommon but should be suspected in lung cancer patients with deteriorated visual acuity. ***(Thorac Med 2023; 38: 142-148)***

Key words: lung cancer, adenocarcinoma, choroidal metastasis

## Introduction

Lung cancer is on the rise globally and is the most common cause of cancer-related deaths. In all, 2.09 million new cases and 1.76 million deaths were estimated for the year 2018, totals that were higher than those reported in 2012 (1.8 million new cases and 1.6 million deaths) [1]. Despite recent advances, lung cancer remains the number 1 cause of cancer death, and is associated with 1 of the lowest 5-year survival rates among all cancer types.

NSCLC is usually diagnosed in the later stages of development [2]. Lung carcinomas metastasize via the lymphatic system and blood vessels. Some preferential sites for metastases of lung cancer are the brain, bones, and adrenal glands. The percentage of patients presenting

[1]Division of Chest Medicine, Department of Internal Medicine, Changhua Christian Hospital Changhua, Taiwan, [2]Department of Ophthalmology, Changhua Christian Hospital, [3]Department of Post-Baccalaureate Medicine, National Chung Hsing University.
Address reprint requests to: Dr. Chin-Shui Yeh, Division of Chest Medicine, Changhua Christian Hospital, 135 Nanxiao St, Changhua, Taiwan

with metastases to various sites for all lung cancer subtypes were liver (33%–40%), brain (15%–43%), kidney (16%–23%), adrenal glands (18%–38%), bone (19%–33%), and abdominal lymph nodes (29%) [3]. In a study involving 1,542 NSCLC patients, 729 had pathologically confirmed NSCLC with distant metastasis. Among the patients, 250 (34.3%), 234 (32.1%), 207 (28.4%), 122 (16.7%), 98 (13.4%), and 69 (9.5%) had bone, lung, brain, adrenal gland, liver, and extrathoracic lymph node metastases, respectively, while 283 (38.8%) patients presented with pleural and/or pericardial fluid effusion [4].

NSCLC patients with mutations in the epidermal growth factor receptor (EGFR) gene are more prone to developing bone and brain metastases [5]. Malignant tumor of the eye is the most common metastatic carcinoma. The incidence of lung cancer with choroidal metastasis is relatively low. Ocular malignant metastases usually involve the uveal tract [6]. Uveal metastatic tumors originating from primary lung cancer have been reported [7], and tumor locations included the choroid (88%), ciliary body (2%), and iris (10%), with bilateral involvement observed in 18% of patients. Patients with choroidal metastases from lung cancer are rarely identified prior to diagnosis of the primary malignancy [8]. Symptomatic choroidal metastasis as the initial presentation of lung cancer is an infrequent occurrence [9]. We herein report a patient with stage IV adenocarcinoma of the lungs with the initial manifestation of symptomatic choroidal metastasis.

## Case Report

A 57-year-old woman, with no history of smoking throughout her lifetime, presented to our ophthalmologist with blurred vision in the left eye for 2 months, with visual acuity of 20/40. A dilated funduscopic examination revealed an amelanotic choroidal mass at the macula in the left eye (figure 1A). Retinal detachment overlying the choroidal mass (figure 1B) was detected on optical coherence tomography. Fundus autofluorescence of the left eye depicted alternance of hypo and hyper autofluorescent lesions (figure 1C). Fundus fluorescein angiography also revealed initial hypofluorescence of the lesions (figure 1D), which changed over time to heterogenous hyperfluorescence (figure 1E). The clinical diagnosis was choroidal metastasis from an occult primary malignancy.

Her chest radiograph revealed several fluffy and nodular opacities in the left lower lung field

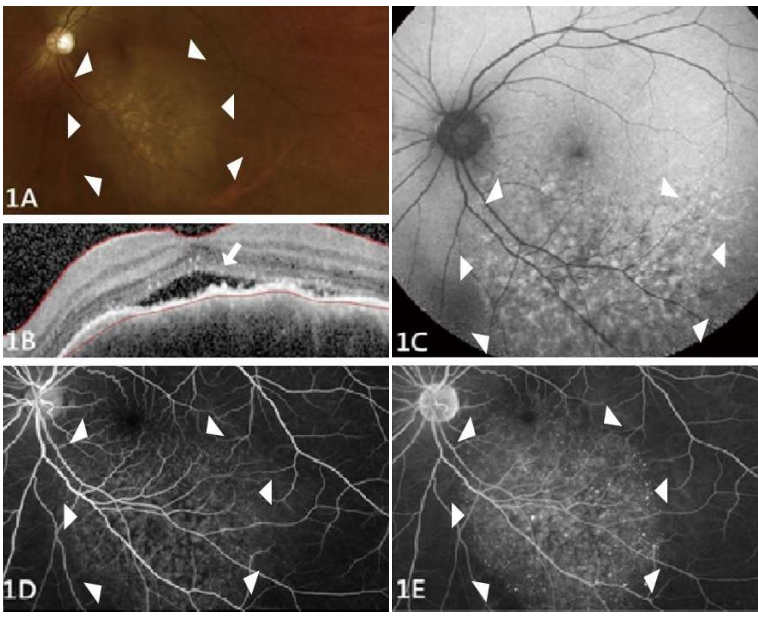


**Fig. 1.** Dilated funduscopic examination disclosed an amelanotic choroidal mass at the macula (arrow heads) of the left eye (1A). OCT showed retinal detachment (arrow) overlying the choroidal mass (1B). Fundus autofluorescence showed alternance of hypo and hyper autofluorescent lesions (arrow heads) (1C). Fundus fluorescein angiography revealed initial hypofluorescence (arrow heads) of lesions (1D) that changed over time to heterogenous hyperfluorescence (arrow heads) (1E).

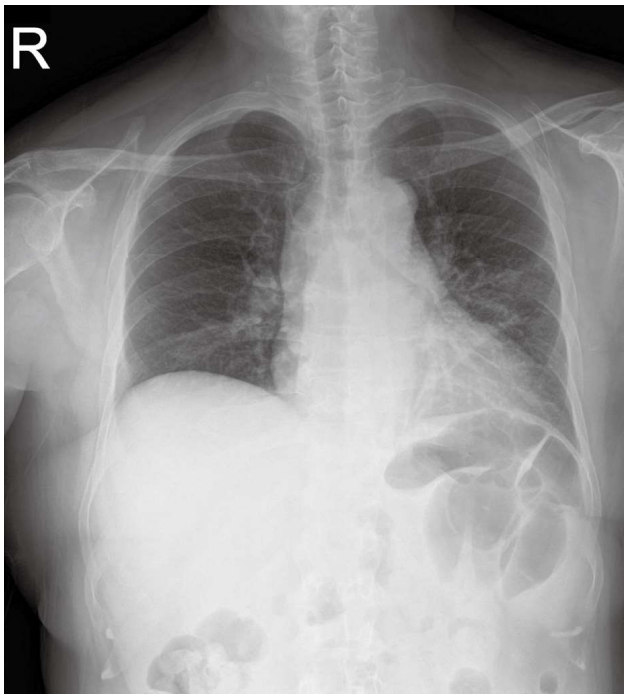


**Fig. 2.** Chest radiography taken at presentation showed increased fluffy and nodular opacities in the left lower lung field.

(Figure 2). The patient was then referred to the chest medicine department. There, a chest CT scan was performed, which revealed malignant invasion in her left lower lung with lymphangitic carcinomatosis and metastasis to the liver, left adrenal gland, and multiple bones (Figure 3). Sonography of the liver indicated liver metastasis, and bone scan revealed multiple bone metastases with increased activity in the skull, cervical-thoracic-lumbar spine, sternum, pelvic bones, bilateral ribs, humerus, femurs, and right tibia. Pathologic diagnosis of CT-guided fine needle aspiration performed on the mass in the left lower lobe revealed adenocarcinoma. The clinical stage was determined to be T2b-N3M1c, stage IVB, as per the Eighth Edition of the American Joint Committee on Cancer staging. Subsequent genetic analysis of the EGFR revealed an exon 19 mutation. Aplastic lymphoma kinase (ALK), ROS1, and programmed cell death ligand 1 (PD-L1) were not detected. The patient began treatment with dacomitinib--a potent, irreversible, highly selective, second-generation EGFR-tyrosine kinase inhibitor. She also received radiation therapy to the posterior pole of the left eye (30 Gy in 10 fractions). However, her visual acuity decreased to 20/200, and progression of retinal detachment at the macula was noted (figure 4A). She was then administered the subtenon triamcinolone acetonide injection monthly, after which the retinal detachment subsided (figure 4B), with visual acuity improving to 20/25 3 months later.

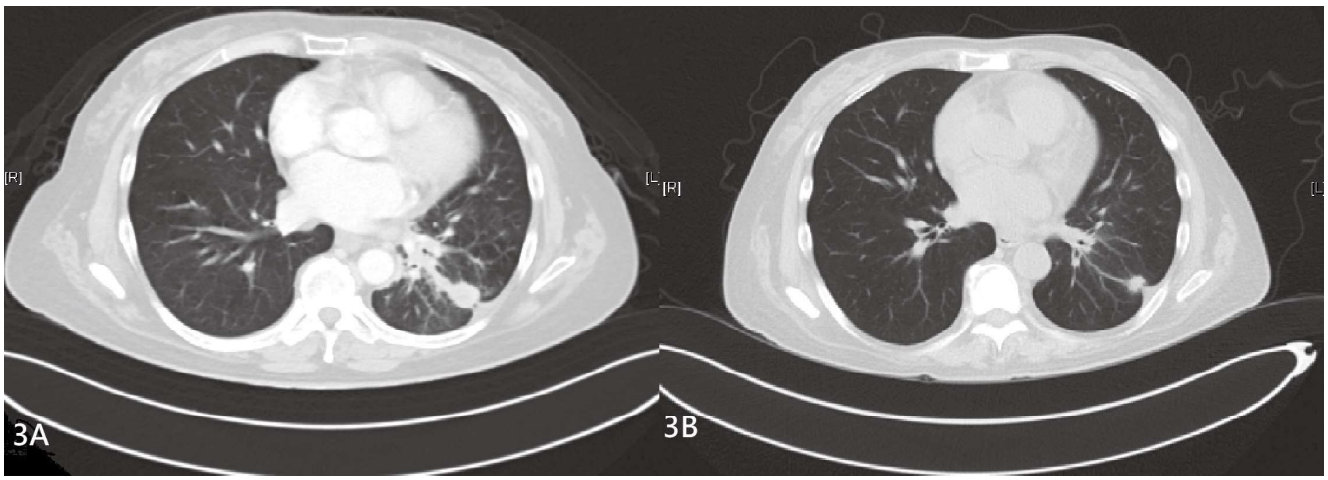


**Fig. 3.** Chest Computed Tomography with a tumor in the left lower lung (3A). Resolution of the tumor after 4 months of TKI targets therapy (3B)

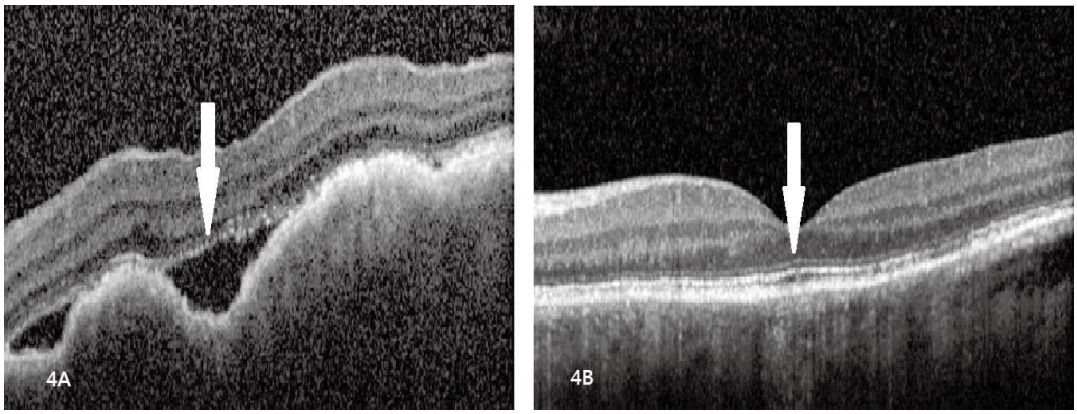


**Fig. 4.** Progression of retinal detachment at macula was noted (4A) after radiotherapy. The retinal detachment subsided after monthly subtenon triamcinolone acetonide injection 3 months later (4B).

Follow up chest CT 4 months after TKI inhibitor therapy showed a decrease in tumor size in the left lower lung, from 4.1 to 1.09 cm (Figure 3). The size of the liver, left adrenal gland, and mediastinal node metastases had also decreased. The patient then was determined to be in a stable disease condition.

## Discussion

Bronchogenic carcinoma metastatic to the choroid was first reported in 1962 [10]. An ocular screening study determined the prevalence of choroidal metastasis in patients with metastatic lung cancer to be 7.1%. The choroid was the sixth most common site of organ metastasis, according to this study [11]. Moreover, choroidal metastasis was detected only when at least 2 other organ systems were affected by metastases. In another study, a total of 36 patients were evaluated for choroidal metastases at National Taiwan University Hospital over an 11-year period [11]. The primary sites of tumors were the lung in 18 (50%) patients, breast in 8 (22.2%), gastrointestinal tract in 3 (8.3%), pancreas in 2 (5.6%), ovaries in 2 (5.6%), kidney in 1 (2.8%), liver in 1 (2.8%), and unknown in 1 case (2.8%). In the case of our patient, 4 organs, including the choroid of the eye, the liver, left adrenal gland, and multiple bones, were affected by metastases.

Symptomatic choroidal metastasis is a rare presenting manifestation of lung cancer. In a systematic literature review, a search of all relevant articles from PUBMED (National Library of Medicine, Bethesda, MD) published in English from 1954 to 2010 was conducted [13]. Occurrence of lung cancer with choroidal metastasis was reported in only 75 cases from 67 publications. Of these, 23 patients reported in 21 publications did not have choroidal metastasis as the presenting manifestation of lung cancer [14-17]. Symptomatic choroidal metastasis from lung cancer in most affected patients presented as a solitary tumor prior to the diagnosis of lung cancer, and is a rare clinical entity contrary to predictions from ocular screening studies [9].

Treatment for choroidal metastasis is usually palliative, since most patients are at a late stage of lung cancer when diagnosed. Treatment decisions should be based on the physical condition of the patient, the location and number of primary tumors, the presence or absence of

distant metastases, and the location and number of intraocular metastases. Approximately two-thirds of lung cancer patients with choroidal metastasis can possibly benefit from treatments; therefore, early diagnosis and interventions are encouraged [18]. Treatments for choroidal metastasis include systemic therapies, systemic therapy combined with local ocular radiotherapy, and local treatment alone. Systemic chemotherapy has been reported to be associated with a good response from patients with malignant lung carcinoma and various metastases including choroidal metastasis, especially for patients without an associated driver gene mutation [19].

Tyrosine kinase inhibitors (TKI) targeting TK-driven oncogenic genes have greatly improved progression-free survival and overall survival for patients with milder adverse events, compared with chemotherapy. The efficacy of TKI agents is known to be equivalent to radiation, and the onset of action is shorter [20]. Osimertinib, a third-generation EGFR TKI, may be considered as a first-line treatment option in patients with choroidal metastases from an EGFR-mutated NSCLC. According to a case report, complete resolution of the subretinal fluid over the choroidal lesion and decreased thickness of the lesion was noted within 1 month of initiating treatment with osimertinib [21], and significant interval decreases in the size and activity of the primary lung lesion was evident after 3 months. After 17 months of follow-up, the choroidal lesion remained involuted. In another case involving a 63-year-old Asian male, and following initiation of osimertinib treatment, ophthalmic and CT imaging revealed regression of both the ocular metastatic disease and the primary malignancy [22].

Alectinib (a second-generation TKI) has also been reported to achieve rapid resolution of choroidal metastatic tumors secondary to lung cancer [23]. TKI administration combined with anti-angiogenic therapy, such as intravitreal bevacizumab, has also been reported to lead to successful regression of choroidal metastasis and improvement of symptoms [24]. The treatment responses observed in patients with choroidal metastases treated with TKI are listed in Table 1 [20-24].

Local ocular radiotherapy has been considered as the cornerstone for ocular malignancies. In terms of choroidal metastatic lesions, optional treatment strategies include external beam radiation therapy, brachytherapy, gamma knife radiosurgery, and proton beam therapy [25]. Although most patients present with multiple metastases and may not be suitable for intervention, surgical resection of the primary lesion following consultation with a multidisciplinary team will help to define the diagnosis and minimize tumor-related symptoms [26].

Analysis of the survival of patients with lung cancer and choroidal metastasis has been reported in a few studies, and found that patients suffering from lung cancer accompanied with metastases to the brain, abdomen and extremities exhibited poorer survival than those without metastases [4]. The mean life span of patients diagnosed with metastatic lung cancer with choroidal metastasis was 1.9 (0.2-5.9) months [11]. In a study involving 36 patients with choroidal metastases following a primary malignancy, mean life span after diagnosis was 4.3 months in 22 patients [12]. Choroidal metastases may indicate a terminal status of the underlying malignancy and a short survival time.

Our current patient was treated with second-generation oral EGFR-TKIs as first-line therapy. Her ocular lesion regressed and blur-

**Table 1.** Published Reports of Patients with NSCLC With Choroidal Metastases Treated With TKI

| Published Reports | Histology | Treatment | Clinical Outcome |
|---|---|---|---|
| Maskell D, *et al*. [20] | EGFR mutation–positive NSCLC | gefitinib | At 33-day assessment, there was complete resolution of the mass and the retinal detachment. Visual acuity had improved to 6/30. |
| Field MG, *et al*. [21] | EGFR exon 19-mutated NSCLC | osimertinib | After 17 months of follow-up, the lesion remained involuted. |
| Vu AN, *et al*. [22] | EGFR mutation–positive adenocarcinuma | osimertinib | Visual symptoms were resolved 9 months after daily treatment with oral osimertinib. CT scan showed improved the right lung mass, paratracheal lymph nodes, and bony metastases |
| Al-Janabi A, *et al*. [23] | NSCLC | alectinib | A few weeks later, his vision had improved and there was complete resolution of the choroidal mass and the associated subretinal fluid. |
| Kim SW, *et al*. [24]. | adenocarcinoma | Combined intravitreal bevacizumab and oral erlotinib | Two months later, the best-corrected visual acuity had improved to 20/40, and the 2 previous masses had completely disappeared. |

ring of her vision was reduced. Repeated chest CT after 4 months of TKI therapy confirmed tumor regression. Adverse reactions to dacomitinib TKI therapy observed in this patient were minor diarrhea and some skin rash.

In conclusion, symptomatic choroidal metastases as the initial presentation of lung cancer is a rare occurrence. Choroidal metastasis is relatively uncommon but should be suspected in lung cancer patients with a deteriorated visual acuity. Early ocular investigation of patients with lung cancer may be helpful in obtaining a confirmed diagnosis. Local ocular treatment and systemic therapy are necessary for lung cancer patients with choroidal metastases. Further molecular studies and immune therapy can play an important role in treatment for these patients. Involvement of a multidisciplinary team in the integrated care and treatment monitoring of these patients will certainly be beneficial.

## References


1. Bade BC, Dela Cruz CS. Lung cancer 2020: epidemiology, etiology, and prevention. Clin Chest Med 2020; 41: 1-24.
2. Kocher F, Hilbe W, Seeber A, *et al*. Longitudinal analysis of 2293 NSCLC patients: a comprehensive study from the TYROL registry. Lung Cancer 2015; 87: 193-200.
3. Quint LE, Tummala S, Brisson LJ, *et al*. Distribution of distant metastases from newly diagnosed non-small cell lung cancer. Ann Thorac Surg 1996; 62: 246-50.
4. Tamura, T, Kurishima, K, Nakazawa, *et al*. Specific organ metastases and survival in metastatic non-small-cell lung cancer. Mol Clin Oncol 2015; 3: 217-21.
5. Hendriks, LEL, Smit, EF, Vosse BAH, *et al*. EGFR mutated non-small cell lung cancer patients: more prone to development of bone and brain metastases? Lung Cancer 2014; 84: 86-91.
6. De Potter P. Ocular manifestations of cancer. Curr Opin Ophthalmol 1998; 9: 100-4.
7. Shah SU, Mashayekhi A, Shields CL, *et al*. Uveal metastasis from lung cancer: clinical features, treatment, and outcome in 194 patients. Ophthalmology 2014; 121: 352-7.

8. Qu Z, Liu J, Zhu L, *et al*. A comprehensive understanding of choroidal metastasis from lung cancer. Onco Targets Ther 2021; 14: 4451-65.
9. Kreusel KM, Bechrakis NE, Krause L, *et al*. Incidence and clinical characteristics of symptomatic choroidal metastasis from lung cancer. Acta Ophthalmol 2008; 86: 515-9.
10. Wright JC, Meger GE. Bronchogenic carcinoma metastatic to the choroid. Am J Ophthalmol 1962; 53: 1003-5.
11. Kreusel KM, Wiegel T, Stange M, *et al*. Choroidal metastasis in disseminated lung cancer – frequency and risk factors. Am J Ophthalmol 2002; 134: 445-7.
12. Wang TJ, Yang CM, Ho TC, *et al*. Metastatic choroidal tumors in Taiwan: an 11-year experience. Am J Ophthalmol 2005; 140: 735-7.
13. Singh N, Kulkarni P, Aggarwal AN, *et al*. Choroidal metastasis as a presenting manifestation of lung cancer: a report of 3 cases and systematic review of the literature. Medicine 2012; 91: 179-94.
14. Abundo RE, Orenic CJ, Anderson SF, *et al*. Choroidal metastases resulting from carcinoma of the lung. J Am Optom Assoc 1997; 68: 95-108.
15. Arevalo JF, Fernandez CF, Garcia RA. Optical coherence tomography characteristics of choroidal metastasis. Ophthalmology 2005; 112: 1612-9.
16. Chong JT, Mick A. Choroidal metastasis: case reports and review of the literature. Optometry 2005; 76: 293-301.
17. George B, Wirostko WJ, Connor TB, *et al*. Complete and durable response of choroid metastasis from non-small cell lung cancer with systemic bevacizumab and chemotherapy. J Thorac Oncol 2009; 4: 661-2.
18. Simomura I, Tada Y, Miura G, *et al*. Choroidal metastasis of non-small cell lung cancer that responded to gefitinib. Case Rep Ophthalmol Med 2013; 2013: 213124. doi: 10.1155/2013/213124
19. Singh A, Singh P, Sahni K, *et al*. Non-small cell lung cancer presenting with choroidal metastasis as first sign and showing good response to chemotherapy alone: a case report. J Med Case Rep 2010; 4: 185.
20. Maskell D, Geropantas K, Kouroupis M, *et al*. Treatment of choice for patients with EGFR mutation-positive non-small cell lung carcinoma presenting with choroidal metastases: radiotherapy or TKIs? Can J Ophthalmol 2017; 52: 22–e25. doi: 10.1016/j.jcjo.2016.09.010
21. Field MG, Boldt HC, Hejleh TA, *et al*. Successful response to first-line treatment with osimertinib for choroidal metastasis from EGFR-mutated non-small-cell lung cancer. Am J Ophthalmol Case Rep 2022 1; 6: 01459.
22. Vu AN, Mehta UV, Israelsen P, *et al*. Treatment of choroidal metastasis from epidermal growth factor mutant non-small cell lung cancer with first-line osimertinib therapy. J Ophthalmic Vis Res 2022 21; 17: 130-4.
23. Al-Janabi A, Han MT, Busby D, *et al*. Rapid resolution of choroidal metastatic tumour secondary to lung cancer following treatment with alectinib. BMJ Case Rep 2021 24; 14: e238573.
24. Kim SW, Kim MJ, Huh K, *et al*. Complete regression of choroidal metastasis secondary to non-small-cell lung cancer with intravitreal bevacizumab and oral erlotinib combination therapy. Ophthalmologica 2009; 223: 411–3.
25. Jardel P, Sauerwein W, Olivier T, *et al*. Management of choroidal metastases. Cancer Treat Rev 2014; 40: 1119–28.
26. Guo Y, Wang X, Xiao J, *et al*. Lung squamous cell carcinoma with solitary ocular metastasis and its successful treatment with thoracic surgery and chemotherapy: an interesting and rare case report. BMC Cancer 2018; 18: 1004.

# Cavernous Sinus Metastasis of Lung Adenocarcinoma: A Case Report With A Literature Review

Chien-Yeh Chi[1], Cheng-Chia Lee[2], Heng-sheng Chao[1]

Cavernous sinus metastasis is rare. Its symptoms vary widely, and it is commonly confused with pituitary gland adenoma due to the lack of clear radiological criteria differentiating the 2 conditions. We present the case of a 54-year-old woman who had been diagnosed with non-small cell carcinoma of the right upper lung, with brain, bone, and lung-to-lung metastases. She presented intermittent dizziness, headache, vertigo, right eye ptosis, blurred vision, and diplopia during regular follow-up. Contrast brain magnetic resonance imaging revealed a mixed-intensity nodular lesion measuring 1.4 x 1 cm in the pituitary gland with a deviation of the pituitary stalk from right to left. Due to suspicion of a new metastatic lesion on the right side of the pituitary gland, the patient underwent an endoscopic trans-sphenoidal excision for removal of the pituitary tumor. Repeated brain computed tomography showed postoperative change and no residual pituitary tumor. This case report is a reminder that physicians should be aware of pituitary and cavernous sinus metastasis with its diverse clinical manifestations. And we should keep in mind that it is important to trace along the cranial nerve path if symptoms and signs of manifestations of the cranial nerve develop. ***(Thorac Med 2023; 38: 149-153)***

Key words: Cavernous sinus metastasis, lung adenocarcinoma

## Introduction

Cavernous sinus tumors include pituitary gland tumors, craniopharyngiomas, germ cell tumors, epidermoid cysts, meningiomas, gliomas, and metastatic tumors. The incidence of pituitary and cavernous sinus metastases among all intracranial metastases, including lung cancer, is rare [1,2]. However, it is a life-threatening disease associated with a poor prognosis. The most common clinical manifestations of pituitary and cavernous sinus metastases are diabetes insipidus, headache, ophthalmoplegia, visual disturbance, or panhypopituitarism [4,5]. Early detection of its clinical manifestations could lead to earlier diagnosis, appropriate therapy, and potentially improved quality of life. However, brain magnetic resonance imaging (MRI) or computed tomography (CT) examinations lack clear radiological features to differen-

[1]Department of Chest Medicine, Taipei Veterans General Hospital, Taipei, Taiwan, [2]Department of Neurosurgery, Neurological Institute, Taipei Veterans General Hospital, Taipei, Taiwan.
Address reprint requests to: Dr. Heng-sheng Chao, Division of General Chest Medicine, Department of Chest Medicine, Taipei Veterans General Hospital, Taipei, Taiwan,No. 201, Sec. 2, Shih-Pai Rd., Beitou District, Taipei 11217, Taiwan, ROC

tiate pituitary adenoma from a metastatic lesion [3,6]. Therefore, surgical intervention, such as endoscopic trans-sphenoidal excision, plays an important role in alleviating symptoms, improving quality of life, and confirming the diagnosis [7]. Stereotactic radiosurgery, as a minimally invasive procedure, also plays a crucial role in the treatment of pituitary and cavernous sinus metastases [8-9].

## Case Report

A 54-year-old woman had been diagnosed with non-small cell carcinoma of the right upper lung, most likely adeno-squamous carcinoma, cT4N2M1c. The epidermal growth factor receptor (EGFR) mutation test showed a deletion of exon 19. After diagnosis, erlotinib was administered as initial therapy. However, after a 6-month treatment regimen with the EGFR-tyrosine kinase inhibitor (EGFR-TKI), disease progression developed with multiple brain metastases in the bilateral cerebral and cerebellar region. The patient then received gamma knife radiotherapy for metastatic brain lesions and chemotherapy with paclitaxel and cisplatin.

Six months later, she complained of intermittent dizziness, headache, and vertigo for several days during the regular follow-up period. It was accompanied by ptosis of the right eye, blurred vision, and diplopia. No seizure, fever, weakness, change in sensation, or other discomfort was reported, and she also had no history of trauma. On examination, the patient was found to have right-side eyelid ptosis, right eye ophthalmoplegia, and diplopia when looking to the left side. The pupil light reflexes were intact. Otherwise, the rest of the neurological examination was within a normal range. Contrast brain MRI revealed multiple newly developed tiny enhancing nodules in the right occipital lobe, right hippocampus, left occipital lobe and left lentiform nucleus. A heterogeneously enhancing lesion was found in the sella turcica (seen not only in T2) (Figure 1A, 1B). It was a mixed intensity nodular lesion measuring 1.4 x 1 cm in the pituitary gland in the post-contrast axial T1-weighted image (Figure 1B). The post-

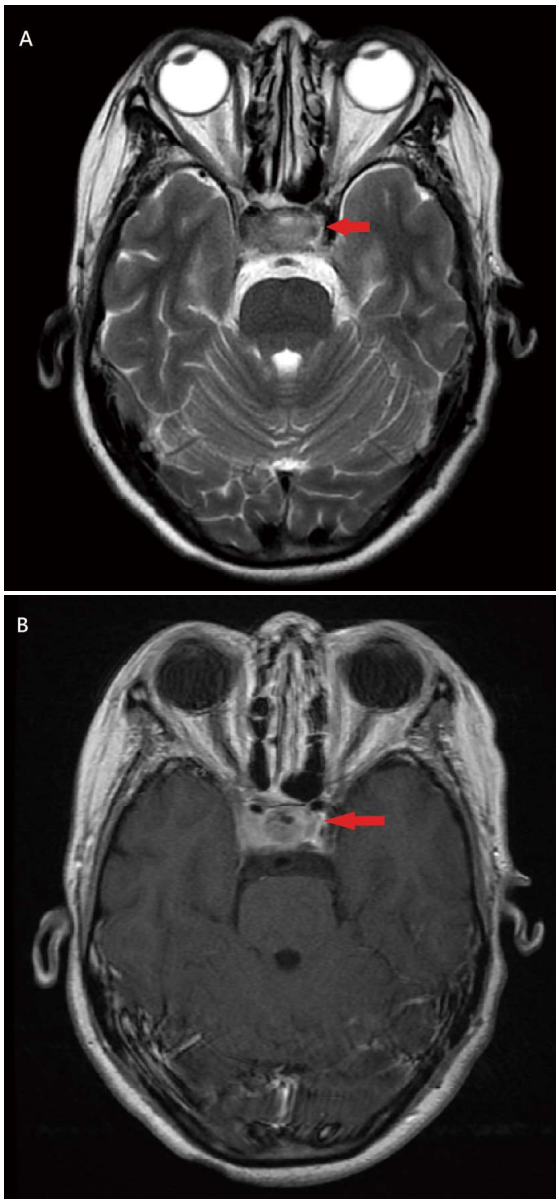


**Fig. 1.** Axial view of a pre-contrast T2-weighted image (A) showing a heterogeneously enhancing lesion in the sella turcica (arrow). Post-contrast axial T1-weighted image (B) revealed a mixed intensity nodular lesion measuring 1.4 x 1 cm in the pituitary gland, which was more on the right side (arrow).

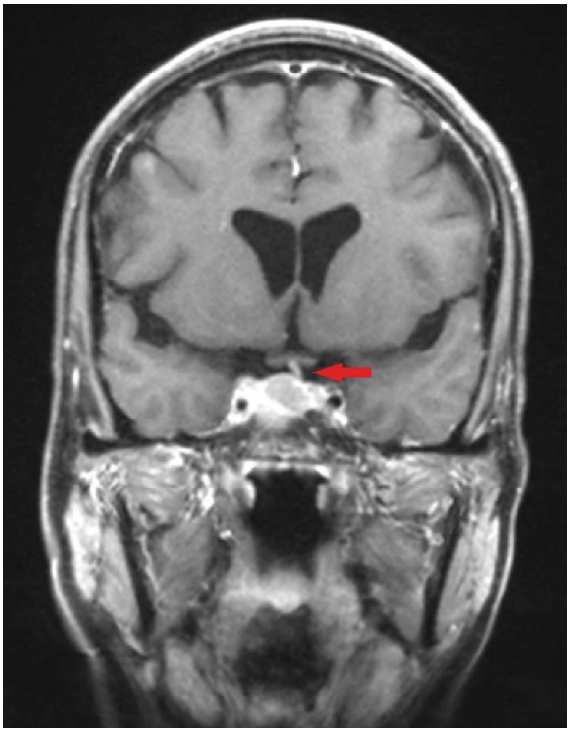

**Fig. 2.** Post-contrast coronal T1-weighted image shows a deviating pituitary stalk from the right to the left side (arrow).

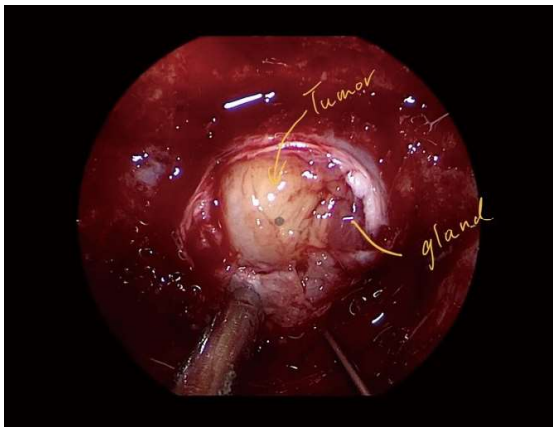


**Fig. 3.** Tumor was located on the right side (arrow), and the normal pituitary gland was located on the left aspect (line) of the sellar region.

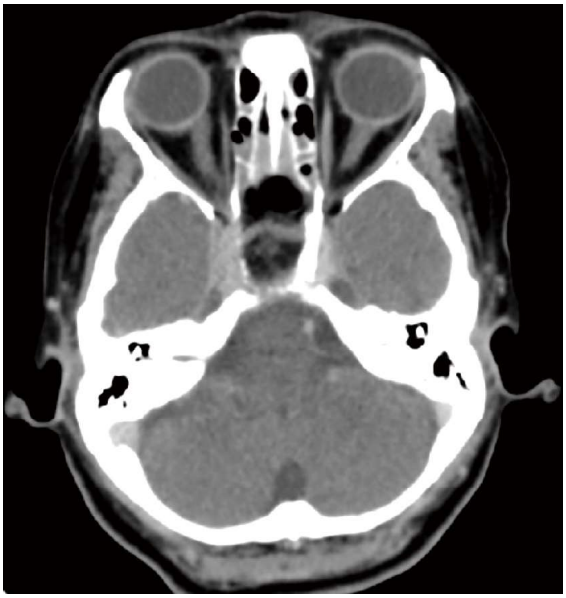

**Fig. 4.** Brain CT showed postoperative change and no residual pituitary tumor.

contrast coronal T1-weighted image revealed a pituitary stalk deviating from right to left (Figure 2). In addition, laboratory data showed an increased prolactin level (52.70 ng/ml, normal range 4.79-23.3 ng/ml).

Due to suspicion of a new metastatic lesion on the right side of the pituitary gland with visual tract compression, the patient underwent endoscopic trans-sphenoidal excision for removal of the pituitary tumor. During the operation, erosion of the dorsum sella, right posterior clinoid process, and upper part of the middle clivus by the tumor was observed. The normal pituitary gland was located on the left side of the sellar region (Figure 3). The frozen section during operation was reported to be metastatic carcinoma, and tumor debulking was performed. The interclinoid ligament was exposed and the oculomotor triangle with cranial nerve III (the oculomotor nerve) could be identified after tumor removal. Pathology revealed metastatic carcinoma-indicated adenohypophyseal tissue. The tumor cells were immunoreactive for P40 and the EGFR 19 deletion. Together with the clinical history of lung cancer, this was compatible with a metastatic carcinoma originating from the lung. After surgery, the prolactin level became normal (8.18 ng/ml). Brain CT showed a postoperative change and no residual pituitary tumor (Figure 4). However, the patient

passed away due to further cancer progression 2 months after surgery.

## Discussion

The cavernous sinus is a complex area rich in vital neurovascular structures. Approximately 90% of cavernous sinus tumors are pituitary adenomas. Metastatic lesions comprise approximately 1% of tumors in the cavernous sinus area [1].

The incidence of pituitary and cavernous sinus metastases among all intracranial metastases is 0.87% (95% CI: 0.56, 1.18) [1,2]. However, in autopsy series, latent pituitary metastases are revealed in approximately 5% of patients with known malignancy [3]. In a 380-case statistical analysis of the origin of primary tumors metastatic to the pituitary gland, patients with breast cancer or lung cancer had a higher incidence rate (39.7% and 23.7%, respectively) than those with other types of cancer [3].

Symptoms vary from nonspecific manifestations, such as fatigue and headache, to more specific symptoms of ophthalmoplegia, visual disturbance, ptosis, polyuria, and polydipsia. According to the literature review, visual problems are the most common first manifestation (48.8%) in cases of pituitary and cavernous sinus metastases. Cranial nerve palsies can be isolated, with the third (oculomotor) and sixth (abducens) nerves being the most commonly involved, followed by the fourth (trochlear) nerve [1,4]. Other primary clinical presentations are diabetes insipidus (38.4%), panhypopituitarism (37.7%), and headache (35.3%) [4-5].

Pituitary and cavernous sinus metastases are associated with a poor prognosis. However, it is hard to differentiate pituitary metastases from other cavernous sinus lesions on brain MRI or CT examination due to a lack of clear radiological features. Metastatic lesions are usually located within the sella and grow primarily in the suprasellar region. Therefore, the most common finding on MRI is an enhancing pituitary lesion with suprasellar extension [6]. Rapid growth of the lesion and erosion of cavernous sinus bony structures are also more likely to be metastases. Other findings that suggest the diagnosis of metastasis are a dumbbell-shaped appearance, stalk enhancement with thickening, and loss of the bright spot of the posterior lobe [3].

Treatments for pituitary and cavernous sinus tumors include surgery, radiation therapy, and chemotherapy. Most importantly, the tumor treatment strategy is mainly focused on local symptoms related to the tumor, such as visual problems and ophthalmoplegia. However, only surgery can confirm the diagnosis. Therefore, the endoscopic trans-sphenoidal excision and debulking procedure plays an important role in alleviating symptoms, improving quality of life, and confirming the diagnosis [7]. Radiotherapy also plays a crucial role in the management of pituitary and cavernous sinus metastases. One study reported that 6 of 7 patients achieved regional control and improved symptoms after stereotactic radiosurgery [8]. Another study revealed that 43% of patients had improvement in their diabetes insipidus and 50% of patients had improvement in their neurological symptoms or signs [9]. With regard to the limited life expectancy of patients with pituitary and cavernous sinus metastases, stereotactic radiosurgery is minimally invasive and appears to improve quality of life.

Pituitary and cavernous sinus tumors often result in panhypopituitarism. However, some patients with nonfunctioning pituitary adenoma had an elevated serum prolactin level. Lesser

degrees of hyperprolactinemia (typically in the range of 30 to 150 ng/ml) may likely indicate the presence of the "stalk effect". Only 4.2% of patients had a serum prolactin concentration higher than 90 ng/ml [10]. As in our case, the "stalk effect" indicates the compression of the pituitary stalk and interrupts the delivery of inhibitory dopamine from the hypothalamus, resulting in the disruption of prolactin control. A prolactin level of more than 200 ng per milliliter is usually diagnostic of macroprolactinoma [11].

## Conclusion

Metastasis to the pituitary or cavernous sinus is rare. Physicians should recognize any symptoms and signs indicating cranial nerve involvement, especially when the patient has a history of cancer. A high level of awareness of this condition coupled with immediate treatment is crucial to a favorable response to this urgent situation.

## References

1. Altay T, Krisht KM, Couldwell WT. Sellar and parasellar metastatic tumors. Int J Surg Oncol 2012; 2012: 647256.
2. He W, Chen F, Dalm B, *et al*. Metastatic involvement of the pituitary gland: a systematic review with pooled individual patient data analysis. Pituitary 2015; 18(1): 159-168.
3. Komninos J, Vlassopoulou V, Protopapa D, *et al*. Tumors metastatic to the pituitary gland: case report and literature review. J Clin Endocrinol Metab 2004; 89(2): 574-580.
4. Javanbakht A, D'Apuzzo M, Badie B, et al. Pituitary metastasis: a rare condition. Endocr Connect 2018 August; 7(10): 1049-1057.
5. Ahn Y, Yang JH, Kim HJ, *et al*. Cavernous sinus metastasis of non-small cell lung cancer. Tuberc Respir Dis 2010; 69(5): 381-384.
6. Schill F, Nilsson M, Olsson DS, *et al*. Pituitary metastases: a nationwide study on current characteristics with special reference to breast cancer. J Clin Endocrinol Metab 2019 August; 104(8): 3379-3388.
7. Alhashema A, Tahab M, Almomenc A. Pituitary metastasis of lung adenocarcinoma: Case report and literature review. Int J Surg Case Rep 2020; 67: 98-101.
8. Habu M, Tokimura H, Hirano H, *et al*. Pituitary metastases: current practice in Japan. J Neurosurg 2015 Oct; 123(4): 998-1007.
9. Kano H, Niranjan A, Kondziolka D, *et al*. Stereotactic radiosurgery for pituitary metastases. Surg Neurol 2009 Sept; 72(3): 248-255.
10. Kawaguchi T, Ogawa Y, Tominaga T. Diagnostic pitfalls of hyperprolactinemia: the importance of sequential pituitary imaging. BMC Res Notes 2014 August; 7: 555.
11. Melmed S. Pituitary-tumor endocrinopathies. N Engl J Med 2020 March; 382(10): 937-950.

# Anti-Melanoma Differentiation-Associated gene 5 Antibody-Positive Dermatomyositis With Rapidly Progressive Interstitial Lung Disease Following SARS-CoV-2 Infection: a Case Report

Bing-Chen Wu[1,2], Shu-Min Lin[1,2]

Anti-melanoma differentiation-associated gene 5 (MDA5) antibody-positive dermatomyositis (DM) is an uncommon autoimmune disorder, particularly clinically amyopathic dermatomyositis, and has a high risk of causing severe rapidly progressive interstitial lung disease (RP-ILD), with poor survival rates. It is hypothesized that SARS-CoV-2 infections may trigger autoimmune diseases, such as DM. We described a patient who was newly diagnosed with anti-MDA5 DM after SARS-CoV-2 infection. ***(Thorac Med 2023; 38: 154-160)***

Key words: Anti-MDA5 antibody-positive dermatomyositis, SARS-CoV-2 infection, rapidly progressive interstitial lung disease

## Introduction

The anti-melanoma differentiation-associated gene 5 (MDA5) is a myositis-specific autoantibody (MSA) linked to dermatomyositis (DM), particularly clinically amyopathic dermatomyositis (CADM). CADM is a form of DM characterized by classic skin symptoms without muscle weakness. The anti-MDA5 antibody has a high risk of causing severe, rapidly progressive interstitial lung disease (RP-ILD), with poor survival rates [1, 2]. Despite the implementation of early detection and a powerful combination of immunosuppressive treatments (including high-dose glucocorticoids, cyclosporine, and intravenous cyclophosphamide pulse) potentially improving the survival rate for anti-MDA5 DM patients, the mortality rate still remains considerable at 25%, even when employing triple therapy [3].

The development of new autoimmune diseases following severe acute respiratory syndrome coronavirus 2 (SARS-CoV-2) infection has been reported, encompassing both single-

[1]Department of Thoracic Medicine, Chang Gung Memorial Hospital, No.5, Fuxing St., Guishan Dist., Taoyuan County 333, Taiwan (R.O.C.), [2]School of Medicine, Chang Gung University, No.259, Wen-Hwa 1st Road, Guishan Dist., Taoyuan County 333, Taiwan (R.O.C.).
Address reprint requests to: Dr. Shu-Min Lin, 1Department of Thoracic Medicine, Chang Gung Memorial Hospital, No.5, Fuxing St., Guishan Dist., Taoyuan County 333, Taiwan (R.O.C.)

organ and systemic rheumatological conditions [4]. Recent studies suggest a potential connection between anti-MDA5 DM and SARS-CoV-2 infection, as well as other viruses [5-7]. However, definitive evidence for a direct correlation is lacking, and more research is needed. These findings highlight the need for a deeper understanding of viruses, especially the interplay between SARS-CoV-2 and the host immune response, leading to autoantibody production. Here, we document the case of a patient newly diagnosed with anti-MDA5 DM following a SARS-CoV-2 infection.

## Case Report

A 64-year-old woman with no known systemic diseases presented with 3 months of dyspnea, dry cough, and bilateral arthralgia. She had a 30-year history of working in a chemical fiber plant and was a non-smoker. She tested positive for coronavirus disease 2019 (COVID-19) on July 1, 2022, using a rapid test, and exhibited symptoms of dry cough and sore throat, indicating a mild disease. Shortness of breath and joint pain, involving distal and proximal interphalangeal joints, metacarpophalangeal joints, temporomandibular joint, elbows, shoulders, hips, back, and toes, developed after the SARS-CoV-2 infection on July 30, 2022. The joint pain was more severe in the mornings. She had received 4 doses of the SARS-CoV-2 vaccine, one each on July 25, 2021 (AstraZeneca), October 21, 2021 (AstraZeneca), January 15, 2022 (Moderna), and June 17, 2022 (Moderna). She experienced no fever, headache, nausea, vomiting, abdominal pain, or diarrhea.

Due to worsening shortness of breath, she visited the emergency room at St. Paul Hospital on October 17, 2022. Initial physical examination revealed Gottron's papules (Figure 1A & 1B). High-resolution computed tomography (HRCT) disclosed reticulation, thickened interlobular septum, and ground-glass opacities,

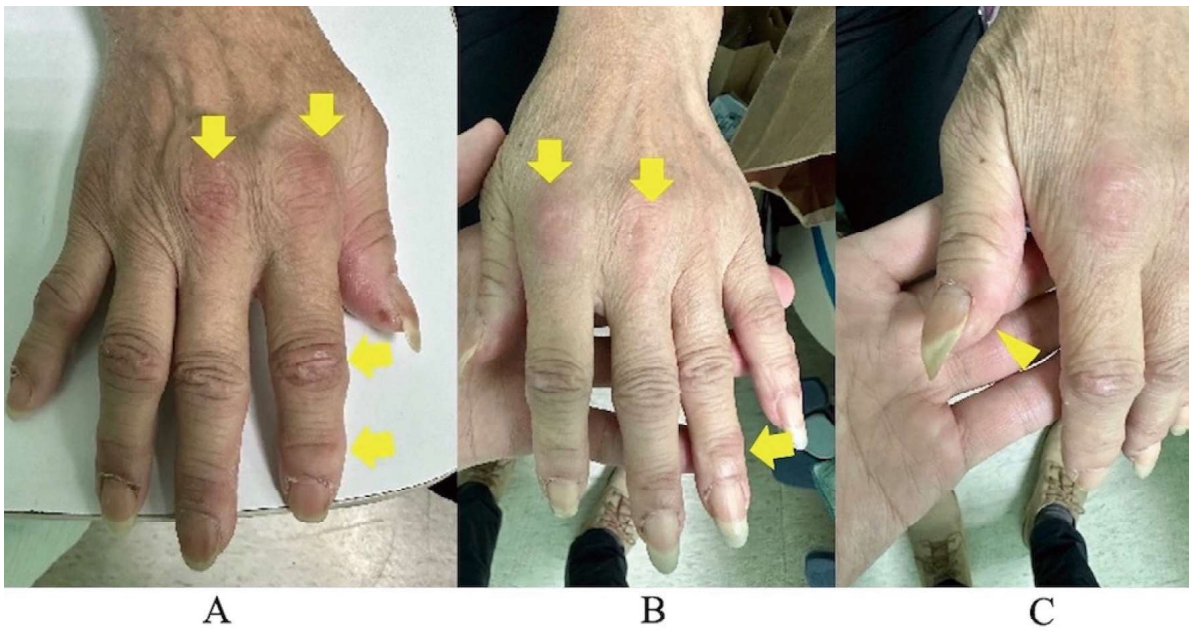


**Fig. 1.** (A, B) Flat erythema at the metacarpophalangeal (MCP) joints, proximal interphalangeal (PIP) joints and distal interphalangeal (DIP) joints (arrow) is referred to as Gottron's papules or Gottron's sign. (C) Periungual erythema was noted. (arrowhead)

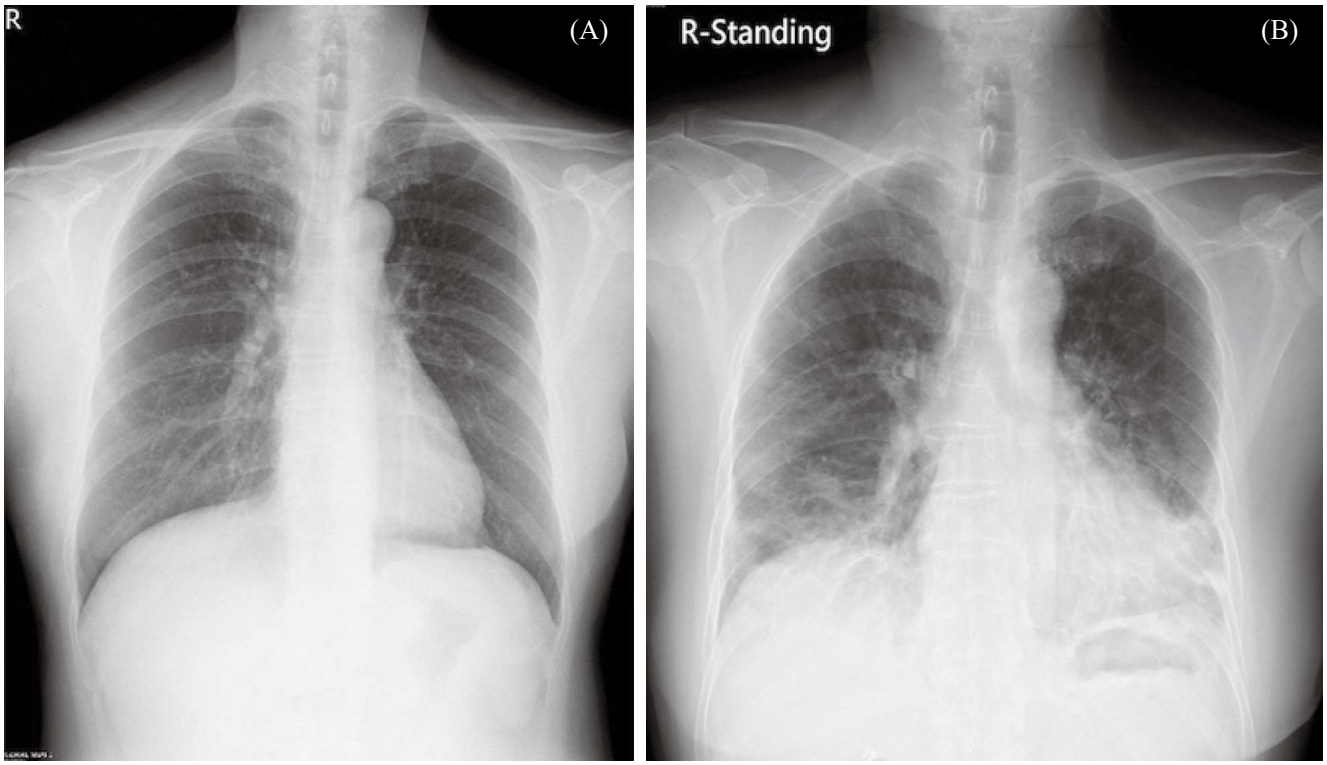


**Fig. 2.** (A) Baseline chest X-ray in 2016. (B) Chest X-ray on admission date revealed bilateral lower lung infiltrates.

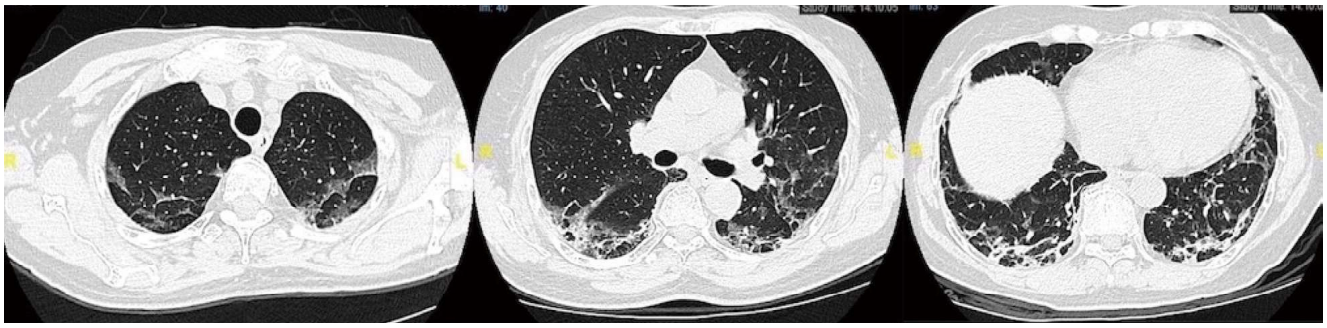

(A)

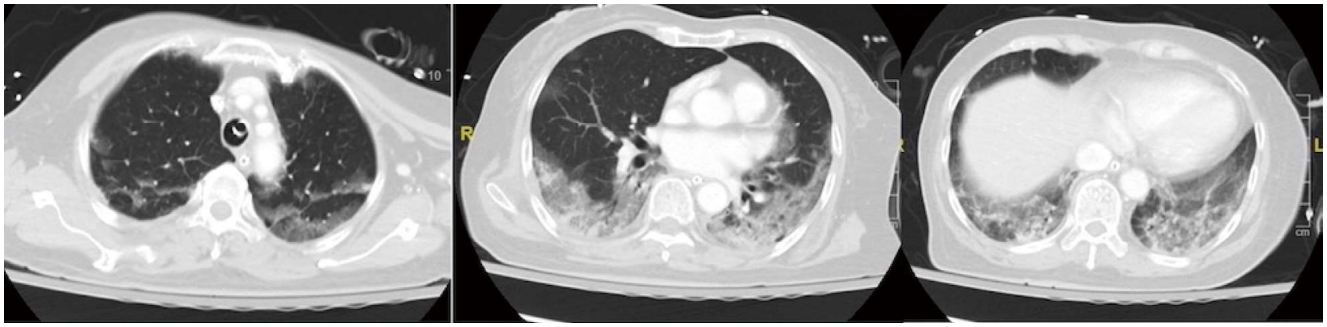

(B)

**Fig. 3.** (A) High-resolution computed tomography revealed reticulation, thickened interlobular septum, and ground-glass opacities. (B) Chest CT on the ninth day after admission showed peri-bronchial ground-glass and consolidative opacities with reticulation in both lungs, particularly the lower lobes.

suggesting interstitial lung disease (Figure 3A). She was subsequently transferred to our emergency department.

At the emergency department, her vital signs included a body temperature of 35.8°C, blood pressure of 128/60 mmHg, respiratory rate of 24 breaths per minute, and heart rate of 78 beats per minute. Her oxygen saturation was 92% on room air. Physical examination revealed bibasilar crackles in both lungs, a positive Gottron's sign, periungual erythema (Figure 1C), and proximal limb weakness. Laboratory results showed a white blood cell count of 9,700/ul with 88.8% neutrophils, 6.0% lymphocytes, and 5.1% monocytes, hemoglobin of 10.0 g/dl, a platelet count of 282,000/ul, and C-reactive protein of 9.06 mg/l. Her ferritin level was elevated at 1,415 ng/ml. Chest X-ray showed bilateral lower lung infiltrates (Figure 2B), compared with a baseline plain film in 2016 (Figure 2A). Sputum and blood cultures for any bacteria or atypical pathogen were negative. An immunoblot myositis panel revealed a strong positive result for MDA5. She was diagnosed with anti-

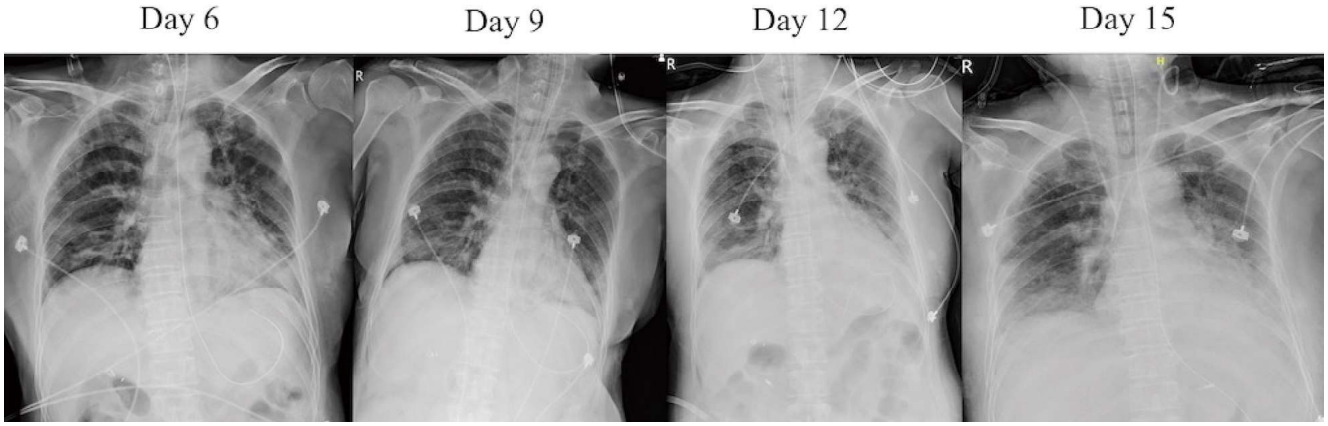


**Fig. 4.** Serial chest X-ray during hospitalization on days 6, 9, 12 and 15.

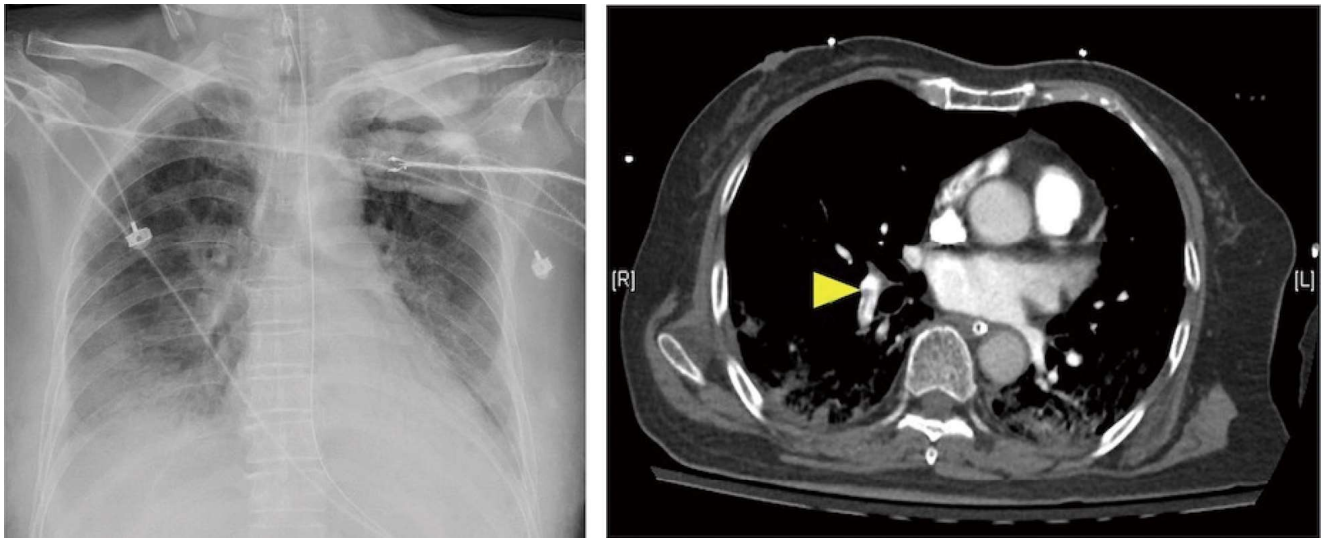


(A) (B)

**Fig. 5.** (A) Chest X-ray on the 19th day after admission revealed right lower lobe consolidation. (B) Chest CT showed filling defect in the right lower lobe segmental and subsegmental pulmonary arteries (arrowhead).

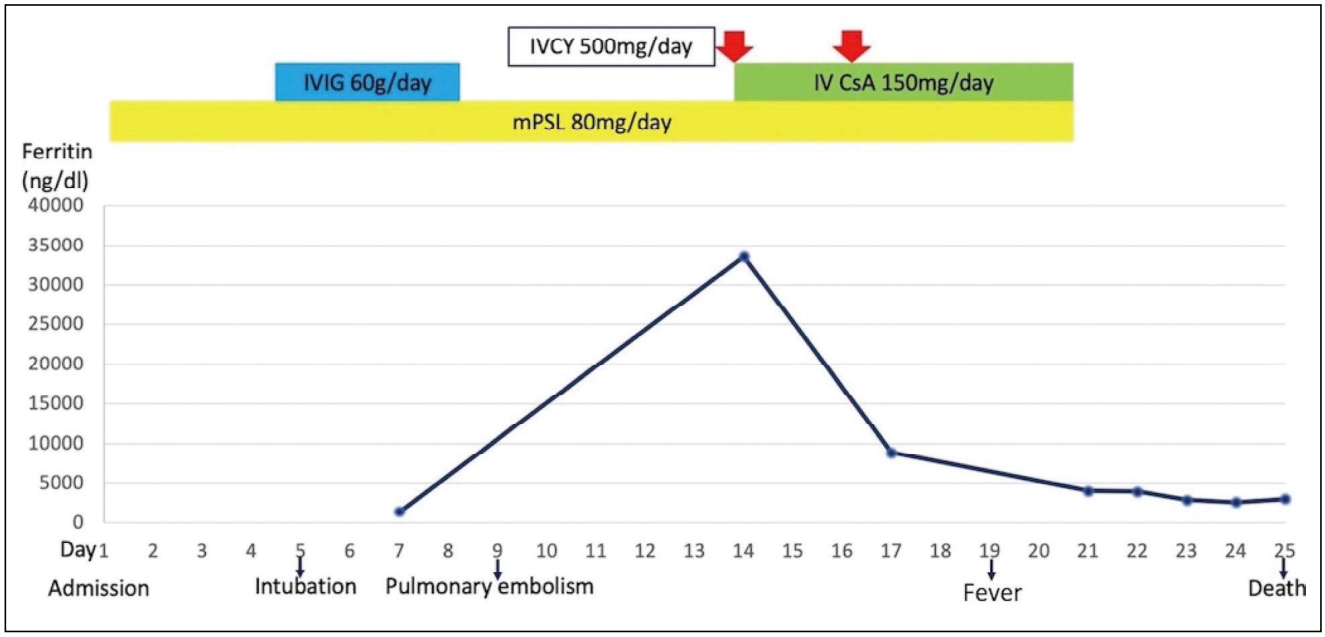


**Fig. 6.** Clinical course of the patient. IVCY=intravenous cyclophosphamide (red arrows), IVIG=intravenous immunoglobulin, CsA=cyclosporin, mPSL=methylprednisolone.

MDA5 dermatomyositis with interstitial lung disease and admitted to the rheumatology ward.

Upon admission, she received methylprednisolone (80 mg/day). On the fifth day after admission, she developed hypoxemic respiratory failure and was placed on mechanical ventilation. Intravenous immunoglobulin (IVIG, 60 g/day) was administered. A subsequent chest CT scan on the ninth day after admission showed peri-bronchial ground-glass and consolidative opacities with reticulation in both lungs, particularly the lower lobes (Figure 3B), and acute pulmonary embolism in the right lower lobe segmental and subsegmental pulmonary arteries (Figure 5B).

Bronchoalveolar lavage was performed, and showed no evidence of pulmonary infection. All tests for hyper-coagulation status, including anti-phospholipid syndrome, were negative. Enoxaparin was given, but she experienced upper gastrointestinal bleeding on the second day of enoxaparin use. Intravenous cyclosporine (150 mg/day) and cyclophosphamide (500 mg, twice a week) were added due to a further increase in ferritin levels (33,565 ng/ml) (Figure 6). (Serial chest X-rays are shown in Figure 4.)

She developed a fever on the 19th day after admission. Blood and sputum cultures identified multi-drug-resistant Acinetobacter baumannii, indicating sepsis. Chest X-ray also showed development of consolidation in the right lower lung (Figure 5A). All immunosuppressant agents were halted and an intensive course of antibiotics was initiated. Despite these efforts, the patient's condition deteriorated due to sepsis and she passed away on the 25th day after admission.

## Discussion

We presented a case of fatal anti-MDA5 DM-associated RP-ILD occurring after SARS-CoV-2 infection, providing valuable insights into the potential association between CO-

VID-19 and this rare autoimmune condition, although a definitive causal link remains to be established.

Viral infections, including SARS-CoV-2, are theorized to trigger autoimmune diseases like inflammatory myopathies [8], potentially through molecular mimicry [9]. In DM patients, researchers have discovered immunogenic epitopes similar to SARS-CoV-2 proteins, which could explain how autoantibody production is initiated [10]. Autoantibodies targeting antiviral signaling proteins, MDA5 and retinoic acid-inducible gene I (RIG-I), have been reported in COVID-19 patients. These proteins play a role in innate antiviral immunity, detecting double-stranded ribonucleic acid (dsRNA) intermediates and activating a signaling pathway that results in type I interferon (IFN) production. Both RNA viruses and IFN can increase MDA5 expression, enhancing the overall process. Following viral-induced cell destruction, dsRNA-MDA5/RIG-I complexes can serve as cryptic antigens, promoting autoantibody production [9]. It is still unclear whether these autoantibodies have a harmful effect or merely signify an abnormal immune response.

Patients with anti-MDA5 DM often experience RP-ILD, which can lead to a poor prognosis due to the disease's severity and rapid progression. In Asia, the 90-day survival rate for these patients is only 67% [11]. While early detection and treatment of anti-MDA5 DM are crucial for improving patient outcomes, distinguishing rapidly worsening symptoms such as shortness of breath, weakness, increased muscle enzymes, and pulmonary involvement associated with anti-MDA5 DM from those caused by severe bacterial pneumonia can be challenging.

Prompt initiation and aggressive combination therapy with immunosuppressants are crucial for survival in patients with anti-MDA5-associated RP-ILD [12, 13]. Retrospective studies suggest benefits from initial combination therapies, including steroids, tacrolimus, cyclophosphamide, mycophenolate mofetil, and rituximab [14, 15]. A recent study showed that adjunct IVIG therapy is highly effective as a first-line treatment for anti-MDA5 DM-related RP-ILD patients, improving survival and remission by reducing ferritin concentration [16]. Poor prognostic indicators identified in 1 study include serum ferritin levels over 1000 ng/mL before therapy, ground-glass opacities in all 6 lung fields before therapy, and worsening pulmonary infiltrates during therapy. Patients with all 3 factors typically succumb to the disease despite receiving triple immunosuppressive therapy [17].

## Conclusion

This case report highlights the potential association between SARS-CoV-2 infection and the development of anti-MDA5 DM with RP-ILD. Clinicians should be aware of this possible relationship; however, further research is needed to understand the underlying mechanisms and establish a definitive link between COVID-19 and this rare autoimmune condition. Early recognition and prompt treatment initiation may improve outcomes for these patients.

## References

1. Rebendenne A, Chaves Valadão AL, Tauziet M, *et al*. SARS-CoV-2 triggers an MDA-5-dependent interferon response which is unable to control replication in lung epithelial cells. J Virol 2021; 95(8): e02415-20.
2. Yin X, Riva L, Pu Y, *et al*. MDA5 governs the innate immune response to SARS-CoV-2 in lung epithelial cells. Cell Rep 2021; 34(2): 108628.

3. Nakashima R, Hosono Y, Mimori T. Clinical significance and new detection system of autoantibodies in myositis with interstitial lung disease. Lupus 2016; 25(8): 925-933.
4. Tonutti A, Motta F, Ceribelli A, *et al*. Anti-MDA5 antibody linking COVID-19, type I interferon, and autoimmunity: a case report and systematic literature review. Front Immunol 2022; 13: 937667.
5. Wang Y, Du G, Zhang G, *et al*. Similarities and differences between severe COVID-19 pneumonia and anti-MDA-5-positive dermatomyositis-associated rapidly progressive interstitial lung diseases: a challenge for the future. Ann Rheum Dis 2022; 81(10): e192-e192.
6. Carrasco L, Arthur A, Rueda JG, *et al*. A rapidly progressive and rare illness: autoantibodies against melanoma differentiation-associated protein 5 (anti-MDA5): amyopathic dermatomyositis with progressive interstitial lung disease that developed after covid-19 vaccine. Chest 2021; 160(4): A680-A681.
7. Mehta P, Machado PM, Gupta L. Understanding and managing anti-MDA 5 dermatomyositis, including potential COVID-19 mimicry. Rheumatol Int 2021; 41(6): 1021-1036.
8. Ercolini A, Miller S. The role of infections in autoimmune disease. Clin Exp Immunol 2009; 155(1): 1-15.
9. De Santis M, Isailovic N, Motta F, *et al*. Environmental triggers for connective tissue disease: the case of COVID-19 associated with dermatomyositis-specific autoantibodies. Curr Opin Rheumatol 2021; 33(6): 514-521.
10. Brito-Zerón P, Acar-Denizli N, Zeher M, *et al*. Influence of geolocation and ethnicity on the phenotypic expression of primary Sjögren's syndrome at diagnosis in 8310 patients: a cross-sectional study from the Big Data Sjögren Project Consortium. Ann Rheum Dis 2017; 76(6): 1042-1050.
11. Hozumi H, Fujisawa T, Nakashima R, *et al*. Comprehensive assessment of myositis-specific autoantibodies in polymyositis/dermatomyositis-associated interstitial lung disease. Respir Med 2016; 121: 91-99.
12. Chen Z, Cao M, Plana MN, *et al*. Utility of anti–melanoma differentiation–associated gene 5 antibody measurement in identifying patients with dermatomyositis and a high risk for developing rapidly progressive interstitial lung disease: a review of the literature and a meta-analysis. Arthritis Care Res 2013; 65(8): 1316-1324.
13. Kurtzman DJ, Vleugels RA. Anti-melanoma differentiation–associated gene 5 (MDA5) dermatomyositis: a concise review with an emphasis on distinctive clinical features. J Am Acad Dermatol 2018; 78(4): 776-785.
14. Nara M, Komatsuda A, Omokawa A, *et al*. Serum interleukin 6 levels as a useful prognostic predictor of clinically amyopathic dermatomyositis with rapidly progressive interstitial lung disease. Mod Rheumatol 2014; 24(4): 633-636.
15. Mao MM, Xia S, Guo BP, *et al*. Ultra-low-dose rituximab as add-on therapy in anti-MDA5-positive patients with polymyositis/dermatomyositis associated ILD. Respir Med 2020; 172: 105983.
16. Wang LM, Yang QH, Zhang L, *et al*. Intravenous immunoglobulin for interstitial lung diseases of anti-melanoma differentiation-associated gene 5-positive dermatomyositis. Rheumatology 2021; 61(9): 3704-3710.
17. Kurasawa K, Arai S, Namiki Y, *et al*. Tofacitinib for refractory interstitial lung diseases in anti-melanoma differentiation-associated 5 gene antibody-positive dermatomyositis. Rheumatology 2018; 57(12): 2114-2119.

# A Case of Pseudoachalasia Secondary to Adenocarcinoma of the Lung

Cheng-Hsi Yang[1], Yuan-Ming Tsai[1], Kuan-Hsun Lin[1], Tsai-Wang Huang[1]
Hsu-Kai Huang[1,2]

Achalasia is a rare disease, with an annual incidence of approximately 1.6 cases per 100,000 individuals and a prevalence of 10 cases per 100,000 individuals. Achalasia is usually diagnosed in patients between the ages of 25 and 60 years. The onset of symptoms, including dysphagia and body weight loss, is usually progressive. Differential diagnosis between idiopathic achalasia and pseudoachalasia is important. Due to the rarity and clinical similarity of these 2 conditions, these patients may be misdiagnosed and receive relatively ineffective treatment. Here we present the case of a patient who was diagnosed initially as having achalasia by esophageal manometric examination, but was eventually found to have adenocarcinoma of the lung. Relevant literature is also reviewed. ***(Thorac Med 2023; 38: 161-165)***

Key words: Pseudoachalasia; lung cancer

## Introduction

Achalasia is a rare disease, with an annual incidence of approximately 1.6 cases per 100,000 individuals and a prevalence of 10 cases per 100,000 individuals. Achalasia is usually diagnosed in patients between the ages of 25 and 60 years. The onset of symptoms, including dysphagia and body weight loss, is usually progressive. Differential diagnosis between idiopathic achalasia and pseudoachalasia is important. Due to the rarity and clinical similarity, these patients may be misdiagnosed and receive relatively ineffective treatment. Here, we present the case of a patient who was diagnosed initially as having achalasia by esophageal manometric examination, but was eventually found to have adenocarcinoma of the lung. Relevant literature is also reviewed.

## Case Report

A 70-year-old man visited our clinic because of dysphagia lasting for 2 weeks and

[1]Division of Thoracic Surgery, Department of Surgery, Tri-service General Hospital, National Defense Medical Center, Taipei, Taiwan, ROC, [2]Penghu Branch, Tri-service General Hospital, National Defense Medical Center, Taipei, Taiwan, ROC.
Address reprint requests to: Dr. Hsu-Kai Huang, Penghu Branch, Tri-service General Hospital, National Defense Medical Center, Taipei, Taiwan, ROC

body weight loss, from 78 kg to 56 kg, within 1 month. Physical examination showed no particular abnormality except the appearance of cachexia. Laryngoscope showed a cobblestone appearance at the posterior pharyngeal wall. After examination with upper-gastrointestinal endoscopy, which showed no intraluminal tumor, he was referred to our chest surgery department due to dysphagia, and a suspicion of achalasia. Upper gastrointestinal series with an air and barium double-contrast study revealed a bird-beak sign and segmental narrowing with a relatively intact mucosal pattern at the lower third of the esophagus, just above the esophagogastric junction. A dilated proximal esophagus was also noted (Figure 1). Chest X-ray film revealed a suspicious mass at the left lower field of the lung.

The Eckardt score was 8 during manometry. Esophageal manometry revealed no relaxation of the lower esophageal sphincter and pan-esophageal pressurization during swallowing. The elevated integrated resting pressure was 43 mmHg. A decreased distal contractile index, 102 mmHg*sec*cm, was recorded. Based on the Chicago classification, type II achalasia could be diagnosed (Figure 2).

Elevated carcinoembryonic antigen level was found via blood examination. Chest computed tomography (CT) revealed a lobulated, heterogeneous, and hypo-dense mass at the left lower lobe of the lung. Dilated esophagus was found (Figure 3). CT-guided biopsy of the lung tumor, brain magnetic resonance imaging, and

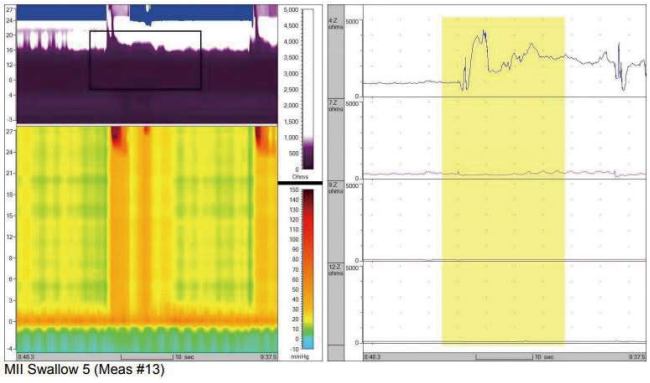


**Fig. 2.** Pan-esophageal pressurization was found in more than 50% of swallows, and an elevated integrated resting pressure up to 43 mmHg was recorded, manifesting as typical type II achalasia. The bolus clearance rate was almost zero.

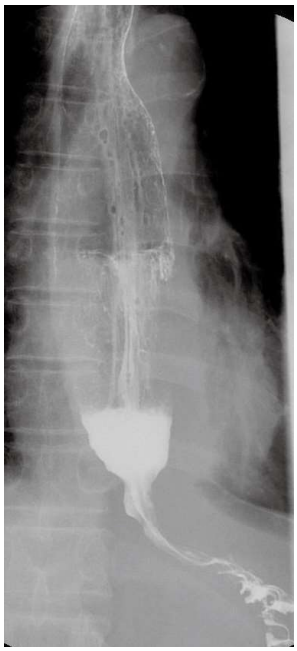

**Fig. 1.** Upper gastrointestinal series with an air and barium double-contrast study revealed a bird-beak sign and segmental narrowing with a relatively intact mucosal pattern at the lower third of the esophagus, just above the esophagogastric junction. Dilatation of the proximal esophagus was also noted.


**Fig. 3.** Chest computed tomography (CT) revealed a lobulated, heterogeneous, and hypo-dense mass at the left lower lobe of the lung, near the lower third of the esophagus. A dilated esophagus was found.

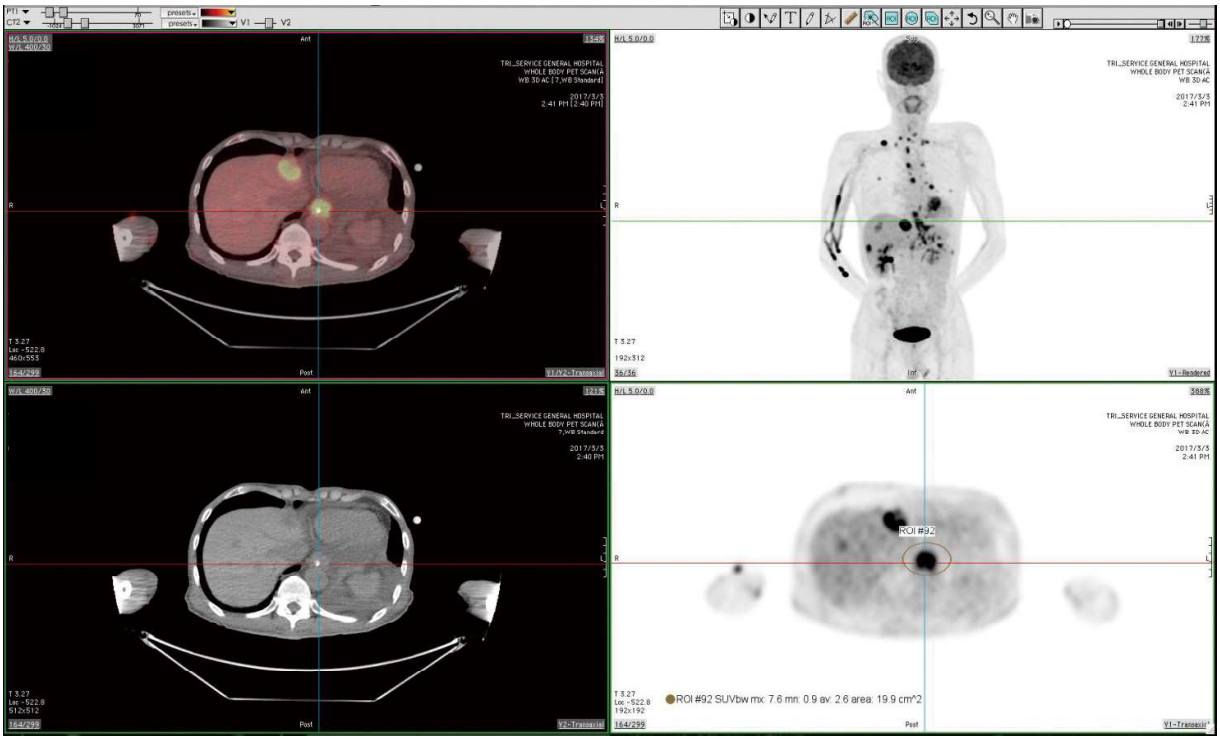


**Fig. 4.** The PET scan showed an ill-defined 18-F-fluorodeoxyglucose uptake avidity near the esophagogastric junction with wall thickening.

a whole-body positron emission tomography (PET) scan were performed. The PET scan showed an ill-defined 18-F-fluorodeoxyglucose uptake avidity near the esophagogastric junction, with wall thickening; the maximum standardized uptake value was around 7.6 (Figure 4). Adenocarcinoma of the left lower lobe of the lung, moderately differentiated, with metastases to the left upper lobe of the lung, the brain, liver, bone, and probably the lower mediastinum, cT4N3M1b, stage IVB, was diagnosed. We inserted a nasogastric tube to maintain the patient's enteral feeding. Target therapy with Tarceva, shifted to chemotherapy with concurrent radiotherapy, was arranged. During the treatment period, the nasogastric tube was removed and he was able to resume his oral intake of food. However, the disease still progressed. The patient died 1 year later.

## Discussion

Most cases of achalasia are idiopathic in nature. The progressive loss of inhibitory neurons of the myenteric plexus within the esophageal wall is the underlying mechanism [1,2]. Disease onset is seldom rapid. A small proportion of patients diagnosed as having achalasia initially are eventually found to have an underlying disease driving the process. They are diagnosed as "pseudoachalasia". Achalasia-like syndrome might be caused by submucosal infiltration of the myenteric plexus by tumor cells producing secondary neuronal inhibition of esophageal peristalsis. Another hypothesis is localized peripheral neuropathy of the vagus nerve [3,4]. The most common cause of pseudoachalasia secondary to neoplasia was adenocarcinoma of the esophagus or stomach, followed by breast

and non-small cell lung cancer. Renal cell carcinoma, cholangiocarcinoma, and even malignant mesothelioma have been reported as potential etiologies [5,6,7].

Achalasia is not prevalent among older patients – just 15% of patients more than 60 years old are diagnosed as having achalasia [8]. Patients with pseudoachalasia had symptomatic dysphagia for a much shorter time than did patients with idiopathic achalasia [9,10]. Patients at a higher risk of developing pseudoachalasia versus idiopathic achalasia include those with an older age (≥55 years old), shorter duration of dysphagia (≤12 months), and pronounced weight loss (≥10 kg) [11,12,13]. Considering of our case's age and the rapid onset of his symptoms and signs, we hypothesized a causal relationship between the primary lung adenocarcinoma and his pseudoachalasia, via mechanisms such as paraneoplastic neurologic syndromes or direct tumor invasion of the myenteric plexus. This was demonstrated via the improvement in the patient's esophageal mobility when the nasogastric tube was removed during the treatment of his lung cancer.

The paraneoplastic effect driven by primary lung cancer that causes pseudoachalasia has been reported. The most common histologic type was small-cell lung carcinoma. Primary adenocarcinoma of the lung has been reported rarely – there are only 3 reported cases, 1 with concrete serological evidence and the others without [14-15]. In our literature review, we found no primary data for analysis of the relationship between disease stage and pseudoachalasia. The diagnosis of paraneoplastic syndrome was uncertain in this case, because there was a lack of evidence from surveillance of serological markers; therefore, specific medical treatment for paraneoplastic syndrome was not administered. Based on the image manifestation, tumor cells that infiltrated the vagus nerve or the myenteric plexus of the esophageal wall would be much more likely to have contributed to his dysphagia. The patient received radiotherapy for local control and his enteral nutrition recovered temporarily.

The true diagnosis is so important because the curative treatment for the 2 conditions is absolutely different. If the patient is misdiagnosed as having idiopathic achalasia, esophagoscopic dilatation is often the first-line treatment. However, this not only provides a short duration of symptomatic relief, but also delays the diagnosis and treatment of the underlying malignancy.

## Conclusion

Dysphagia might be a manifestation of adenocarcinoma of the lung. When achalasia is diagnosed via esophageal manometry, detailed history-taking, physical examination, and endoscopic and image examinations are mandatory to exclude pseudoachalasia. The proper treatment can then be administered based on the primary cause.

## References

1. Spechler SJ, Castell DO. Classification of oesophageal motility abnormalities. Gut 2001; 49:145- 51.
2. Goldblum JR, Whyte RI, Orringer MB, *et al*. Achalasia. A morphologic study of 42 resected specimens. Am J Surg Pathol 1994; 18: 327-37.
3. Bholat OS, Haluck RS. Pseudoachalasia as a result of metastatic cervical cancer. JSLS 2001; 5: 57-62.
4. Shulze KS, Goresky CA, Jabbari M, *et al*. Esophageal achalasia associated with gastric carcinoma: lack of evidence for widespread plexus destruction. Can Med Assoc J 1975; 112: 857-64.
5. Katzka DA, Farrugia G, Arora AS. Achalasia secondary

to neoplasia: a disease with a changing differential diagnosis. Dis Esophagus 2012 May; 25(4): 331-336.
6. Campo SM, Zullo A, Scandavini CM, *et al*. Pseudoachalasia: a peculiar case report and review of the literature. World J Gastrointest Endosc 2013; 5: 450-4.
7. Gockel I, Eckardt VF, Schmitt T, *et al*. Pseudoachalasia: a case series and analysis of the literature. Scand J Gastroenterol 2005; 40: 378-85.
8. Reynolds JC, Parkman HP. Achalasia. Gastroenterol Clin North Am 1989; 18: 223-55.
9. Tracey JP, Traube M. Difficulties in the diagnosis of pseudoachalasia. Am J Gastroenterol 1994; 89: 2014-8.
10. Kahrilas PJ, Kishk SM, Helm JF, *et al*. Comparison of pseudoachalasia and achalasia. Am J Med 1987; 82: 439-46.
11. Kahrilas PJ, Kishk SM, Helm JF, *et al*. Comparison of pseudoachalasia and achalasia. Am J Med 1987; 82: 439-46.
12. Ponds FA, Moonen A, Smout A, *et al*. Screening for dysplasia with Lugol chromoendoscopy in longstanding idiopathic achalasia. Am J Gastroenterol 2018; 113: 855-62.
13. Rozman RW Jr, Achkar E. Features distinguishing secondary achalasia from primary achalasia. Am J Gastroenterol 1990; 85:1327-30.
14. Lee HR, Lennon VA, Camilleri M. Paraneoplastic gastrointestinal motor dysfunction: clinical and laboratory characteristics. Am J Gastroenterol 2001 Feb; 96(2):373-9. doi: 10.1111/j.1572-0241.2001.03454.x.
15. Hirano T, Miyauchi E, Inoue A, *et al*. Two cases of pseudo-achalasia with lung cancer: case report and short literature review, Respir Investig 2016 Nov; 54(6): 494-499.

# Linezolid-Induced Discoloration of the Teeth and Tongue in Patients With Drug-Resistant Tuberculosis: A Report of Two Cases

Pei-Ya Liao[1], Ko-Yun Chang[1], Ming-Feng Wu[1,2], Hui-Chen Chen[1]
Wei-Chang Huang[1,3], Cha-Wen Lee[4*], Shin-Shin Liu[5*]

The purpose of this report was to describe the cases and different pathophysiology of two patients with drug-resistant tuberculosis (TB) who experienced the embarrassing side effects of oral discoloration after using linezolid. One patient had pre-extensively drug-resistant TB (pre-XDR TB), and the other had multidrug-resistant TB (MDR-TB). The former received a bedaquiline-pretomanid-linezolid (BPaL) regimen, and the latter was treated with moxifloxacin, bedaquiline, linezolid and cycloserine. The first patient developed discoloration of her tongue around one and a half months after treatment with the BPaL regimen, while the other patient developed discoloration of her teeth following one month of treatment with the linezolid-containing regimen, with linezolid being considered the culprit causing these anomalies. We referred the patients to a dentist, who excluded other possible etiologies (such as poor oral hygiene), and cleaned their oral cavities. This substantially improved the black hairy tongue and tooth pigmentation despite the continued use of linezolid-containing regimens. To determine whether linezolid is the offending agent, other predisposing conditions should be excluded and the culprit drugs discontinued. However, considering that linezolid plays an important role in the treatment of drug-resistant TB in international guidelines, continued use of linezolid and early referral to a dentist for multidisciplinary combined care are warranted. ***(Thorac Med 2023; 38: 166-172)***

Key words: Black hairy tongue; tooth discoloration; drug-resistant tuberculosis; linezolid

[1]Division of Chest Medicine, Department of Internal Medicine, Taichung Veterans General Hospital, Taichung, Taiwan, [2]Department of Medical Laboratory Science and Biotechnology, Central Taiwan University of Science and Technology, Taichung, Taiwan, [3]Department of Post-Baccalaureate Medicine, College of Medicine, National Chung Hsing University, Taichung, Taiwan, [4]Department of Internal Medicine, Taichung Veterans General Hospital, Taichung, Taiwan, [5]Nursing Department, Taichung Veterans General Hospital, Taichung, Taiwan, *These authors contributed equally to this work.
Address reprint requests to: Dr. Pei-Ya Liao, Division of Chest Medicine, Department of Internal Medicine,Taichung Veterans General Hospital,1650 Taiwan Boulevard Sect. 4, Taichung, Taiwan 40705

## Introduction

Tuberculosis (TB) is one of the most infectious diseases worldwide, and is spread via the inhalation of aerosol droplets containing Mycobacterium tuberculosis complex (MTBC). The disease most often affects the lungs and is considered to be curable and preventable. The World Health Organization (WHO) reported in 2020 that an estimated 10 million people had TB [1]. Furthermore, 1.3 million human immunodeficiency virus (HIV)-negative people and an additional 208,000 HIV-positive people died from TB globally in 2020 [1]. In addition, 132,222 cases of multidrug-resistant (MDR)/rifampin-resistant (RR)-TB and 25,681 cases of pre-extensively drug-resistant TB (pre-XDR TB) or XDR-TB were detected globally in 2020 [1].

The WHO guidelines for the treatment of drug-resistant TB recommend linezolid, a bacteriostatic antibiotic in the oxazolidinone class [2]. Linezolid has a unique binding site located on the 50S subunit of 23S ribosomal RNA, which prevents 70S ribosomal unit formation and inhibits protein synthesis. It is used in the treatment of infections caused by aerobic Gram-positive bacteria, particularly vancomycin-resistant enterococcus, non-tuberculous mycobacteria, and drug-resistant TB [3-4]. Common side effects following linezolid treatment include diarrhea, gastrointestinal upset, changes in the patient's sense of taste, rashes, irreversible peripheral and optic neuropathy, and bone marrow suppression [2]. Herein, we present the two cases with drug-resistant TB with rare adverse effects that originated from different pathophysiology but resulted in embarrassing discoloration following the use of linezolid.

## Case Report

### *Case 1*

A 35-year-old female who had moved to Taiwan from China visited the outpatient department of Taichung Veterans General Hospital with the presentations of productive cough and excessive sweating over a period of two months, although no fever was noted during her visit, and she had no underlying comorbidities. A chest X-ray (Figure 1) and computed tomography (CT) (Figure 2) showed several micronodular lesions at the bilateral upper lungs, and alveolar infiltrates at the left retrocardiac region. Sputum specimens were collected and underwent acid-fast staining, which showed positive results, and a culture yielded MTBC. Owing to her history of previously residing in China, a country with a high burden of drug-resistant TB, the Xpert MTB/RIF test was performed by the

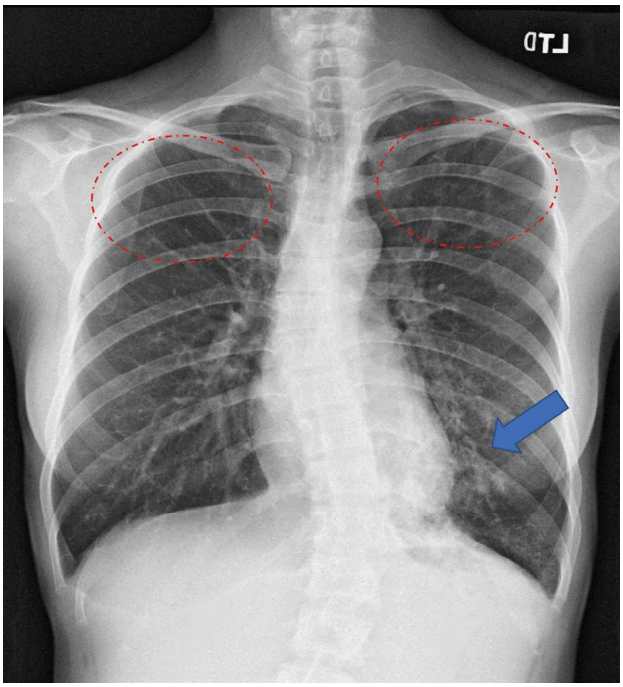

**Fig. 1.** Chest X-ray revealed micronodular lesions (red dashed circles) at the left upper and right upper lung fields, and consolidations (blue arrow) at the left lower lung field.

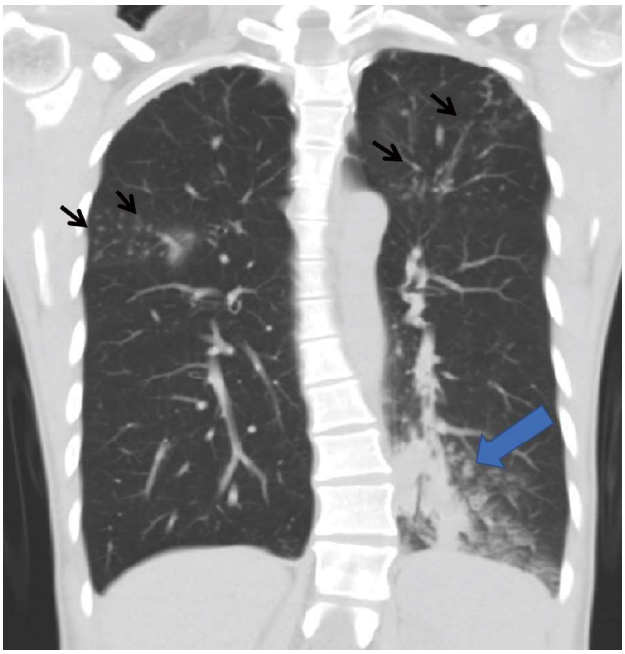

**Fig. 2.** Computed tomography of the chest revealed micronodular lesions (black arrows) at the left upper and right upper lung lobes, and consolidations (blue arrow) at the left lower lung lobe.

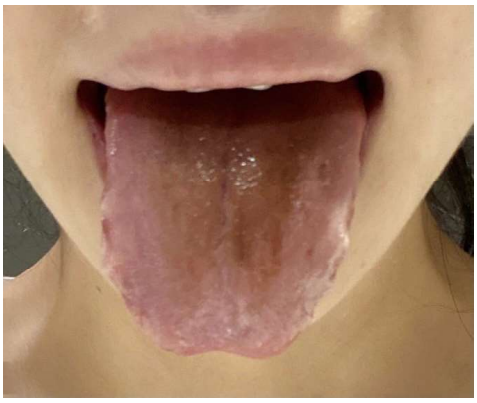

**Fig. 3.** The patient (Case 1) with pre-XDR (pre-extensively drug resistant) TB who received the BPaL (bedaquiline-pretomanid-linezolid) regimen presented with a black hairy tongue.

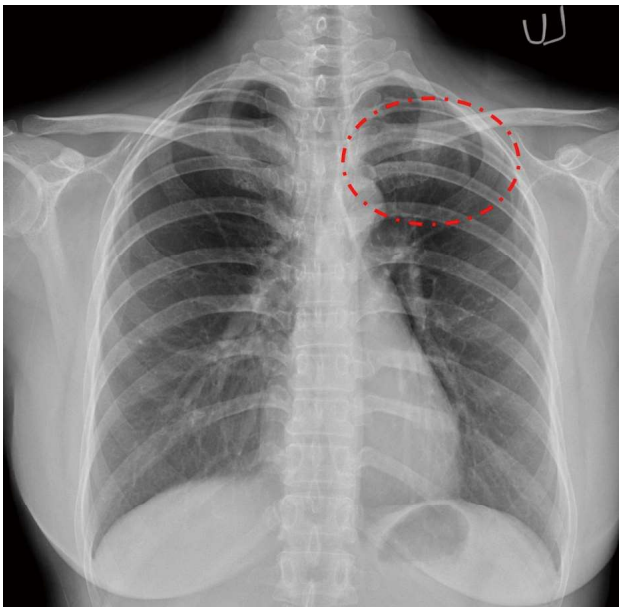

**Fig. 4.** A cavitary lesion at the left upper lung (within the red circle).

national reference laboratory, according to the Taiwan Centers for Disease Control policy, and revealed rifampin resistance. Therefore, further phenotypic and molecular drug susceptibility testing (DST) for first-line and second-line anti-TB drugs was performed. The results showed that the offending MTBC strain was resistant to all of the first-line anti-TB drugs as well as fluoroquinolones, but susceptible to linezolid and bedaquiline. Thus, she was diagnosed with pre-XDR TB [5], and the bedaquiline-pretomanid-linezolid (BPaL) regimen was prescribed [6]. However, a black coating on the surface of her tongue was noted one and a half months after starting the BPaL regimen (Figure 3), although there was no change in her perception of taste. We referred the patient to a dentist, who found no remarkable infections and excluded other possible causes (such as poor oral hygiene) of the tongue discoloration. Therefore, tongue cleaning was performed, and the tongue discoloration subsequently faded.

### *Case 2*

A 41-year-old previously healthy female who had been living in Taiwan for 20 years, but was originally from Vietnam, presented with no history of systemic disorders. She had initially visited another hospital due to persistent cough for two months, where chest X-ray (Figure 4) and CT (Figure 5) revealed the

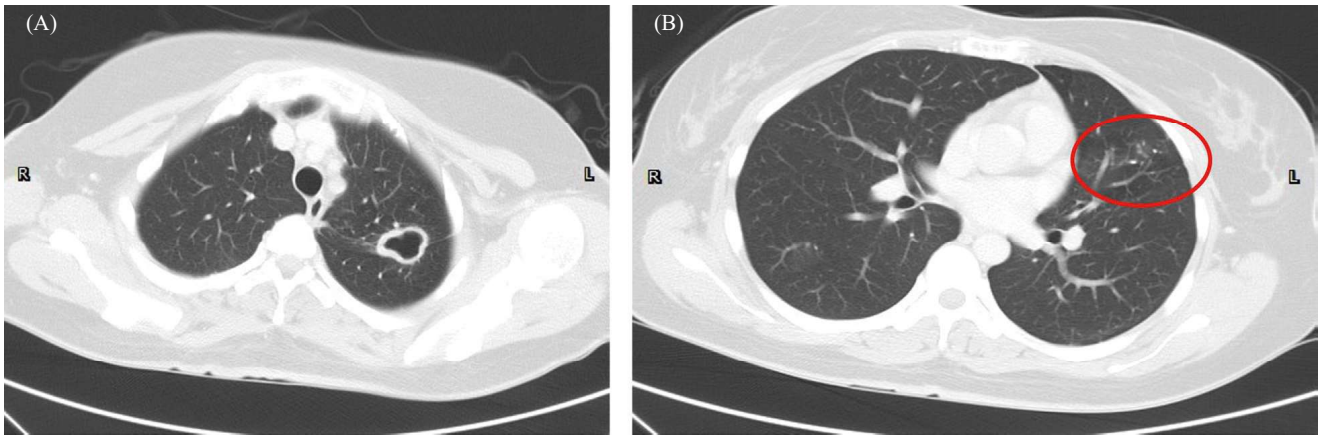


**Fig. 5.** One cavitary lesion (A) and micronodular lesions (B) (within the red circle) at the left upper lung lobe.

abnormal findings of one cavitary lesion along with micronodular lesions at the left upper lobe. Sputum smear examinations, cultures, nucleic acid amplification tests, and bronchoalveolar lavage (BAL) were performed due to the suspicion of pulmonary TB, and the BAL yielded a positive culture for MTBC. She then began anti-TB chemotherapy with isoniazid, rifampin, ethambutol and pyrazinamide. Meanwhile, the MTBC strain was sent to the national reference laboratory for DST due to the patient's history of once residing in Vietnam, a country with a high burden of drug-resistant TB. This was in accordance with the national TB control policy of the Taiwan Centers for Disease Control. The DST concluded that the offending strain was resistant to all of the first-line anti-TB drugs except for pyrazinamide. In addition, the offending strain was susceptible to all tested second-line anti-TB drugs, except for ethionamide. Therefore, she was diagnosed with MDR-TB. Accordingly, her treatment regimen was then shifted to moxifloxacin, bedaquiline, linezolid and cycloserine. However, one month after the initiation of this regimen, she noticed discoloration of her teeth (Figure 6). She then visited a dentist who concluded that the discolored teeth could be related to the use of linezolid rather than poor oral hygiene or other etiologies. She received regular dental scaling treatment, after which the discoloration of her teeth improved.

**Fig. 6.** The patient (Case 2) with multidrug-resistant tuberculosis who received anti-tuberculosis agents presented with discoloration of her teeth.

Both patients denied any history of such discoloration of the tongue and teeth prior to the start of linezolid treatment. They also denied any history of smoking or increased intake of tea, coffee or alcohol that could possibly have

caused the tongue and teeth to become discolored. In addition, the dentists confirmed that neither patient had poor oral hygiene. Both patients were young and had no systemic diseases, and neither was taking any possible culprit drugs. Furthermore, there were no signs of fever, chills, skin rashes or other possible infections. A dentist showed Case 1 how to perform daily tongue brushing, and the dentist performed regular tooth scaling for Case 2. After evaluating the pros and cons and discussing the treatment plans with the patients, it was decided that linezolid would be continued as part of the treatment regimen in both patients.

## Discussion

MDR/RR-TB, pre-XDR TB and XDR-TB are major challenges in terms of achieving a cure and reducing mortality, due to resistance to the most important medications against TB [7]. The WHO updated the guidelines for the treatment of MDR/RR-TB in 2019, and classified anti-TB medications into Group A, B, and C, based on their efficacy (Table 1) [8]. The updated guidelines recommend that ideally all the three Group A agents and at least one Group B agent should be included in the intensive phase, and that at least four effective agents should be used [8]. In addition, if all three Group A agents are not included, both Group B agents should be included and a total of at least five effective agents should be used [8]. The guidelines also recommend that the duration of a longer treatment regimen should be up to 18-20 months or 15-17 months after culture conversion for most patients, although this can be modified based on the response to therapy [8]. Regarding drug intolerance and long treatment duration, the BPaL regimen, containing bedaquiline, pretomanid and linezolid, has recently been recommended for patients with no previous exposure (>2 weeks) to bedaquiline or linezolid and who meet the definition of MDR-TB with additional fluoroquinolone resistance (pre-XDR TB group), with a treatment duration of 6-9 months [8-10].

Linezolid is an oxazolidinone antibiotic

**Table 1.** Classification of Medications for Multidrug-Resistant Tuberculosis in the 2019 World Health Organization Guidelines

| Group | Medicine | Step |
|---|---|---|
| A | Levofloxacin or moxifloxacin<br>Bedaquiline<br>Linezolid | Include all three medicines (unless they cannot be used) |
| B | Clofazimine<br>Cyloserine or terizidone | Add one or both medicines (unless they cannot be used) |
| C | Ethambutol<br>Delamanid<br>Pyrazinamide<br>Imipenem-cilastatin or meropenem<br>Amikacin or streptomycin<br>Ethionamide or prothionamide<br>Para-aminosalicylic acid | Add to complete a four-to five drug regimen when medicine from group A and B cannot be used |

that inhibits bacterial protein synthesis by preventing the fusion of 30S and 50S ribosome subunits. In the 2016 WHO guidelines, linezolid was classified as a Group C agent and recommended as another core drug for MDR-TB treatment [11]. However, in the 2019 WHO guidelines, linezolid was reclassified to Group A, indicating the highest priority for use in the management of patients with MDR/RR-TB [8]. Although linezolid has now become a core agent in the treatment of MDR/RR-TB, its adverse effects and toxicity, particularly critical adverse effects such as peripheral neuropathy, myelosuppression and optic neuropathy, should be closely monitored whenever prescribed [2]. Moreover, linezolid may induce adverse effects that are not life-threatening or permanent, but still have an impact on appearance, including black hairy tongue and teeth discoloration, as seen in our cases.

Black hairy tongue originates from hypertrophy and elongation of the papilla on the surface of the tongue [12]. Bacteria and fungi then coat the structures with delayed shedding compared to a normal course, thus creating hair-like projections. In addition to linezolid treatment as an etiology, it is important to investigate the patient's history in detail to identify any other possible etiologies. Such etiologies may include consuming certain beverages, cigarette smoking and/or betel nut chewing, concurrent treatment involving chemotherapy and/or radiation therapy, or previous tetracycline use during childhood, and even other systemic diseases such as Sjogren's syndrome [12-14].

Tooth discoloration is classified as intrinsic or extrinsic [15-17]. Intrinsic tooth discoloration is caused by endogenous material that is incorporated into the tooth structure during the development of deciduous tooth crowns, while the extrinsic type is caused by material staining the surface of the teeth. Chromogens deposited within the teeth, particularly during odontogenesis, can lead to the intrinsic type of tooth discoloration. Other etiologies, including vitamin D deficiency, infection (such as measles) or trauma during pregnancy, can also lead to discoloration of the teeth. Medications, including tetracycline and minocycline, are well-known causes of the intrinsic type of tooth discoloration, and linezolid has also been reported to be the cause of extrinsic tooth discoloration in several case reports [13,18].

Although linezolid-related black hairy tongue and tooth discoloration originate from different pathophysiology and are not life-threatening adverse effects, they are still important issues for certain patients, as they may cause embarrassment when communicating with others. Fortunately, both conditions are benign and can be improved by discontinuing the offending drug and/or through oral cavity cleaning when linezolid is continued, as in our cases [10,12].

Linezolid plays a critical role in the treatment regimen for MDR/RR-TB, according to the WHO 2019 guidelines [8], and its role has been updated in the 7th edition of the Taiwan Centers for Disease Control Guidelines for Tuberculosis Diagnosis and Treatment [19]. Therefore, clinicians should carefully monitor both the critical and the embarrassing adverse effects of linezolid as it becomes a central part of the treatment regimen for patients with MDR/RR-TB infection. When teeth pigmentation changes or black hairy tongue occurs, and linezolid treatment for drug-resistant TB is maintained, early referral to a dentist for detailed inspection, and multidisciplinary combined care are the crucial clinical strategies.

## References


1. World Health Organization. Global Tuberculosis Report 2020. Geneva: World Health Organization; 2021.
2. Hashemian SMR, Farhadi T, Ganjparvar M. Linezolid: a review of its properties, function, and use in critical care. Drug Des Devel Ther. 2018; 12: 1759-67.
3. Zhang X, Falagas ME, Vardakas KZ, *et al*. Systematic review and meta-analysis of the efficacy and safety of therapy with linezolid-containing regimens in the treatment of multidrug-resistant and extensively drug-resistant tuberculosis. J Thorac Dis. 2015; 7(4): 603-15.
4. Winthrop KL, Ku JH, Marras TK, *et al*. The tolerability of linezolid in the treatment of nontuberculous mycobacterial disease. Eur Respir J. 2015; 45(4): 1177-79.
5. World Health Organization (27,Jan,2021). WHO announces updated definitions of extensively drug-resistant tuberculosis. Available at: https://www.who.int/news/item/27-01-2021-who-announces-updated-definitions-of-extensively-drug-resistant-tuberculosis
6. World Health Organization. WHO consolidated guidelines on tuberculosis, Module 4: treatment: drug-resistant tuberculosis treatment. Geneva: World Health Organization; 2020.
7. Chung-Delgado K, Guillen-Bravo S, Revilla-Montag A, et al. Mortality among MDR-TB cases: comparison with drug-susceptible tuberculosis and associated factors. PLoS One. 2015; 10(3): e0119332.
8. World Health Organization. WHO consolidated guidelines on drug-resistant tuberculosis treatment. Geneva: World Health Organization; 2019.
9. World Health Organization. WHO consolidated guidelines on tuberculosis: tuberculosis preventive treatment: Module 1: prevention. Geneva: World Health Organization; 2020.
10. Ma J-S. Teeth and tongue discoloration during linezolid therapy. Pediatr Infect Dis J. 2009; 28(4): 345-46.
11. World Health Organization. WHO treatment guidelines for drug-resistant tuberculosis 2016 update. Geneva, Switzerland: World Health Organization; 2016.
12. Kobayashi K, Takei Y, Sawada M, *et al*. Dermoscopic features of a black hairy tongue in 2 Japanese patients. Dermatol Res Pract. 2010; 2010: 145878.
13. Petropoulou T, Lagona E, Syriopoulou V, *et al*. Teeth and tongue discoloration after linezolid treatment in children. Pediatr Infect Dis J. 2013; 32(11): 1284-85.
14. Manabe M, Lim HW, Winzer M, *et al*. Architectural organization of filiform papillae in normal and black hairy tongue epithelium: dissection of differentiation pathways in a complex human epithelium according to their patterns of keratin expression. Arch Dermatol. 1999; 135(2): 177-181.
15. Thwaini M. A student's guide to tooth staining: diagnosis and management. BDJ Student. 2021; 28(3): 47-49.
16. Sulieman M. An overview of tooth discoloration: extrinsic, intrinsic and internalized stains. Dent Update. 2005; 32(8): 463-71.
17. Willian D. Basics of tooth staining-diagnosis and management. Eur J Mol Clin Med. 2020; 7(3): 1781-85.
18. Agrawal P, Prakash P, Pursnani N, *et al*. Linezolid-induced dental hyperpigmentation in an adult male being treated for an ulcer caused by atypical mycobacteria. J Family Med Prim Care. 2018; 7(6): 1576-77.
19. Centers for Disease Control, Ministry of Health and Welfare, R.O.C. (Taiwan). Taiwan Guidelines for TB Diagnosis & Treatment (7E). Centers for Disease Control, Ministry of Health and Welfare, R.O.C.(Taiwan), 2022.

# Pulmonary Vein Puncture During Port Implantation: A Rare and Abnormal Route

Chun-Hao Wang[1], Pei-Hsing Chen[2]

This study presents the case of a 56-year-old woman with breast cancer who underwent implanted catheter surgery via the left subclavian vein, under general anesthesia. However, chest radiography revealed the implantation had taken an abnormal route -- the catheter had punctured the pulmonary vein. The implanted catheter was removed and no irreversible complication developed. Most complications related to venepuncture and catheterization have involved the subclavian artery, great artery, or pulmonary artery. Seldom has a case occurred at the left heart level, especially the pulmonary vein. During treatment, physicians should be aware of the risk of a complication, which may lead to a life-threatening event such as pulmonary embolism, stroke, or air-related myocardial infarction. In conclusion, puncture of the pulmonary vein during port implantation is a rare condition with limited treatment suggestions. The successful conservative treatment provided in this case was without long-term impairment, and can be applied in future cases. In all cases, however, the patient needs close observation and monitoring, and the surgical intervention team should always be prepared to provide hemostasis. ***(Thorac Med 2023; 38: 173-176)***

Key words: pulmonary vein puncture, iatrogenic-related injury

## Introduction

Subclavian vein puncture was introduced around 1970 [1], and since then, several hazards and many complications have been described [2, 3], including pneumothorax, hydrothorax, hemothorax, massive subcutaneous emphysema, arteriovenous fistula, brachial plexus injury, and air embolism [4]. However, in previous cases, these complications were almost always at the right heart or pulmonary level. They seldom developed at the left heart or in the pulmonary vein system.

We recently encountered a patient who developed possible embolic complications after accidental port-A catheterization through the left upper lung into the pulmonary vein, with the tip reaching the mitral valve level. This situation of an accidental puncture of the pulmonary vein and left upper lung is rare and has seldom been reported.

[1]National Taiwan University College of Medicine, [2]Division of Thoracic Surgery, Department of Surgery, National Taiwan University Hospital Yun-Lin Branch
Address reprint requests to: Dr. Pei-Hsing Chen, Division of Thoracic Surgery, Department of Surgery, National Taiwan University Hospital Yun-Lin Branch, No. 579, Sec. 2, Yunlin Rd., Douliu City, Yunlin County 640, Taiwan

## Case Report

This 56-year-old woman with breast cancer received port implantation via the left subclavian vein using the infraclavicular approach. However, intraoperative chest radiography (Figure 1) revealed the port implantation had taken an abnormal route. Computed tomography revealed that the port catheter had coursed through the left upper lung into the left superior pulmonary vein, with its tip reaching the mitral valve level (Figures 2, 3, 4). Only minor pneumothorax developed, as a result, without obvious hemothorax or bleeding. A minor stroke symptom was noticed after the port implantation operation, but was relieved spontaneously with conservative treatment. The follow-up brain magnetic resonance imaging showed no obvious lesion. A transient ischemic attack related to the procedure was highly suspected,

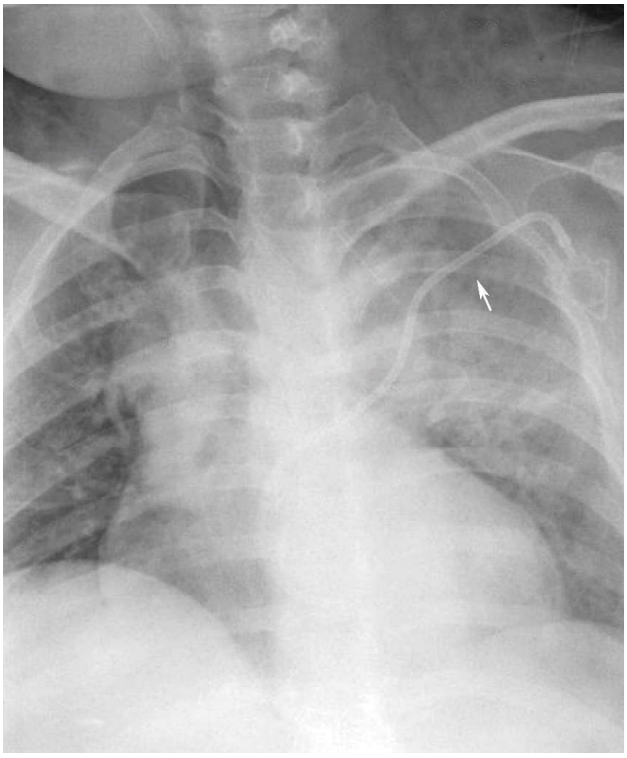

**Fig. 1.** Intraoperative chest radiography revealed the port implantation had taken an abnormal route.

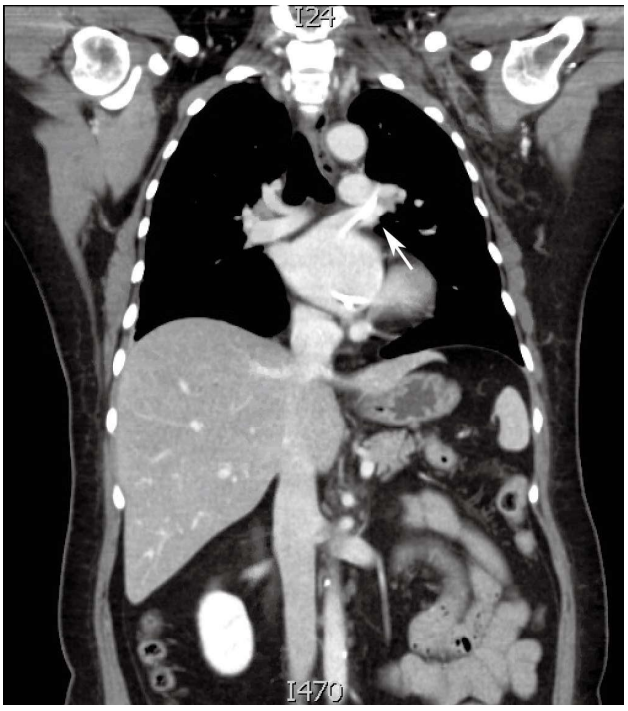


**Fig. 2.** Computed tomography, coronal view, revealed that the port catheter had coursed through the left upper lung into the left superior pulmonary vein, with its tip reaching the mitral valve level.

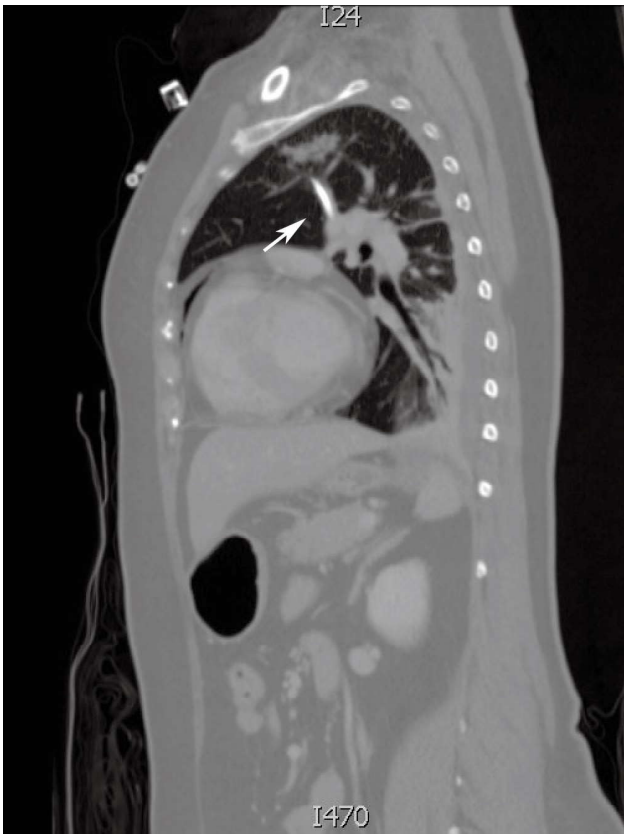


**Fig. 3.** Computed tomography, coronal view, revealed that the port catheter had coursed through the left upper lung into the left superior pulmonary vein, with its tip reaching the mitral valve level.

**Fig. 4.** 3D simulation of the computed tomography

but without image evidence. After evaluation, the implantable port was removed a day after the first operation, with the cardiovascular team standing by. No significant vital sign change was noted post-port removal. After 1 hour of observation following port removal, the patient was extubated, and the postoperative course was smooth. No pneumothorax or hemothorax developed postoperatively. A new implantable port was put in place 10 days later, through the right subclavian vein, using the infraclavicular method with echo-guidance. At the 24-month follow-up, the patient was free of symptoms and signs related to the procedure.

## Discussion

Central venous catheterization is extensively used in unstable patients who need hemodynamic monitoring, and in patients who require prolonged treatment, such as chemotherapy, antibiotics therapy, parenteral nutrition, or temporary hemodialysis [4]. Subclavian vein catheterization is the preferred approach for hemodialysis, especially as it does not restrict the patient. Most of the complications related to this procedure are insignificant. However, at times, some patients present with severe complications, like severe hemothorax, which could eventually cost lives [5].

In general, the life-threatening cases that would require surgical intervention are those in which great vessels are penetrated, and eventually develop massive hemothorax [5-8]. However, we presented a even rarer case, in which the upper left lung and subclavian vein, and eventually the mitral valve area, were accidentally penetrated. The patient experienced a suspected cardioembolism-related transient ischemic attack that caused right hemiplegia accompanied by dysarthria, but other than that, no major complications were noticed.

Most complications related to venepuncture and catheterization have involved the subclavian artery, great artery, or pulmonary artery [3, 7, 9-12]. Seldom has a case occurred at the left-side vessels, especially the pulmonary vein. Most cases involve the risk of an unstable hemodynamic status, which is related to bleeding. But the pressure in these cases is relatively low and has a higher chance of self-healing. However, penetration to the left heart system with relatively high pressure carries a higher risk, which is rarely noticed due to limited experience. In our case, air embolic and cardiac thrombi were the major possible mechanisms that induced the stroke in this case. No obvious vascular injury or intima injury was noticed in the follow-up

image, so the possibility of vascular injury was relative low.

In this case, we had a successful experience with a conservative treatment policy that can be applied in the future. But physicians should always be aware of the risk of an air-embolic event, which may lead to a life-threatening condition such as pulmonary embolism, stroke, or air-related myocardial infarction.

In conclusion, puncture of the pulmonary vein during port implantation is a rare occurrence with limited treatment suggestions. We presented our experience with successful conservative treatment without long-term impairment. But physicians should always be alert to life-threatening illnesses, and the patient needs close observation and monitoring. The surgical intervention team should always be prepared for hemostasis.

## References


1. FFeiler EM, De Alva WE. Infraclavicular percutaneous subclavian vein puncture. A safe technic. Am J Surg 1969; 118(6): 906-8.
2. Trerotola SO, Kuhn-Fulton J, Johnson MS, *et al*., Tunneled infusion catheters: increased incidence of symptomatic venous thrombosis after subclavian versus internal jugular venous access. Radiology 2000; 217(1): 89-93.
3. Samad AMA, Ibrahim YA. Complications of Port A Cath implantation: A single institution experience. Egypt J Radiol Nucl Med 2015; 46(4): 907-911.
4. McGee DC, Gould MK. Preventing complications of central venous catheterization. New Engl J Med 2003; 348(12): 1123-1133.
5. Porter JM, Page R, Wood AE, *et al*. Ventricular perforation associated with central venous introducer-dilator systems. Can J Anaesth 1997; 44(3): 317-320.
6. Arenas-Marquez H, Anaya-Prado R, Barrera-Zepeda LM, *et al*. Complications of central venous catheters. Curr Opin Clin Nutr Metab Care 2001 May; 4(3): 207-210.
7. Hoeper MM, Lee SH, Voswinckel R, *et al*. Complications of right heart catheterization procedures in patients with pulmonary hypertension in experienced centers. J Am Coll Cardiol 2006; 48(12): 2546-52.
8. Fukuda H, Kasuda H, Shimizu R. [Right ventricular perforation and cardiac tamponade caused by a central venous catheter]. Masui 1993; 42(2): 280-3.
9. Leick J, Leinen S, Friedrich I, *et al*. Iatrogenic perforation of a pulmonary artery side branch—a case report. Eur Heart J Case Rep 2021; 5(6).
10. Jahangirifard A, Ahmadi ZH, Khalili A, *et al*. Right ventricular perforation with the body of Swan-Ganz catheter during lung transplantation by ECMO support: a case report. Tanaffos 2017; 16(3): 240-244.
11. Lalwani P, Aggarwal S, Uppal R, *et al*. A case of malpositioned catheter via supraclavicular approach for subclavian vein cannulation: a rare technique revisited. J Anaesthesiol Clin Pharmacol, 2016; 32(1): 120-2.
12. Bossert T, Gummert JF, Bittner HB, *et al*. Swan-Ganz catheter-induced severe complications in cardiac surgery: right ventricular perforation, knotting, and rupture of a pulmonary artery. J Card Surg 2006; 21(3): 292-5.